JPL NO. 9950-580

DRL. No. 74/DRD No. SE
Line Item No. 7

DOE/JPL-955089 81/11
Distribution Category UC-63

SILICON SOLAR CELL PROCESS

DEVELOPMENT, FABRICATION, AND ANALYSIS

NINTH QUARTERLY REPORT

FOR PERIOD COVERING

1 JANUARY 1981 TO 31 MARCH 1981

H.I. Yoo, P.A. Iles, and D.C. Leung

JPL CONTRACT NO. 955089

OPTICAL COATING LABORATORY, INC.
Photoelectronics Division
15251 E. Don Julian Road
City of Industry, California 91746

"The JPL Low-Cost Silicon Solar Array Project is sponsored by the U.S. Government of Energy and forms part of the Solar Photovoltaic Conversion Program to initiate a major effort toward the development of low-cost solar arrays. This work was performed for the Jet Propulsion Laboratory, California Institute of Technology by agreement between NASA and DOE."

DRL. No. 74/DRD No. SE
Line Item No. 7

DOE/JPL-955089 81/11
Distribution Category UC-63

SILICON SOLAR CELL PROCESS DEVELOPMENT, FABRICATION, AND ANALYSIS

NINTH QUARTERLY REPORT

FOR PERIOD COVERING

1 JANUARY 1981 TO 31 MARCH 1981

H.I. Yoo, P.A. Iles, and D.C. Leung

JPL CONTRACT NO. 955089

OPTICAL COATING LABORATORY, INC.
Photoelectronics Division
15251 E. Don Julian Road
City of Industry, California 91746

"The JPL Low-Cost Silicon Solar Array Project is sponsored by the U.S. Government of Energy and forms part of the Solar Photovoltaic Conversion Program to initiate a major effort toward the development of low-cost solar arrays. This work was performed for the Jet Propulsion Laboratory, California Institute of Technology by agreement between NASA and DOE."

ABSTRACT

Extensive evaluation of two large cast ingots by HEM (Crystal Systems) was carried out. Solar cell performance versus substrate position within the ingots was obtained and the results are presented in detail.

Dendritic web samples were analyzed at MRI, in terms of structural defects, and efforts were made to correlate the data with the performance of solar cells made from the webs.

TABLE OF CONTENTS

TABLE OF CONTENTS CONT'D.

LIST OF TABLES

LIST OF FIGURES

1. INTRODUCTION

The objective of this program is to investigate, develop, and utilize technologies appropriate and necessary for improving the efficiency of solar cells made from various unconventional silicon sheets. During the reporting period, work included fabrication and evaluation of solar cells from HEM (Crystal Systems) and dendritic web (Westinghouse). Baseline solar cells were fabricated from HEM wafers cut from two large ingots (40kg) of HEM (HEM #41-41C and HEM #41-48) and detail mapping of solar cell parameters was completed for ingot HEM #41-41C while that for ingot HEM #41-48 was half completed. For dendritic web material, baseline solar cells were fabricated on pre-characterized material to correlate solar cell performance with material properties, such as structural defects.

II. TECHNICAL DISCUSSION

A. HEM Solar Cells

1.0 Solar Cell Fabrication

Baseline solar cells were fabricated wafers cut from two HEM ingots. (Both ingots #41-41C and ingot #41-48 were 12" x 12" x 6" in dimension, 40kg). The positions where the wafers were cut is illustrated in Figure 1. Cross section layers of half ingots were cut at three vertical positions and three horizontal positions for each ingot. About 48 - 2x2cm cells were fabricated on each layer chosen to represent each ingot position. In this report period, cell fabrication was completed in all six layers for ingot #41-41C and for three vertical layers for Ingot #41-48. See Reference (1) for the description of the baseline process, and reference (2) for the details of HEM process.

2.0 Solar Cell Performance and Characterization

Characteristics Under Illumination

Finished baseline solar cells had SiO AR coating and about 90% active area with Ti-Pd-Ag metallization. Solar cell parameters, such as Isc, Voc, CFF, and were measured under AM1 conditions at 28°C test block temperature. Figures 2 to Figure 7 shows the mappings of cells normalized (to CZ control) on all six layers for the ingot #41-41C. Appendix III (vertical layers) and Appendix IV (horizontal layers) provide mappings of individual cell parameters of these layers. This ingot #41-41C demonstrated the best performance for all the HEM ingots measured to date. Except for the region close to the seed at center bottom with some areas, showing low Jsc and shunting problems (top layer), the cell performances were quite uniform throughout the ingot including the polycrystalline area. (See the Figures in text and Appendix). The overall efficiency of the usable area of the ingot is about 87% of the baseline CZ control cells.

For ingot #41-48, Figure 8 to Figure 10 shows mappings of normalized (to CZ control) of cells for each of the three vertically cut layers. Appendix V provides mappings of individual cell parameters for each layer. The solar cell performance of this ingot is much worse than #41-41C. The mappings of Voc and CFF in Appendix V indicated severe shunting problems in relatively large portions of the ingot, especially close to the edge. The cause of the shunting is not immediately known. Portions of the shunting area had high density of micro-precipitates as shown in the microscope pictures of Figure 11. In some cases these micro-precipitates were observed at grain boundaries of very fine grain areas. However, these fine grain areas only account for a small portion of the total shunting area. Inclusions were also noted in some other areas in the bulk. The shunting area is estimated to be about 30 to 35% of the whole ingot, mostly occurring along the edge and on the top of the upper half of the ingot (see figures). The top polycrystalline area where the final solidification occurred seems to be mostly shunted judged by the cell performance. Other areas showing shunting problems are polycrystalline areas along the edge downward. The single crystalline area and the lower polycrystalline areas away from the edge are relatively free of the shunting problems. It could be speculated that the shunting is caused by inclusions, most likely precipitates at the final solidification stage. The results merit further material study. The total effectiveness of the ingot was estimated to be about 60% compared to a Cz control ingot.

Spectral Response

Absolute spectral response (A/W) measurements were made using a filter wheel set-up (see Appendix V of Reference (1) for the details). Response versus wavelength of selected cells are given in Figure 12 to Figure 14 for ingot #41-41C and Figure 15 to Figure 17 for ingot #41-48.

Minority Carrier Diffusion Length

Minority carrier diffusion length (L_D) was measured on the same solar cells used to measure spectral response, using the short circuit current method. The results including the locations of the cells are given in Figure 18 to Figure 23 for the two respective ingots. The results of spectral response and minority carrier diffusion length measurements indicate that there is substantial variation of L_D from top to bottom in the ingots (from 15um to 100um). This is not reflected directly from the Jsc data because Jsc does not drop substantially until $L_D < 40$um. However, one would expect that more pronounced differences will show up when a back surface field is added.

FIGURE 1

WAFER IDENTIFICATION WITHIN THE HEM INGOT

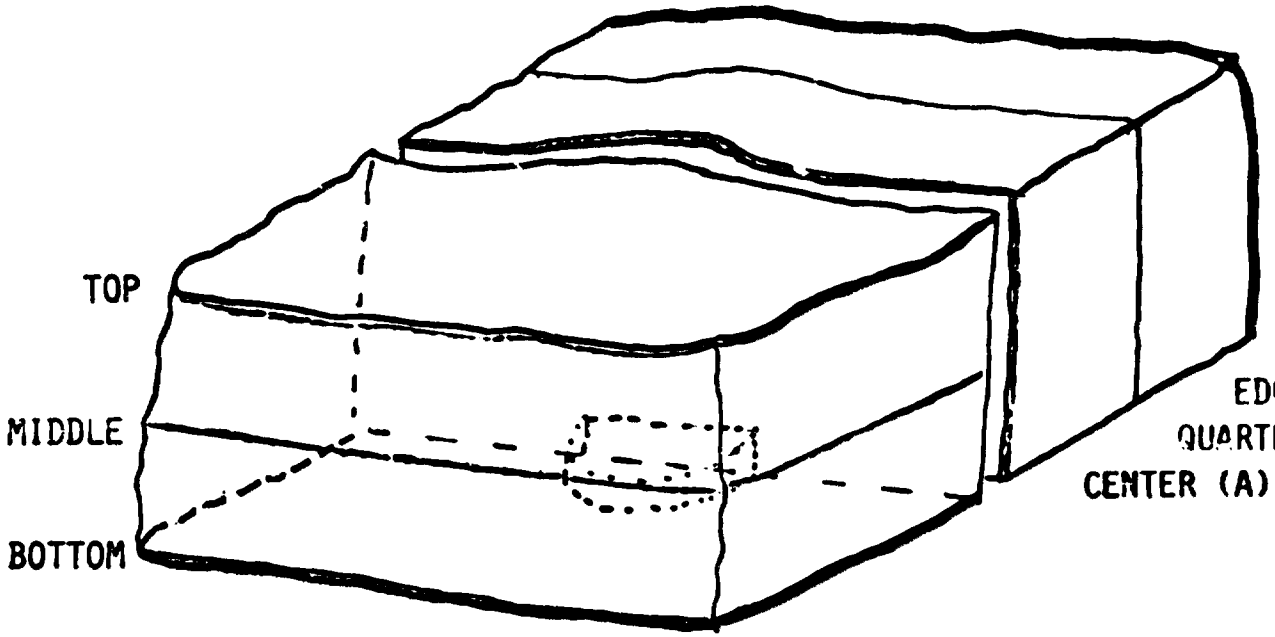

SIZE: 12" x 12" x 6"

WT. ~ 35 kg

FIGURE 2

A MAPPING OF NORMALIZED η (% TO CONTROL) FOR A CENTER LAYER OF VERTICALLY CUT HEM (41-41C)

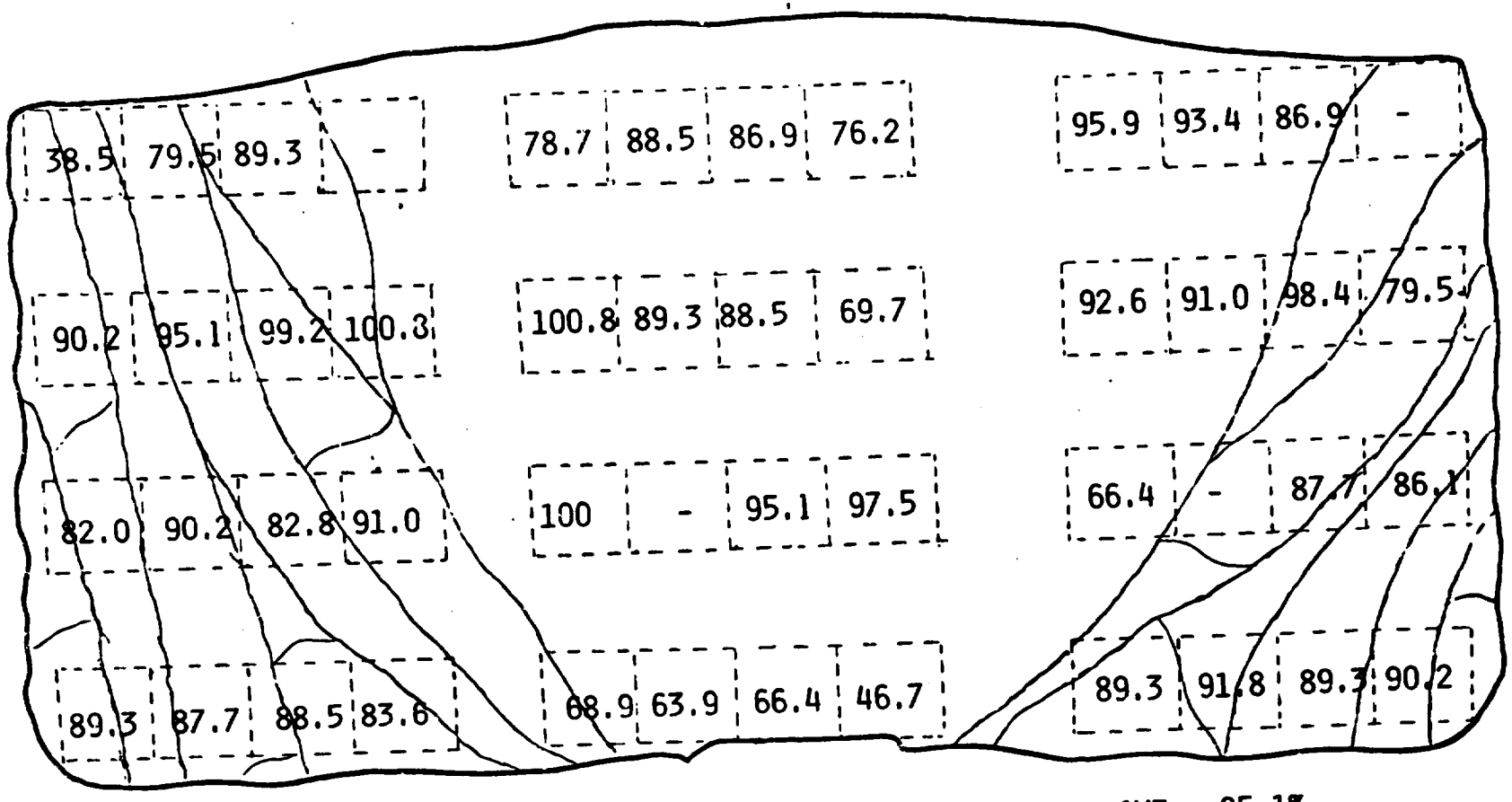

AVE. 85.1%

FIGURE 3

A MAPPING OF NORMALIZED η (% TO CONTROL) FOR A QUARTER LAYER OF VERTICALLY CUT HEM (41-41C)

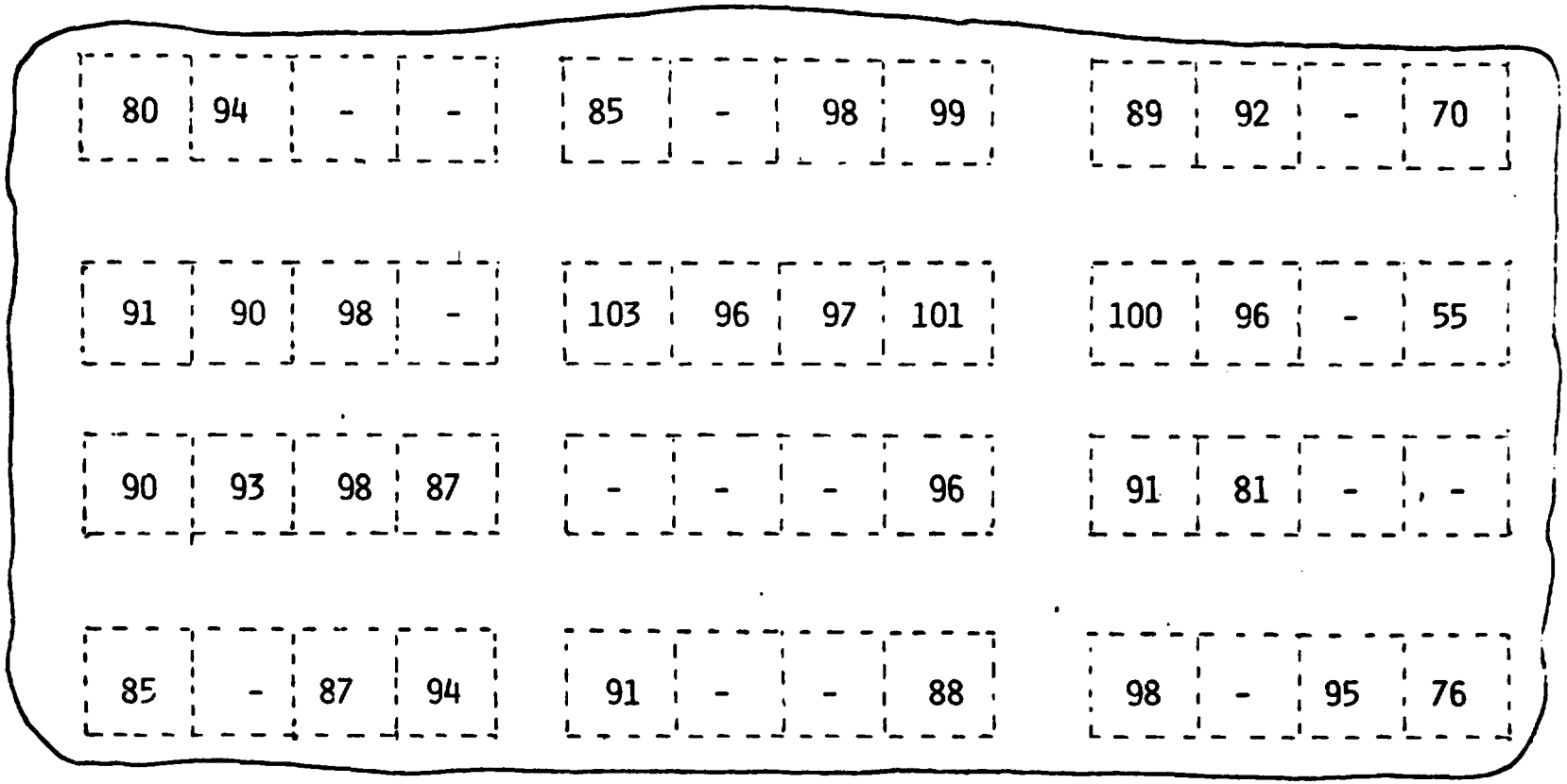

AVE. 90%

FIGURE 4

A MAPPING OF NORMALIZED η (% TO CONTROL) FOR A EDGE LAYER OF VERTICALLY CUT HEM (41-41C)

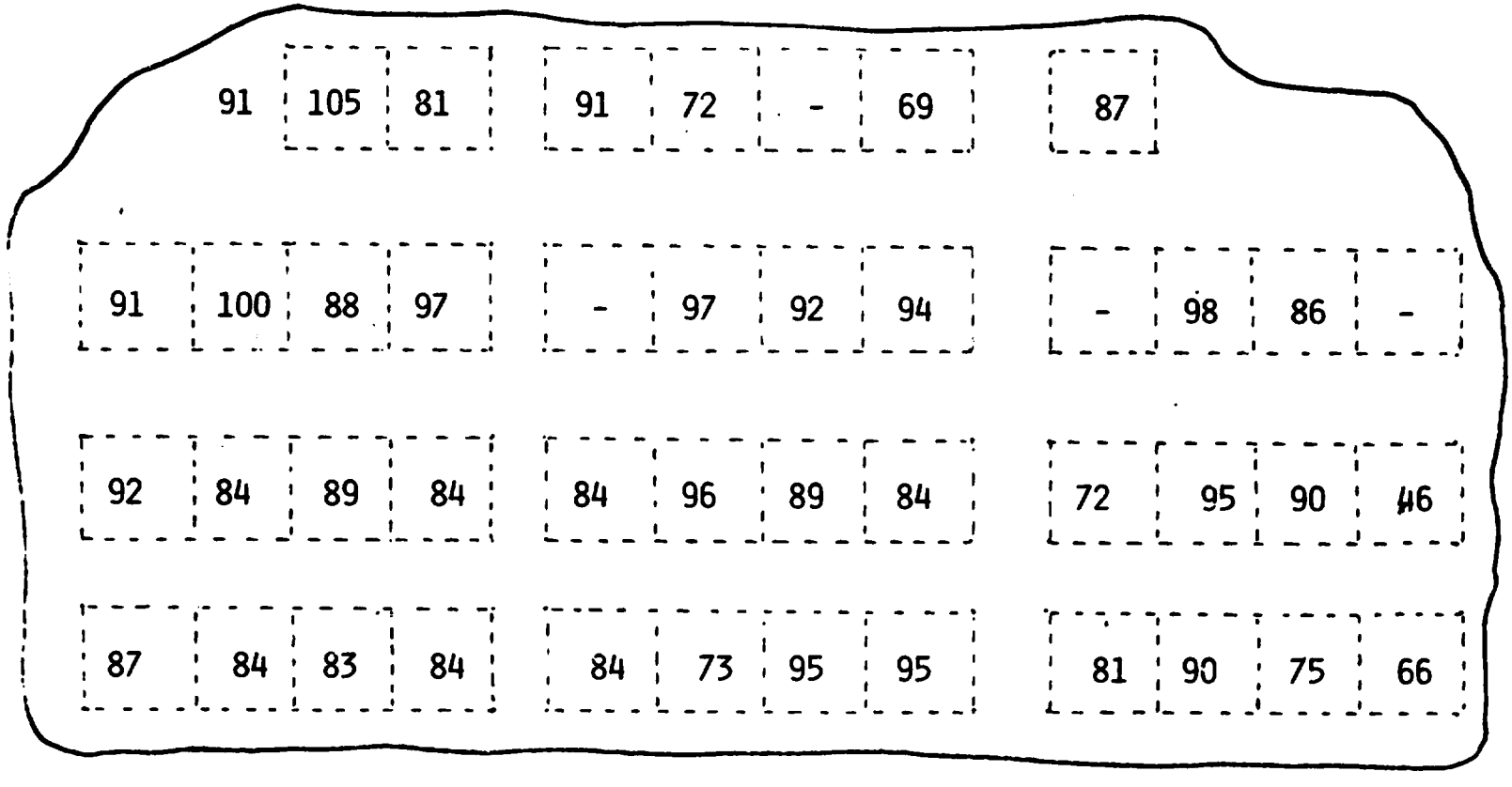

AVE. 86%

FIGURE 5

A MAPPING OF NORMALIZED η (% TO CONTROL) FOR THE TOP HORIZONTAL LAYER OF HEM I.D.41-41C

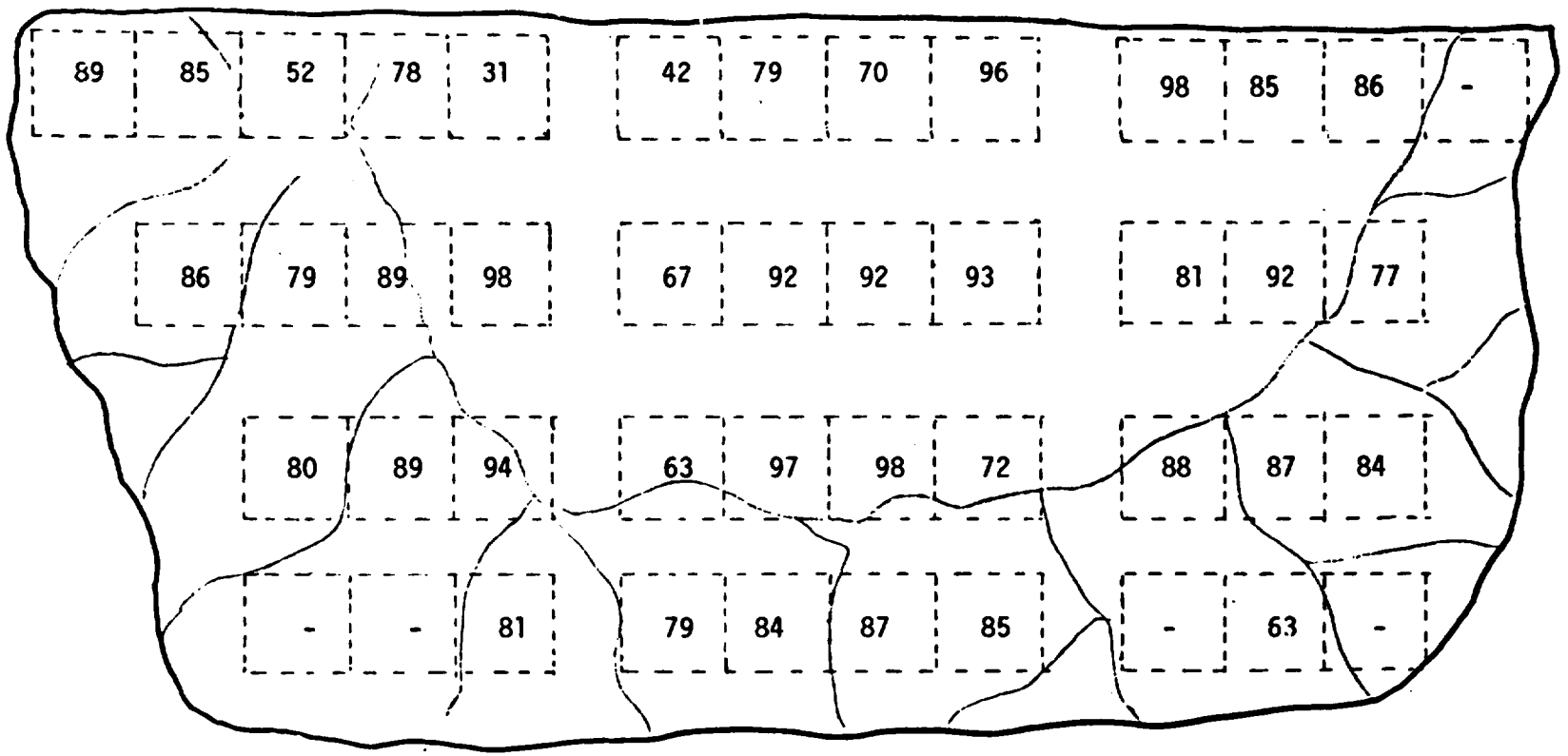

AVE. 82%

FIGURE 6

A MAPPING OF NORMALIZED η (% TO CONTROL) FOR THE MIDDLE HORIZONTAL LAYER OF HEM I.D. 41-41C

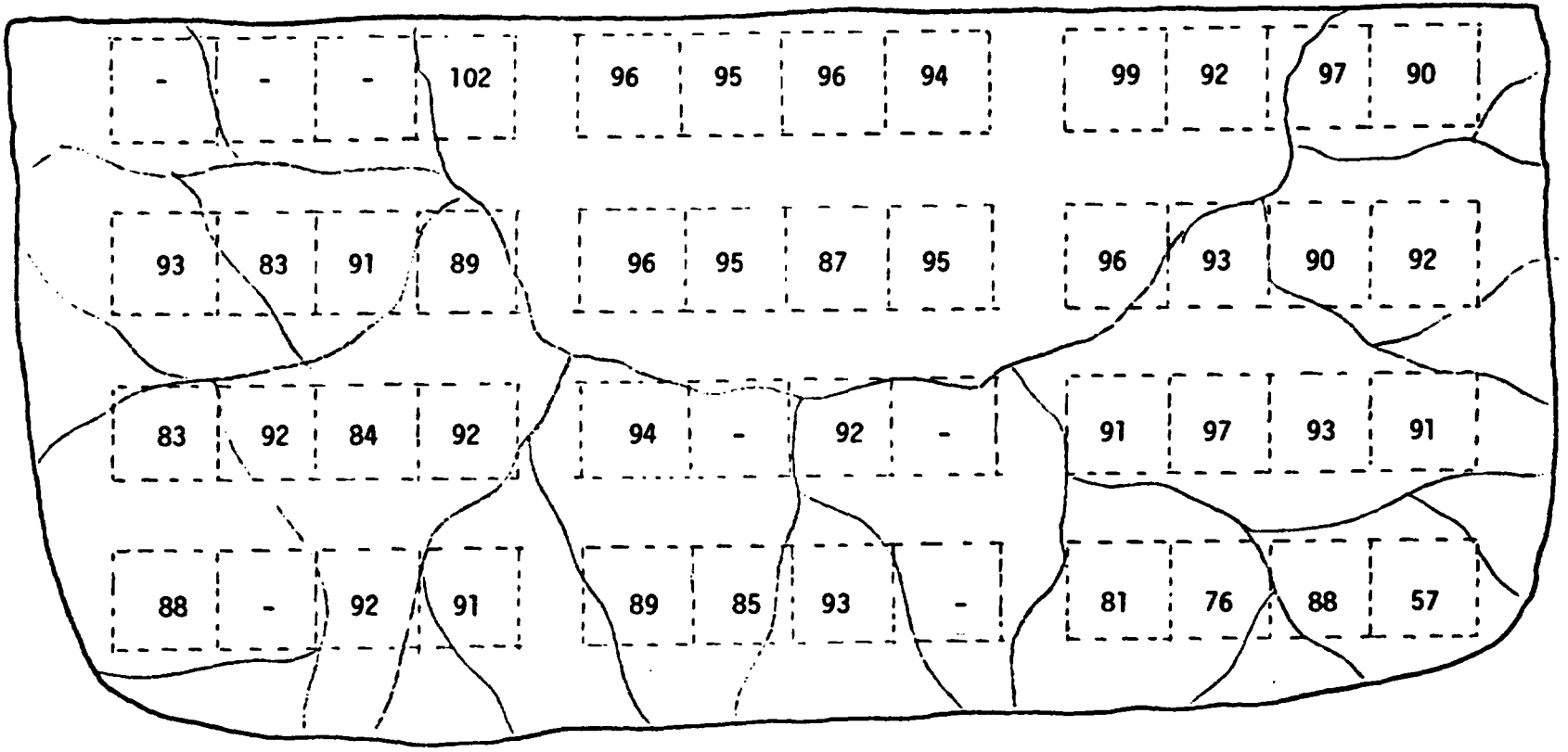

AVE. 90%

FIGURE 7

A MAPPING OF NORMALIZED η (% TO CONTROL) FOR THE BOTTOM HORIZONTAL LAYER OF HEM I.D.41-41C

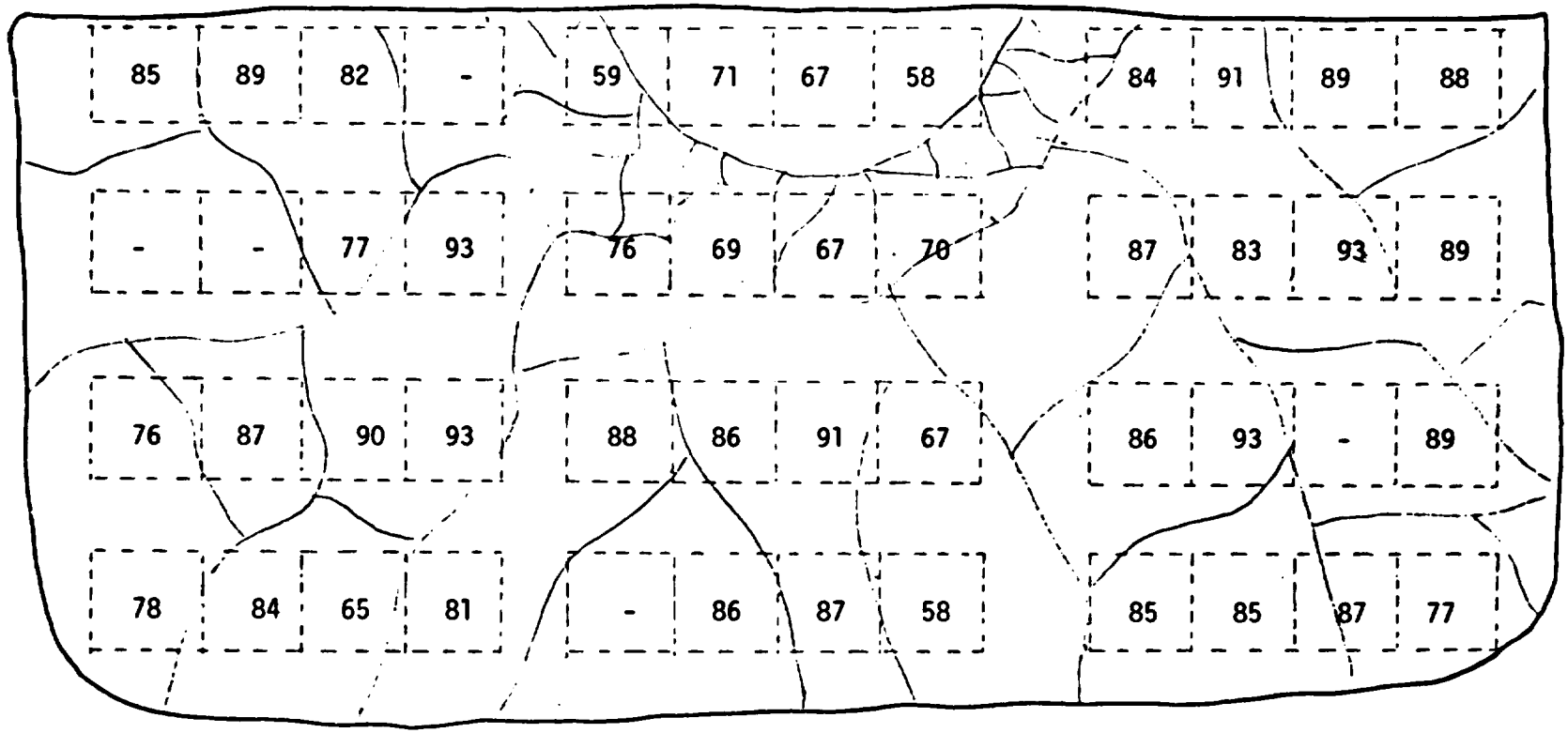

AVE. 81%

FIGURE 8

A MAPPING OF NORMALIZED η (% TO CONTROL) FOR A CENTER LAYER OF VERTICALLY CUT HEM (41-48)

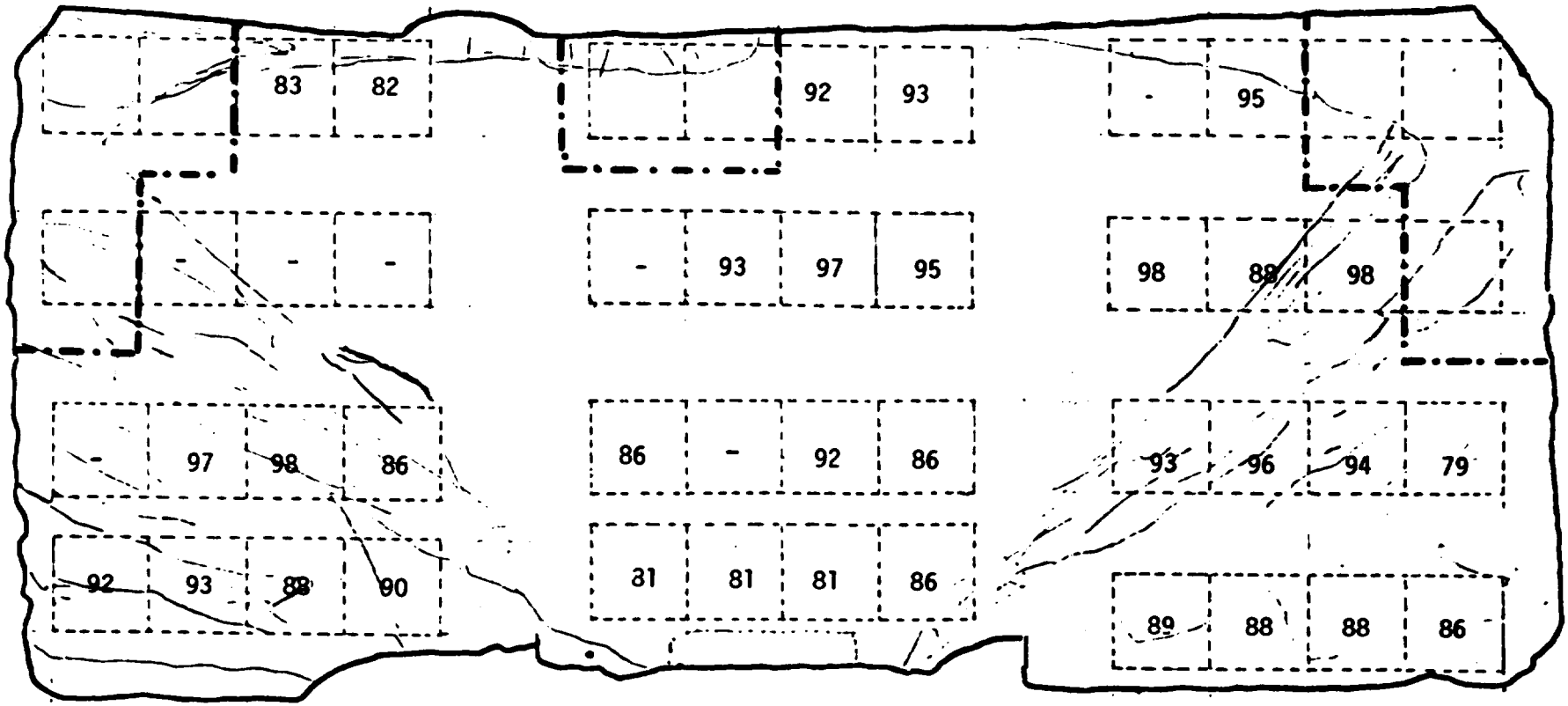

AVE. OF USABLE AREA: 90 (Regions separated by -·- lines are excluded due to shunting.)

FIGURE 9

A MAPPING OF NORMALIZED η (% TO CONTROL) FOR A QUARTER LAYER OF VERTICALLY CUT HEM (41-48)

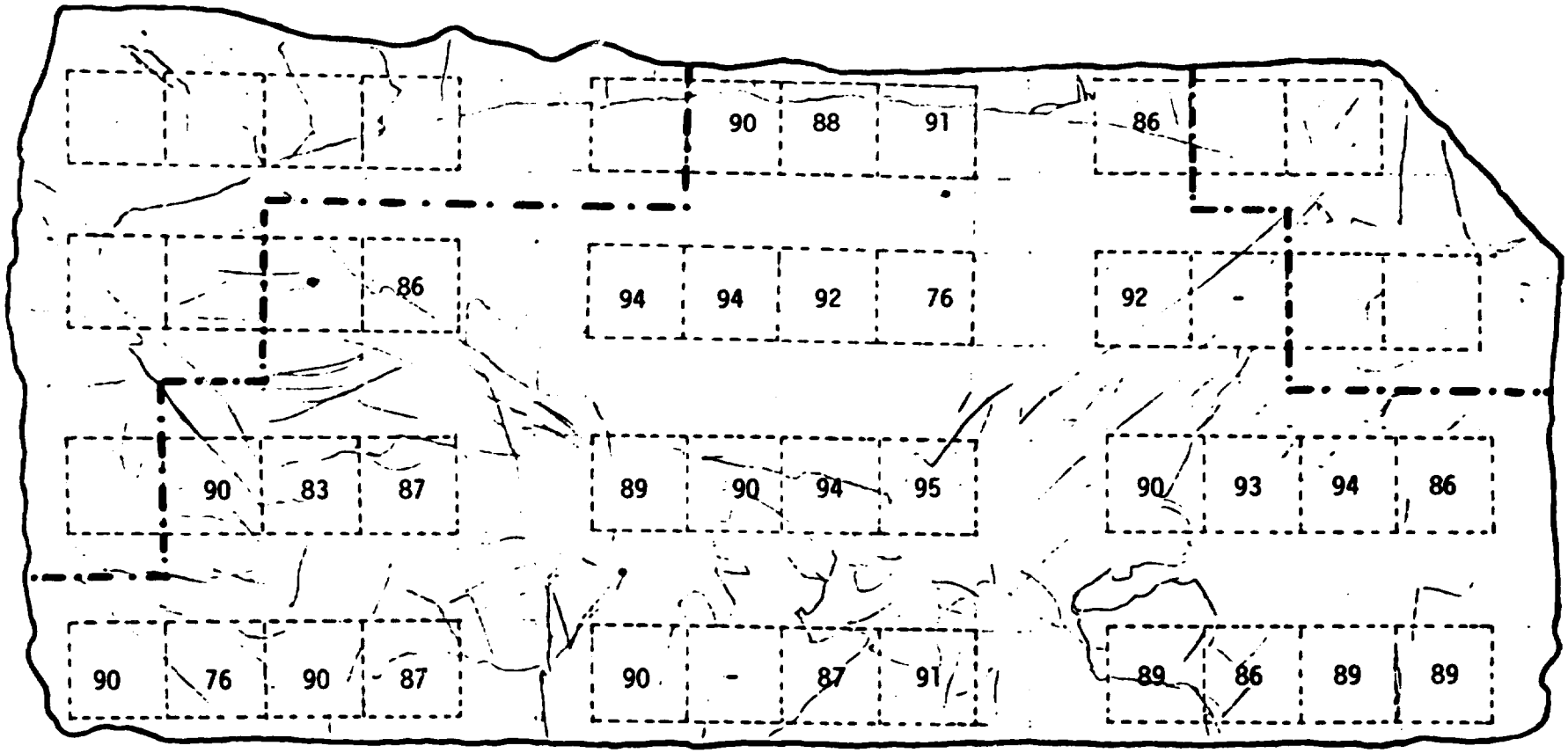

AVE. OF USABLE AREA: 89% (Regions separated by —·— lines are excluded due to shunting.)

FIGURE 10

A MAPPING OF NORMALIZED η (% TO CONTROL) FOR A EDGE LAYER OF VERTICALLY CUT HEM (41-48)

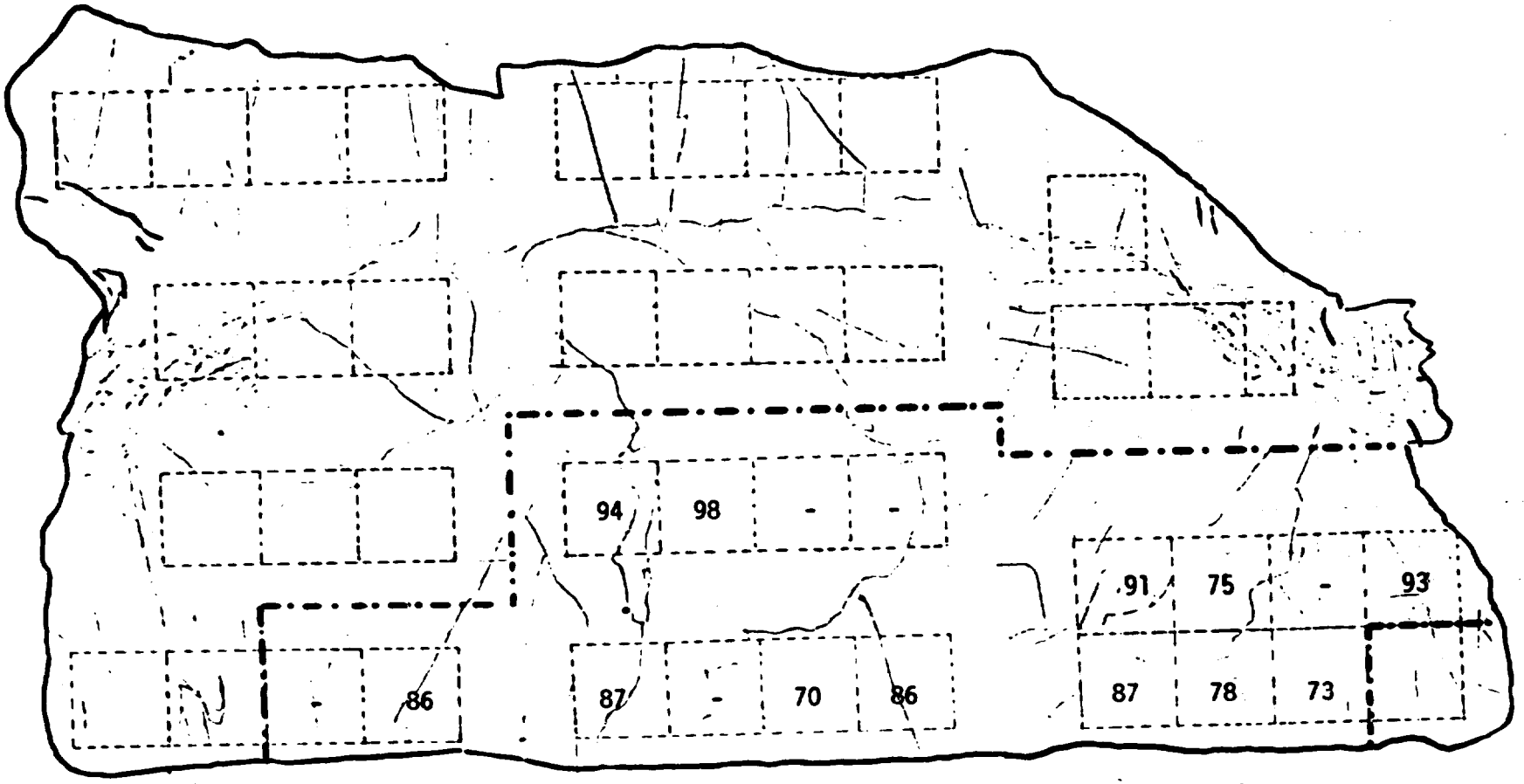

AVE. OF USABLE AREA: 84% (Regions seaprated by —·— lines are excluded due to shunting. In this case, the whole upper region is excluded.)

FIGURE 11

Microscopic Picture of Inclusions Observed in a HEM Ingot (41-48), 200X Magnification

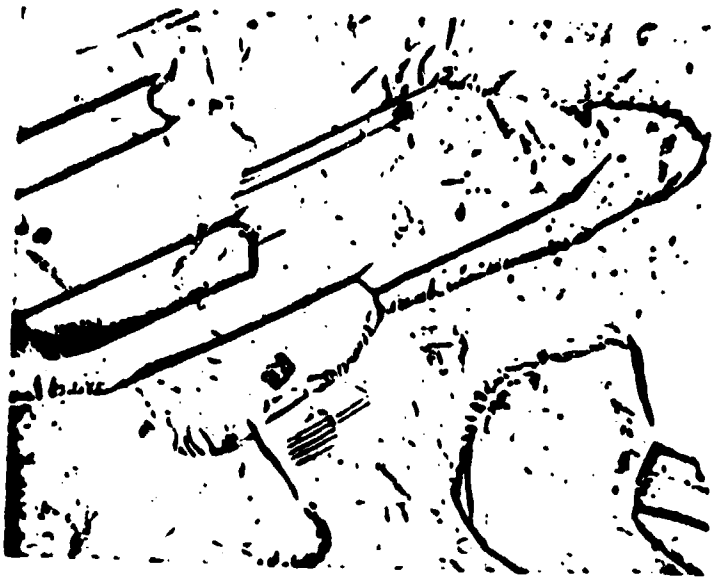

FIGURE 12A

SPECTRAL RESPONSES OF SELECTED SAMPLES FROM A CENTER LAYER OF VERTICALLY CUT HEM(41-41C)

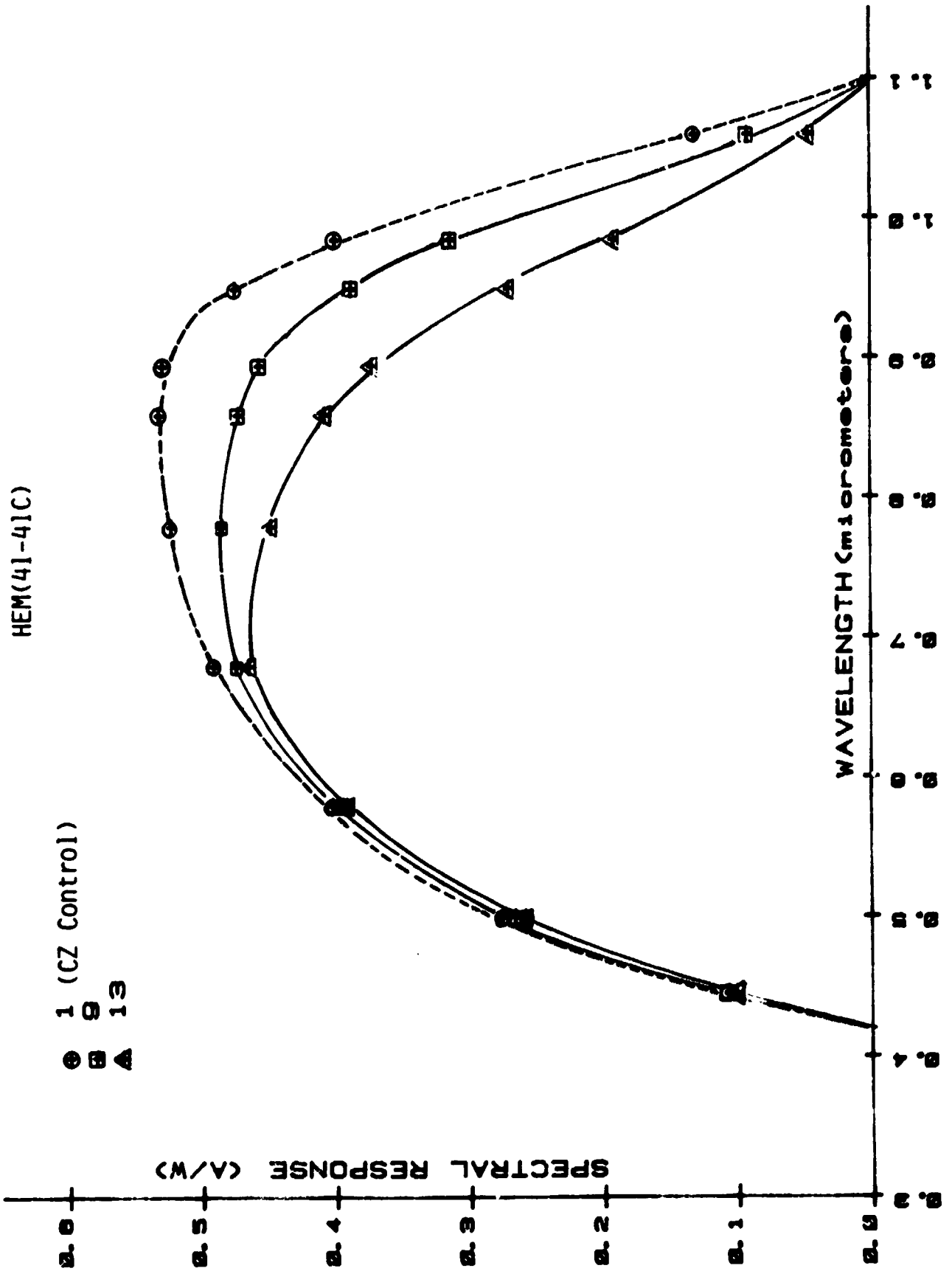

FIGURE 12B

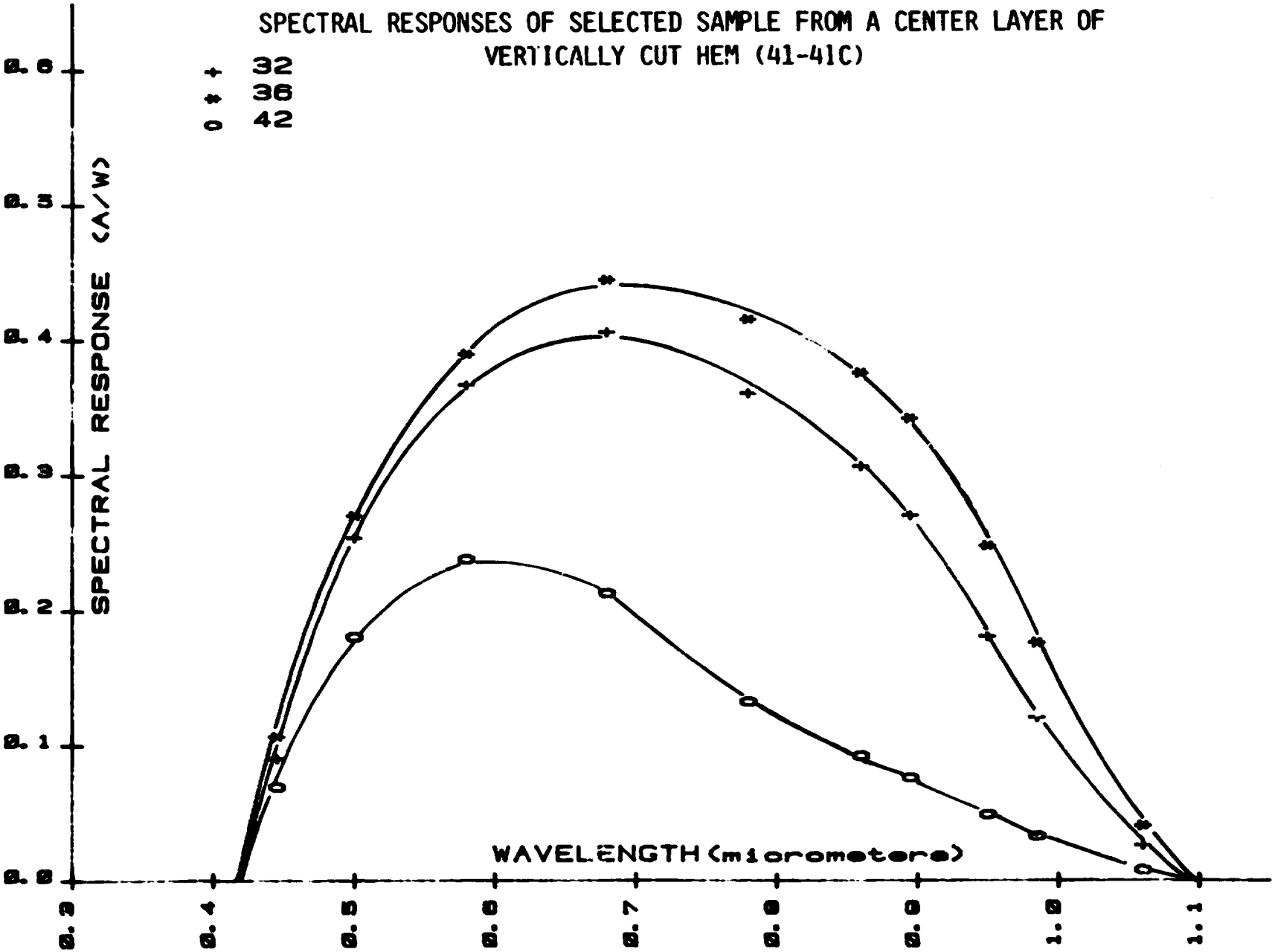
SPECTRAL RESPONSES OF SELECTED SAMPLE FROM A CENTER LAYER OF VERTICALLY CUT HEM (41-41C)
32
36
42
SPECTRAL RESPONSE (A/W)
WAVELENGTH (micrometers)

FIGURE 13

SPECTRAL RESPONSES OF SELECTED SAMPLES FROM A QUARTER LAYER OF VERTICALLY CUT HEM (41-41C)

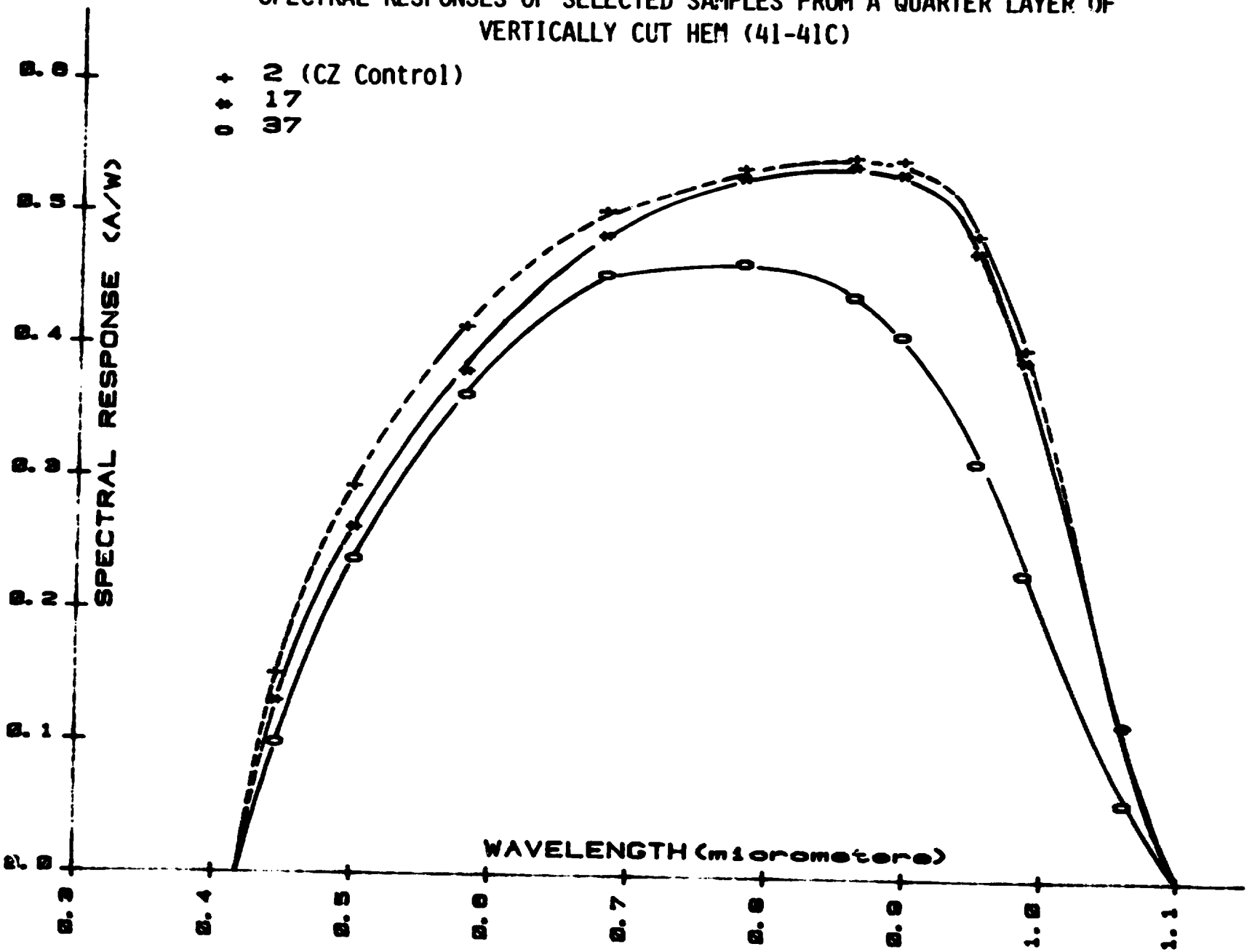

FIGURE 14

SPECTRAL RESPONSES OF SELECTED SAMPLES FROM A EDGE LAYER OF VERTICALLY CUT HEM (41-41C)

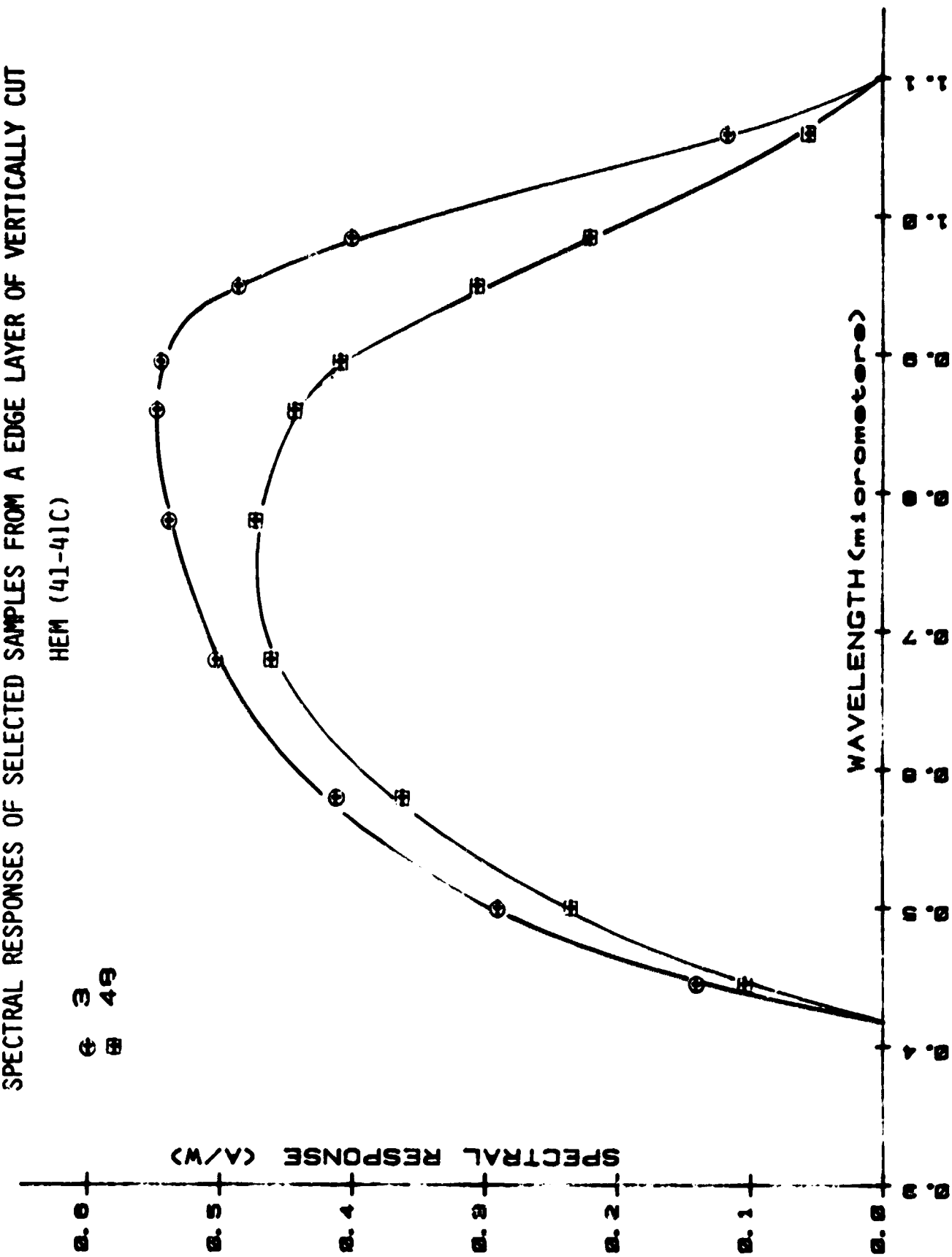

FIGURE 15

SPECTRAL RESPONSES OF SELECTED SAMPLES OF A CENTER LAYER OF VERTICALLY CUT HEM 41-48

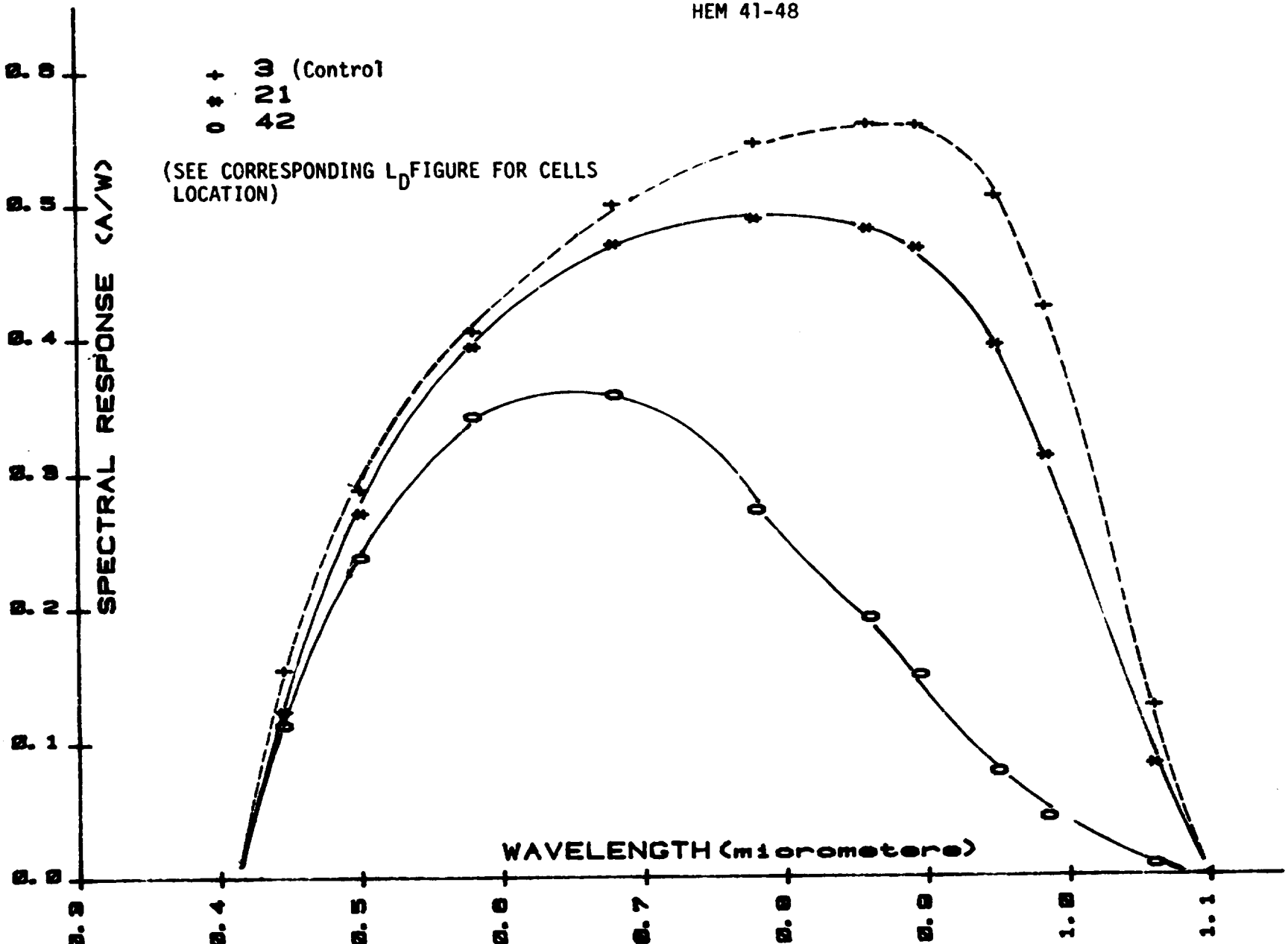

FIGURE 16

SPECTRAL RESPONSES OF SELECTED SAMPLES OF A QUARTER LAYER OF VERTICALLY CUT HEM 41-48

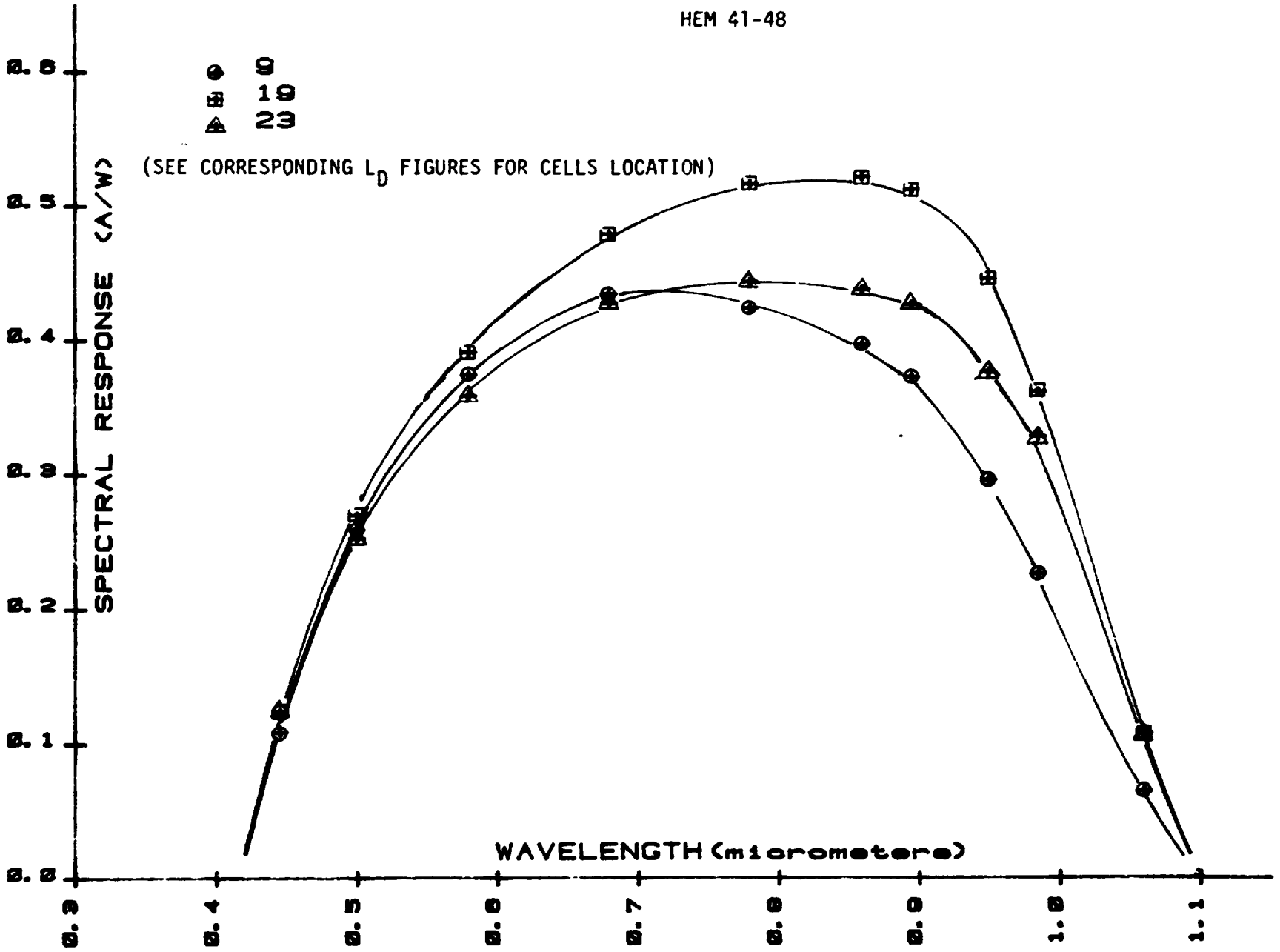

FIGURE 17

SPECTRAL RESPONSES OF SELECTED SAMPLES OF A EDGE LAYER OF VERTICALLY CUT HEM 41-48

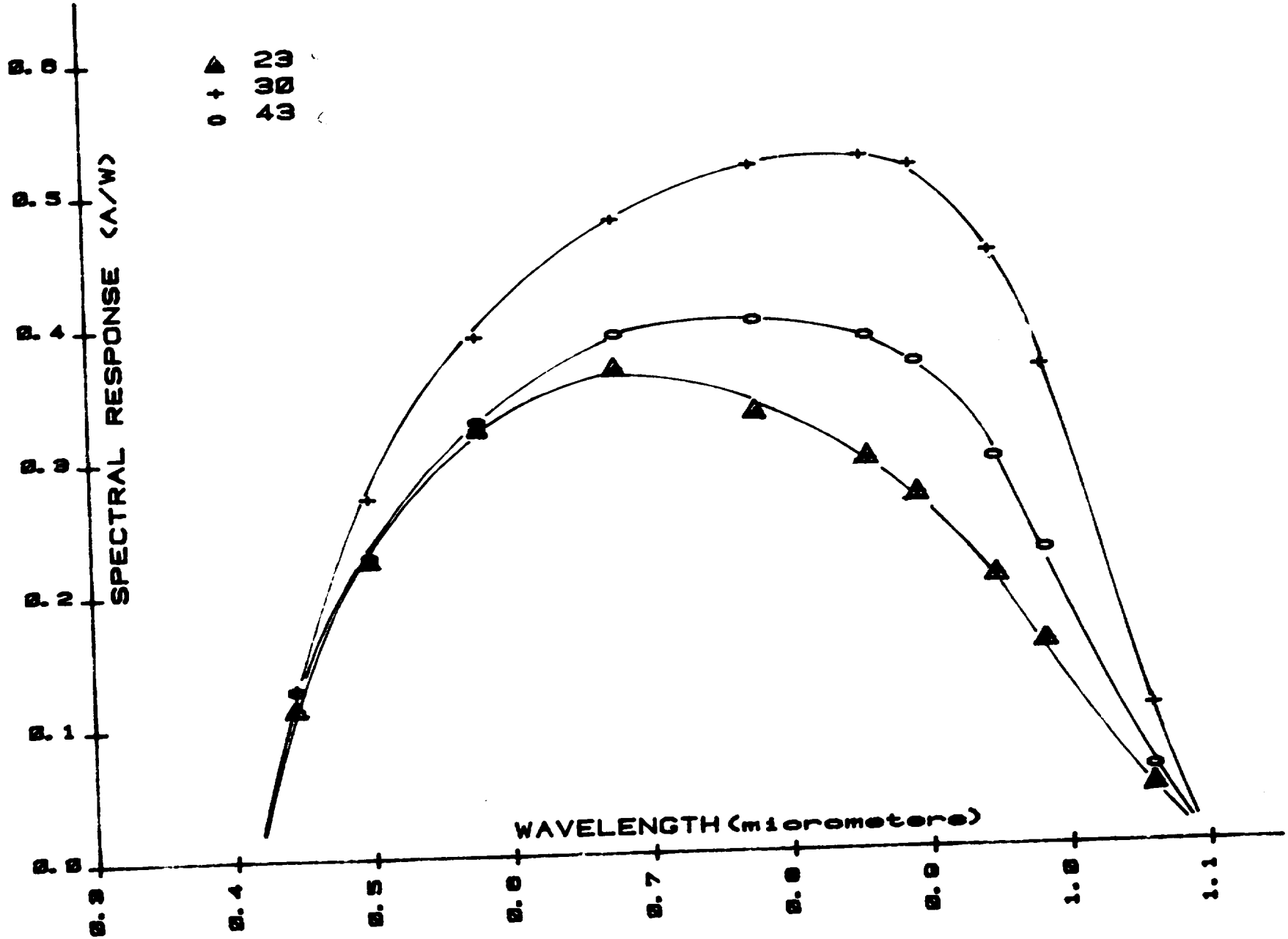

FIGURE 18

DIFFUSION LENGTH L_D (um) OF SELECTED SAMPLES FROM A CENTER LAYER OF VERTICALLY CUT HEM (41-41C)

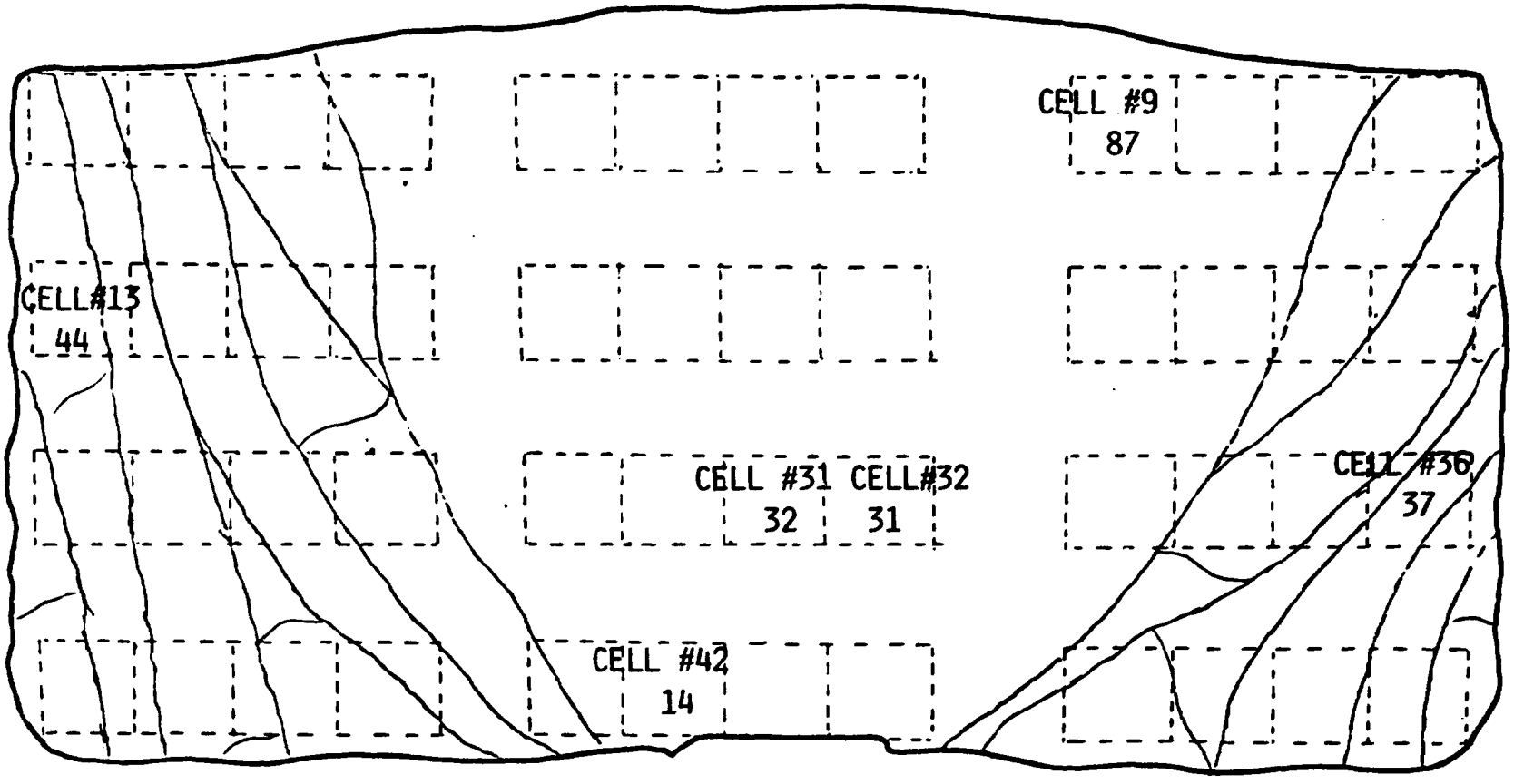

CONTROL CELL (C-1)= 125um

FIGURE 19

DIFFUSION LENGTH L_D (um) OF SELECTED SAMPLES FROM A QUARTER LAYER OF VERTICALLY CUT HEM (41-41C)

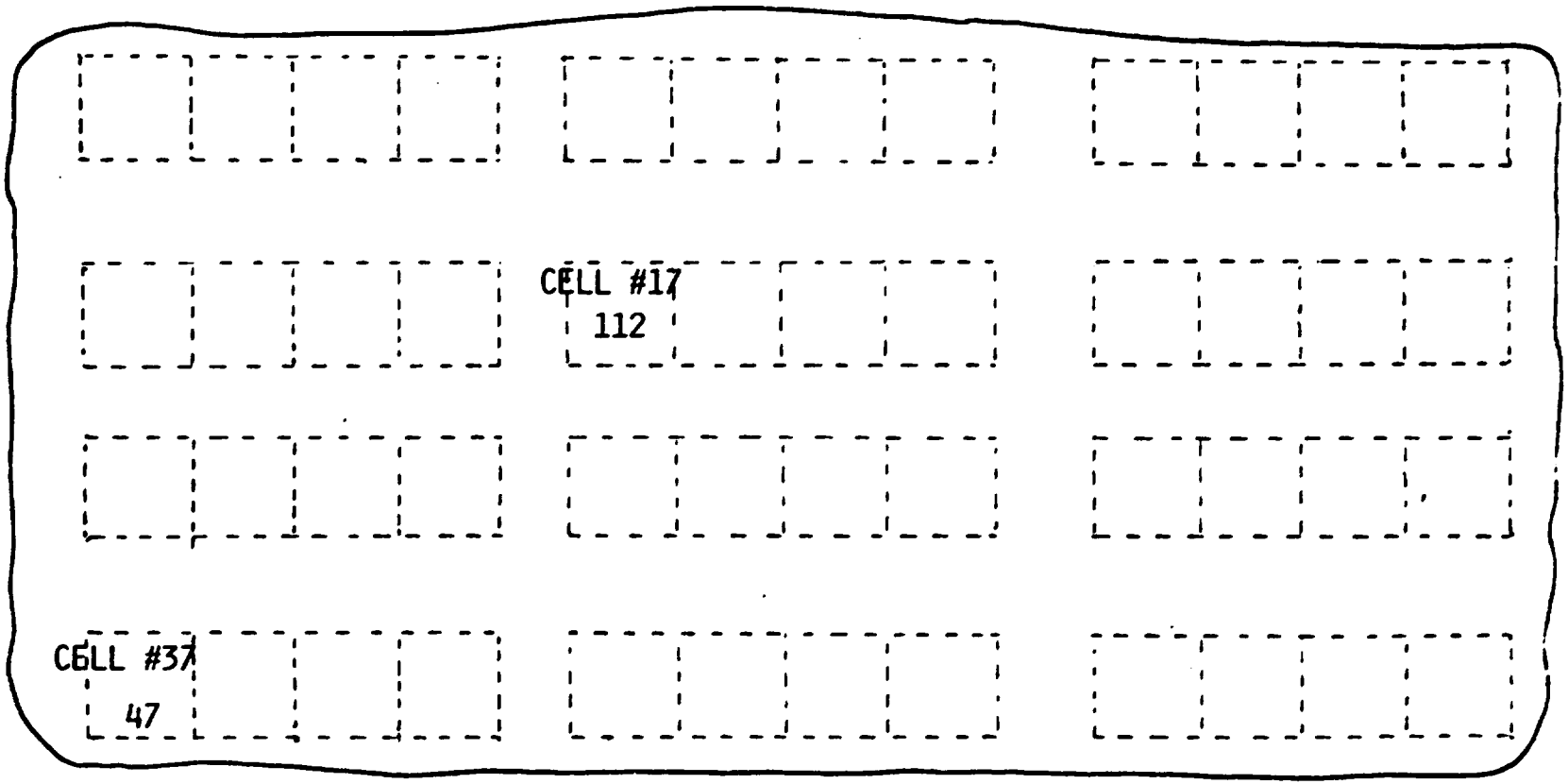

FIGURE 20

DIFFUSION LENGTH L_D (um) FROM SELECTED SAMPLES OF A EDGE LAYER OF VERTICALLY CUT HEM (41-41C)

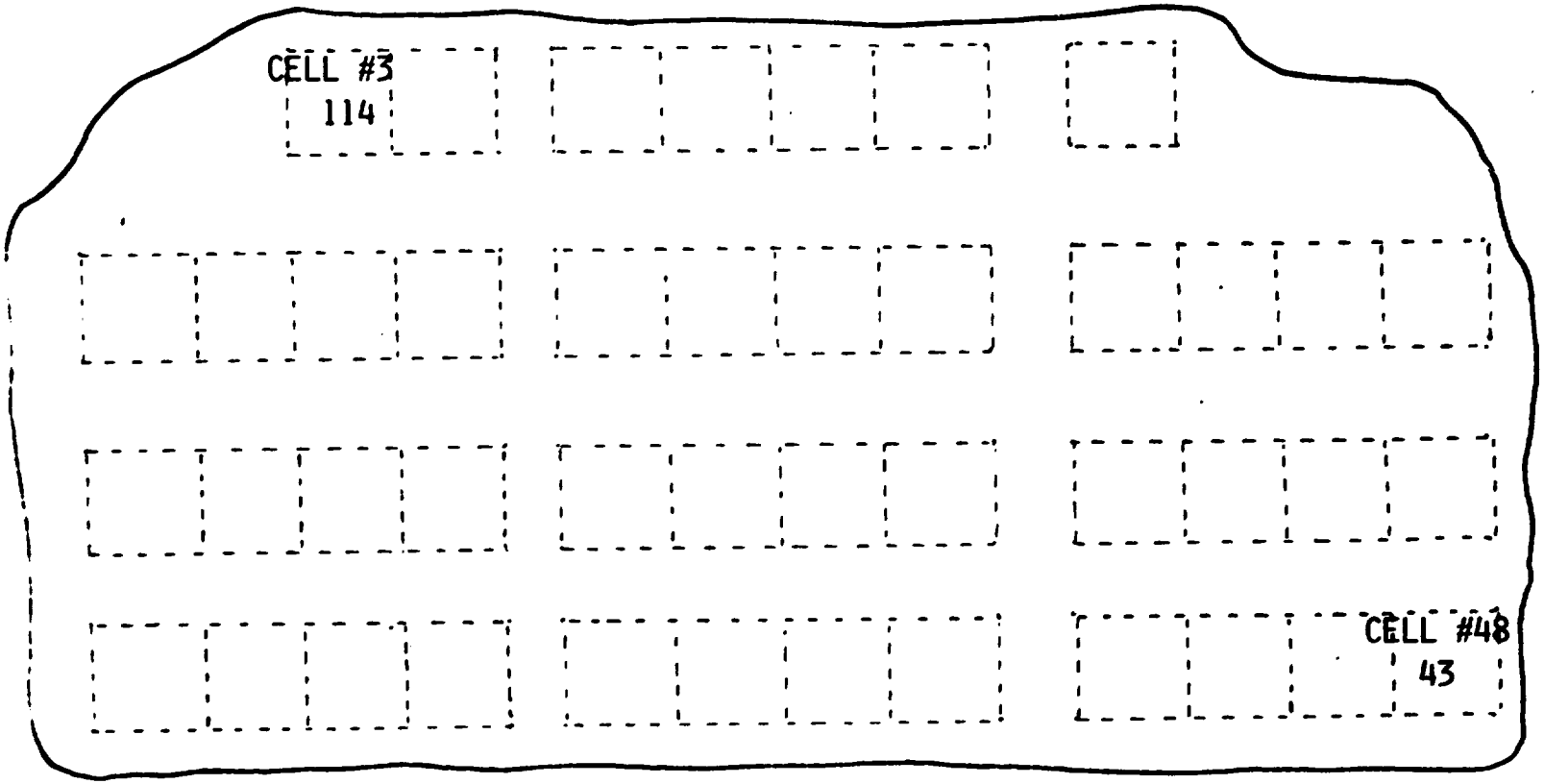

CONTROL #2: 117

FIGURE 21

DIFFUSION LENGTHS L_D (um) OF SELECTED SAMPLES OF A CENTER LAYER OF VERTICALLY CUT HEM 41-48

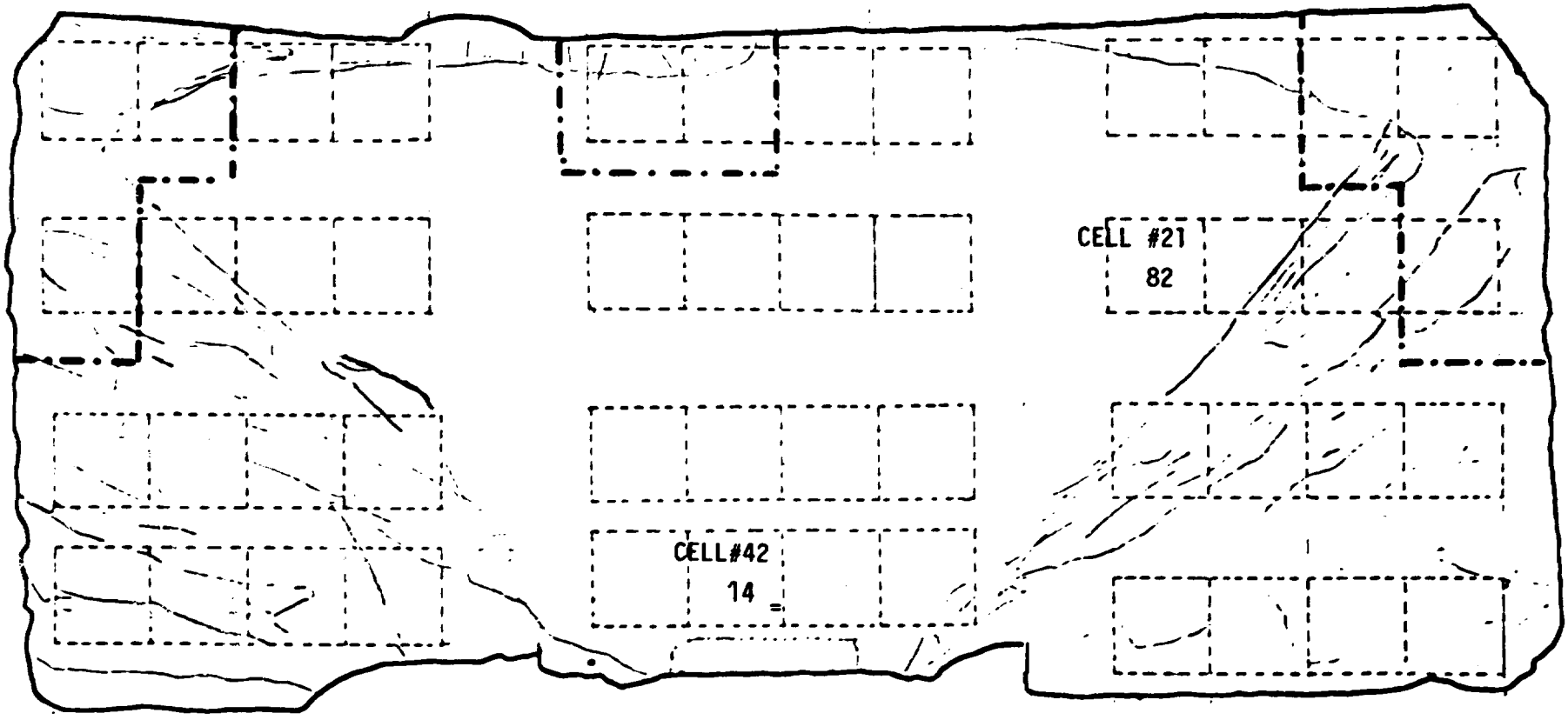

CONTROL CELL #3: 128

FIGURE 22

DIFFUSION LENGTHS L_D (um) OF SELECTED SAMPLES OF A QUARTER LAYER OF VERTICALLY CUT HEM 41-48

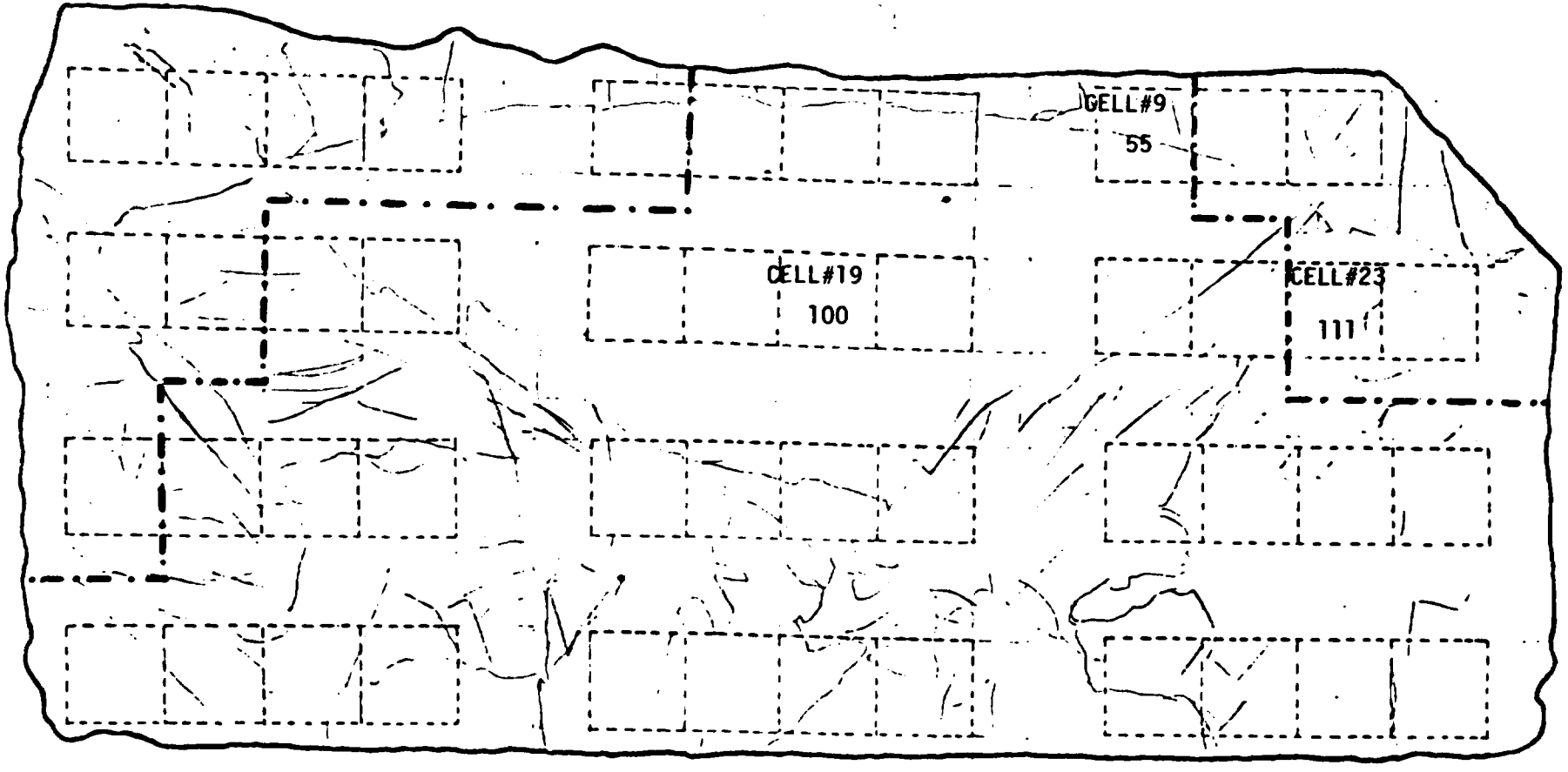

CONTROL CELL #3: 128

FIGURE 23

DIFFUSION LENGTHS L_D (um) OF SELECTED SAMPLES OF A EDGE LAYER OF VERTICALLY CUT HEM 41-48

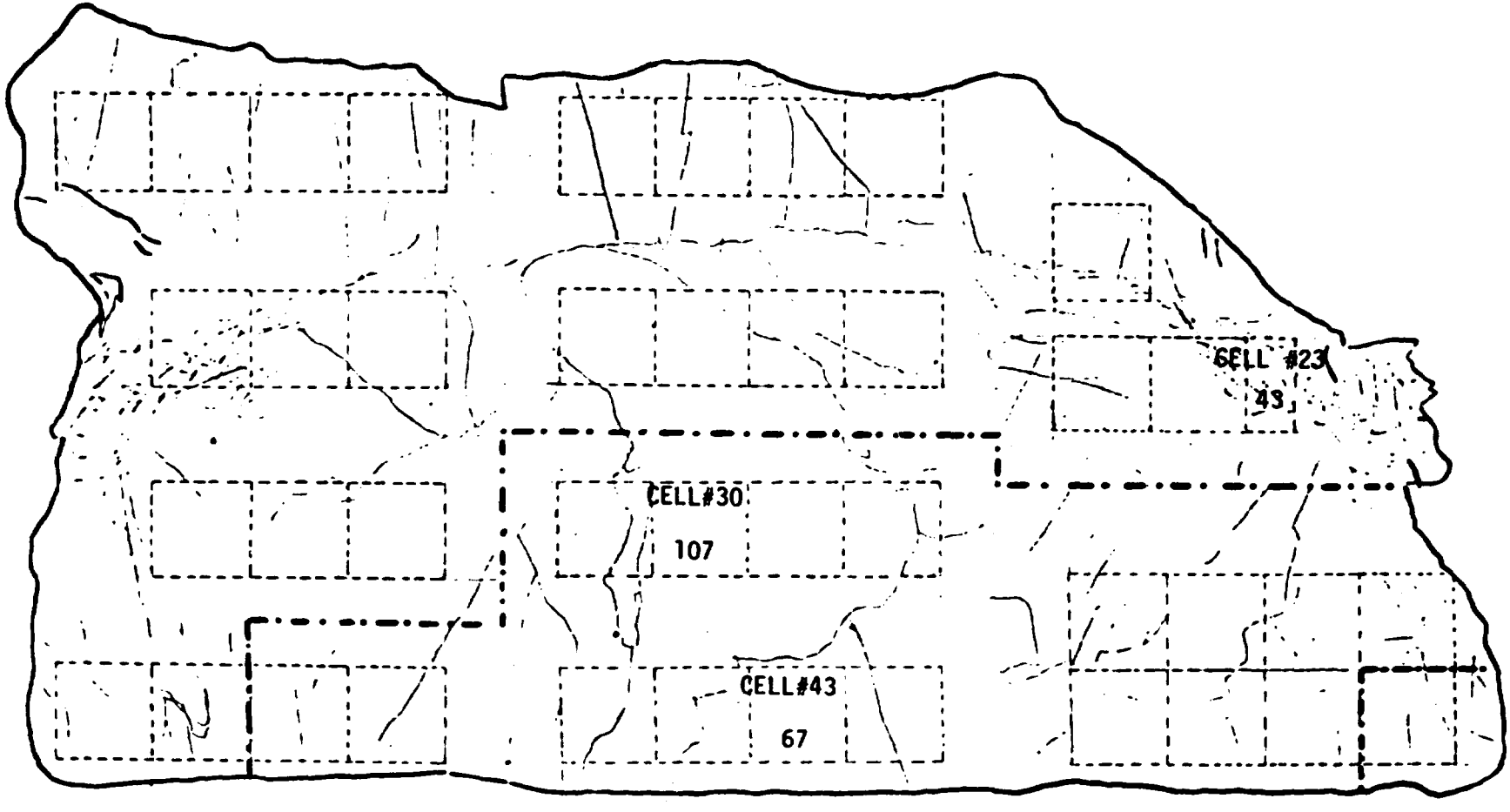

CONTROL CELL #3: 128

B. Dendritic Web Solar Cells

1.0 Solar Cell Fabrication

Baseline solar cells were fabricated on 2x2 wafers pre-characterized in terms of dislocation density by MRI (Utah), in an effort to correlate solar cell parameters with defects. Table 1 shows dislocation densities provided by MRI. The table indicates there is no significant difference in dislocation count between the samples. See reference (3) for the details of Web process.

2.0 Solar Cell Performance and Characterization

Characteristics Under Illumination

Finished solar cells were tested under AM1 conditions at 28°C test block temperature. Individual cell parameters are given in Appendix VI and the results are summarized in Table 2. As expected, no significant difference in various parameters is shown. The average efficiency of about 12.8% is a slightly lower value than that of the Cz control cells of the same resistivity, mainly due to lower Jsc.

Spectral Response

Absolute spectral response (A/W) was obtained using a filter wheel set-up. The result of a typical web cell with a control cell for comparison is in Figure 24. The lower long wavelength response of the web cell indicates lower minority carrier diffusion length.

Minority Carrier Diffusion Length

Minority carrier diffusion length (L_D) was measured on finished solar cells using the short circuit current method. The results of the samples are listed in Table 3 and they are quite uniform. The whole range of variation was between 58 and

65um which could be within the experimental error. This does agree well with the MRI data in terms of defect counts.

TABLE 1

ANALYSIS OF WESTINGHOUSE SAMPLES

JPL SAMPLE #	NO. OF DISLOCATIONS PITS/FIELD	NO. OF DISLOCATIONS PITS/um^2
J250-4.7-A	17.808	2.737×10^{-4}
J250-4.7-B	14.946	2.298×10^{-4}
J250-4.7-C	12.146	1.867×10^{-4}
J250-4.7-D	16.614	2.554×10^{-4}
J250-4.7-E	15.526	2.387×10^{-4}
J250-4.7-F	15.800	2.429×10^{-4}
J250-4.7-K_1	15.828	2.433×10^{-4}
J250-4.7-K_2	16.615	2.554×10^{-4}
J250-4.7-L_1	37.424	5.753×10^{-4}
J250-4.7-L_2	27.082	3.702×10^{-4}

TABLE 2

SUMMARY OF THE PRE-CHARACTERIZED WEB WAFERS

	Voc (mV)	Jsc (mA/cm^2)	CFF (%)	(%)
AVERAGE	534	26.3	77	10.8
STANDARD DEVIATION	1	.1	1	.2
RANGE	532-534	26.2-26.5	76-78	10.6-10.8

TABLE 3

MINORITY DIFFUSION LENGTHS OF THE PRE-CHARACTERIZED WEB CELLS

SAMPLE I.D.	L_D(um)
C	65
T2	62
F	58
K-1	62
K-2	63
L	62
Control #11	121

FIGURE 24

SPECTRAL RESPONSE OF THE BASELINE CELLS FROM A TYPICAL WEB CELL

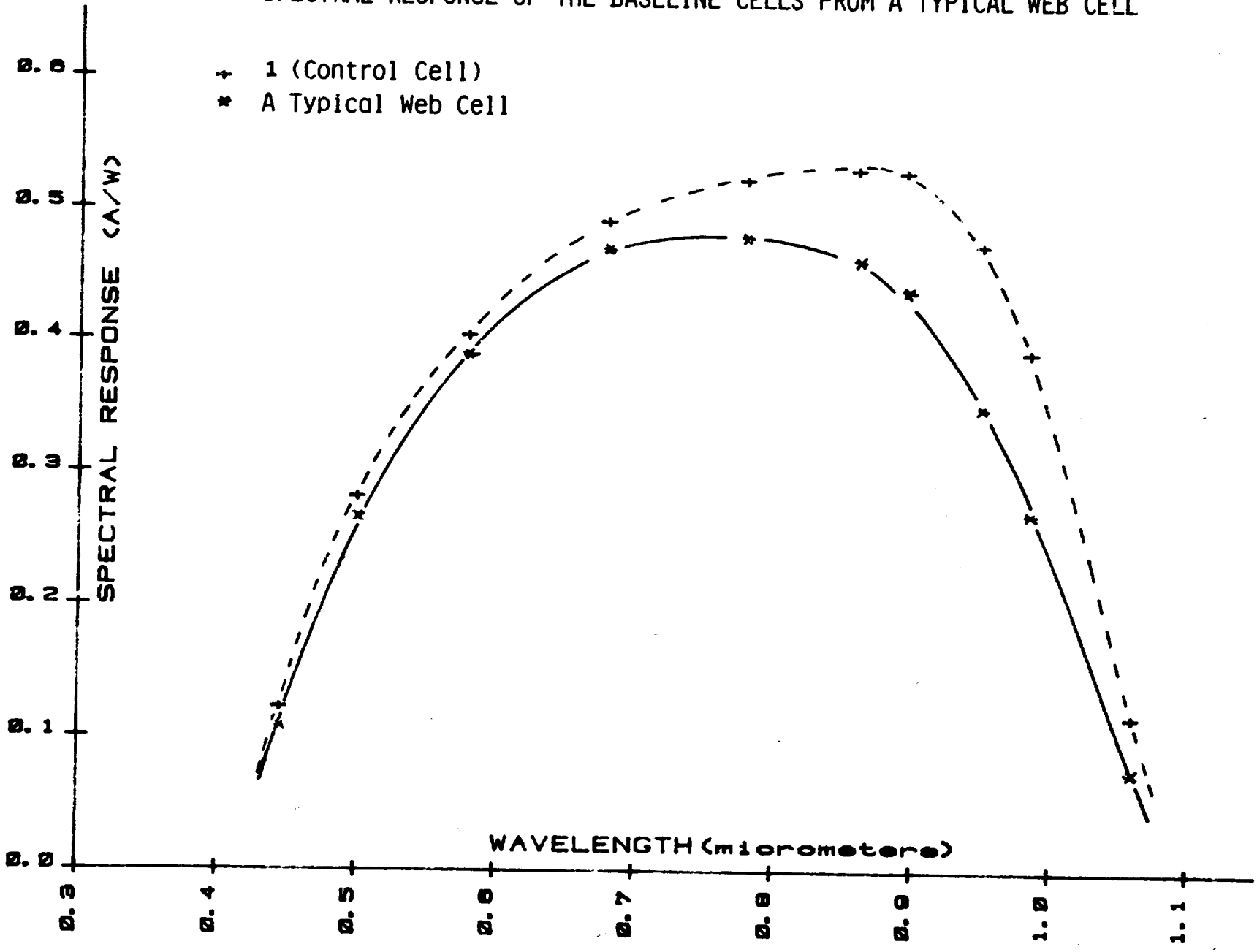

III. CONCLUSIONS AND RECOMMENDATIONS

The following conclusions and recommendations were reached after processing and evaluation of the silicon sheets.

HEM

- Evaluation of the ingot #41-41C indicated that the cell performance was quite uniform throughout the ingot including the polycrystalline area. The overall efficiency of the usable area of the ingot was about 87% of the CZ control cells.

- Partial evaluation of the ingot #41-48 suggested the problems of in homogeneous performance. Junction shunting was major cause of the problem, which could be due to the particulate inclusions observed in the bulk.

Dendritic Web

- Performances of the baseline solar cells agree well with the dislocation counts analyzed by MRI, especially in terms of uniformity.

- Minority carrier diffusion length (L) of the webs was considerably lower than CZ control, about 60um versus 120um. .

  NOTE: Dislocation density $10^5/cm^2$ is not expected to reduce minority carrier lifetime significantly. Further work is required to find the cause of the low L.

IV. WORK PLAN STATUS

The following silicon sheets are expected for processing and evaluation during the next period.

- o Large cast ingots by HEM (Crystal Systems).
- o Wafers from cast ingot by UCP (SEMIX).

V. REFERENCES

1. Yoo et.al., "Silicon Solar Cell Process Development, Fabrication, and Analysis". JPL Contract No. 955089. First Annual Report, June 1979.

2. F. Schmid, et.al., "Silicon Ingot Casting - Heat Exchanger Method, Multi-Wire Slicing - Fixed Abrasive Slicing Technique". JPL Contract No. 954373, Technical Report, Crystal System.

3. C.S. Duncan, et.al., "Silicon Web Process". JPL Contract No. 954654, Technical Report, Westinghouse.

APPENDIX I

TIME SCHEDULE

TIME SCHEDULE

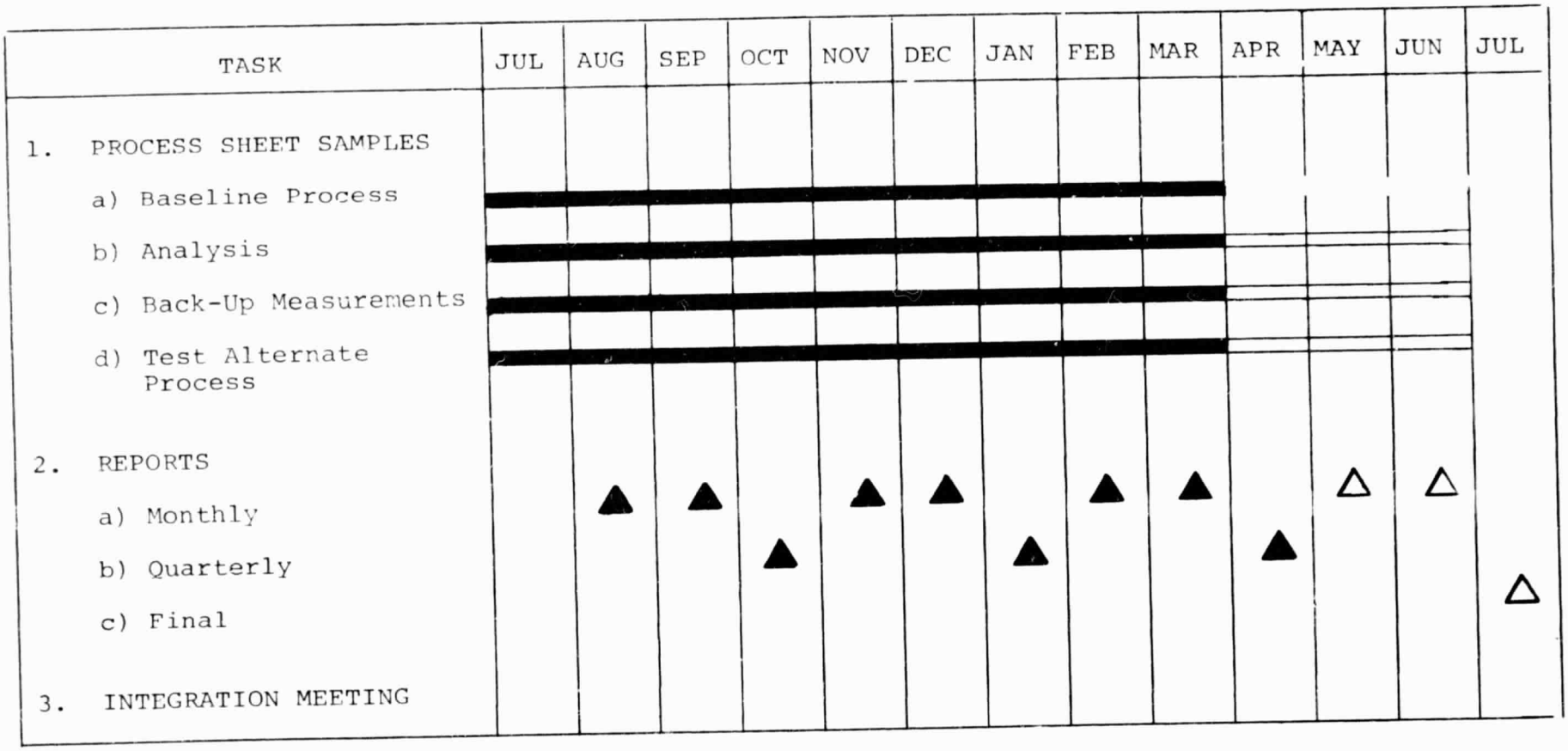

APPENDIX II

ABBREVIATION

V_{OC}:	Open Circuit Voltage
I_{SC}:	Short Circuit Current
J_{SC}:	Short Circuit Current Density
I_{SCR}:	Short Circuit Current (Red Response) at Wavelength Above ~.6um
I_{SCB}:	Short Circuit Current (Blue Response) at Wavelength Below ~.6um
CFF:	Curve Fill Factor
η :	Solar Cell Conversion Efficiency
L:	Minority Carrier Diffusion Length (D.L.)
I_{MAX}:	Current at Maximum Power Point
V_{MAX}:	Voltage at Maximum Power Point
BSF:	Back Surface Field
BSR:	Back Surface Reflector
V_B:	Bias Voltage
I_o:	Diode Saturation Current
HEM:	Heat Exchanger Method
EFG:	Edge Defined Film-Fed Growth
SOC:	Silicon on Ceramic
RTR:	Ribbon-to-Ribbon
SPV:	Surface Photovoltage
MLAR:	Multi-Layer Anti-Reflective
R_s:	Series Resistance

APPENDIX III

MAPPING OF SOLAR CELL PARAMETERS

FROM VERTICALLY CUT HEM (41-41C) LAYERS

A MAPPING OF Voc (mV) FOR A CENTER LAYER OF VERTICALLY CUT HEM (41-41C)

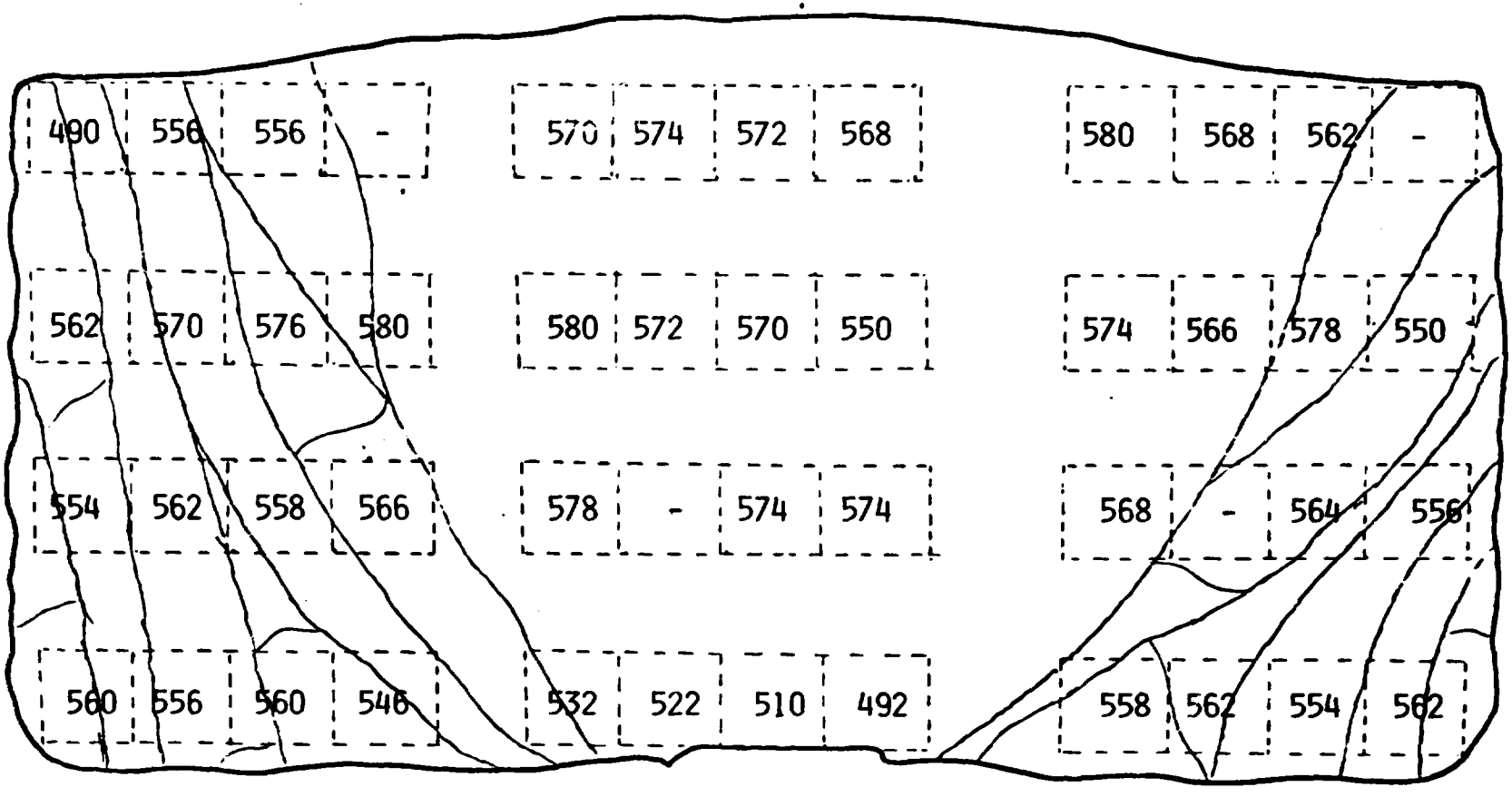

AVERAGE: 559

CONTROL AVE: 577

A MAPPING OF Jsc (mA/cm^2) FOR CENTER LAYER VERTICALLY CUT HEM (41-41C)

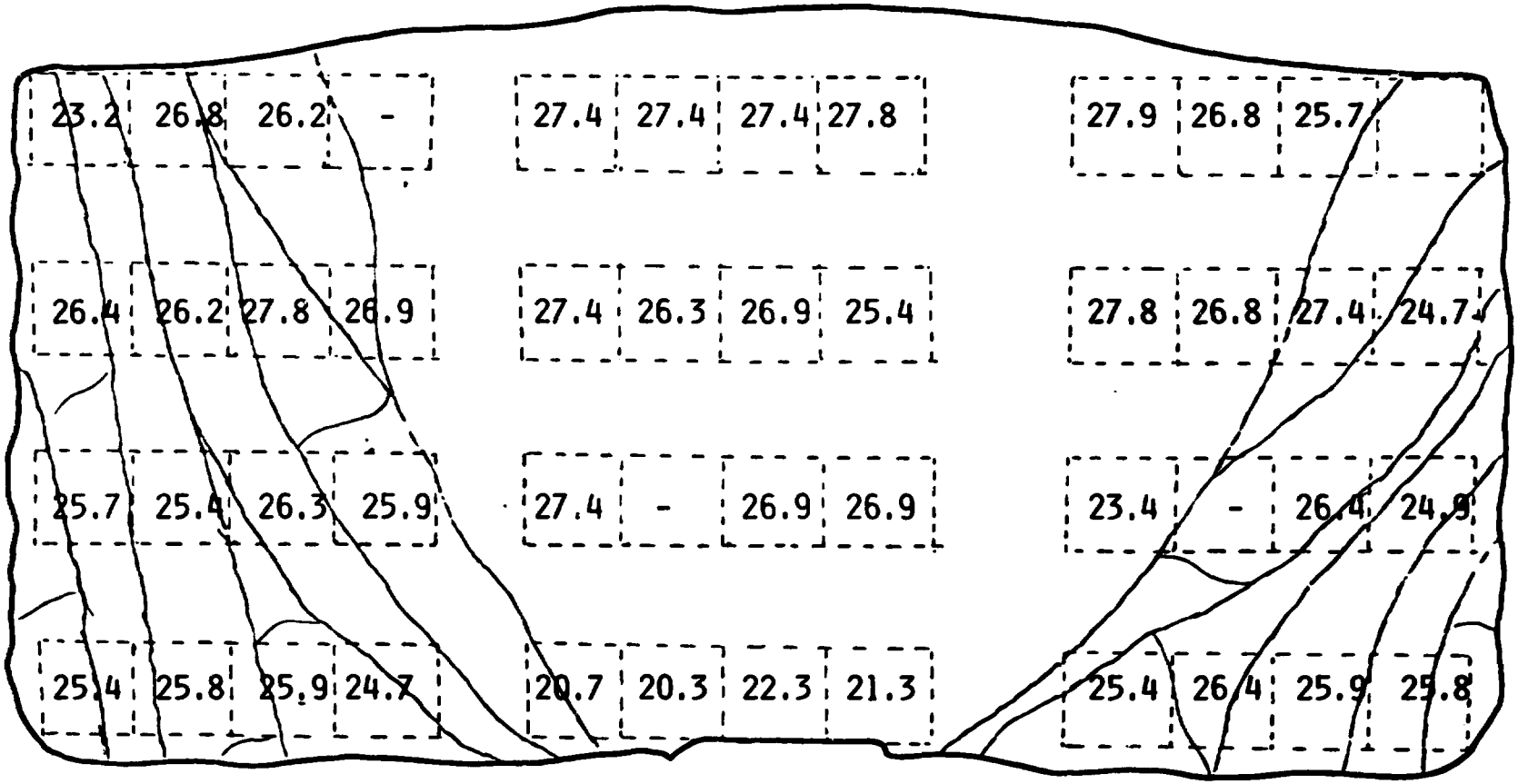

AVE. 25.8

CONTROL AVE. 27.3

A MAPPING OF CFF (%) FOR A CENTER LAYER OF VERTICALLY CUT HEM (41-41C)

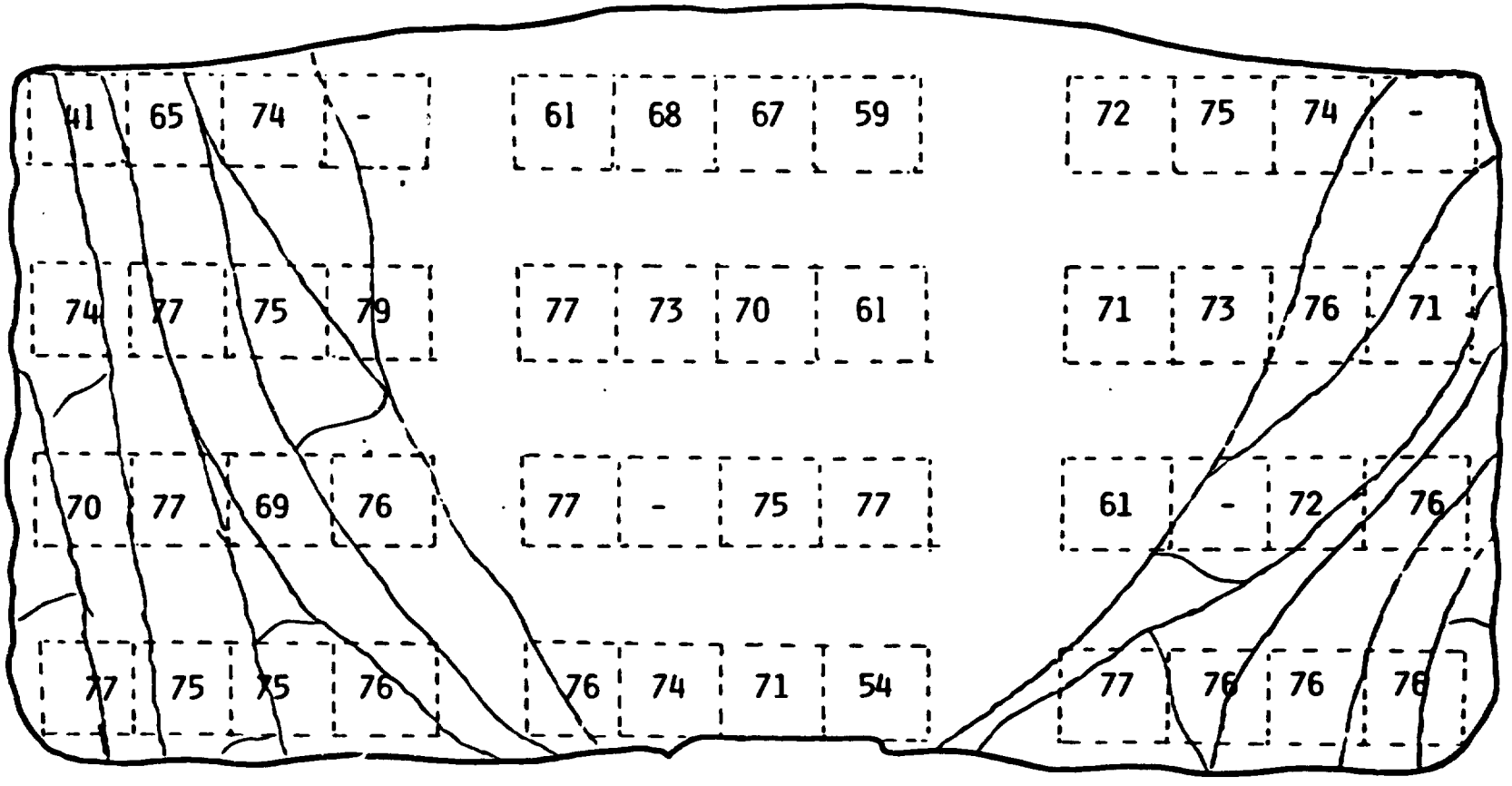

AVE.: 72% (93%)

CONTROL AVE.: 76%

A MAPPING OF η (%) FOR A CENTER LAYER OF VERTICALLY CUT HEM (41-41C)

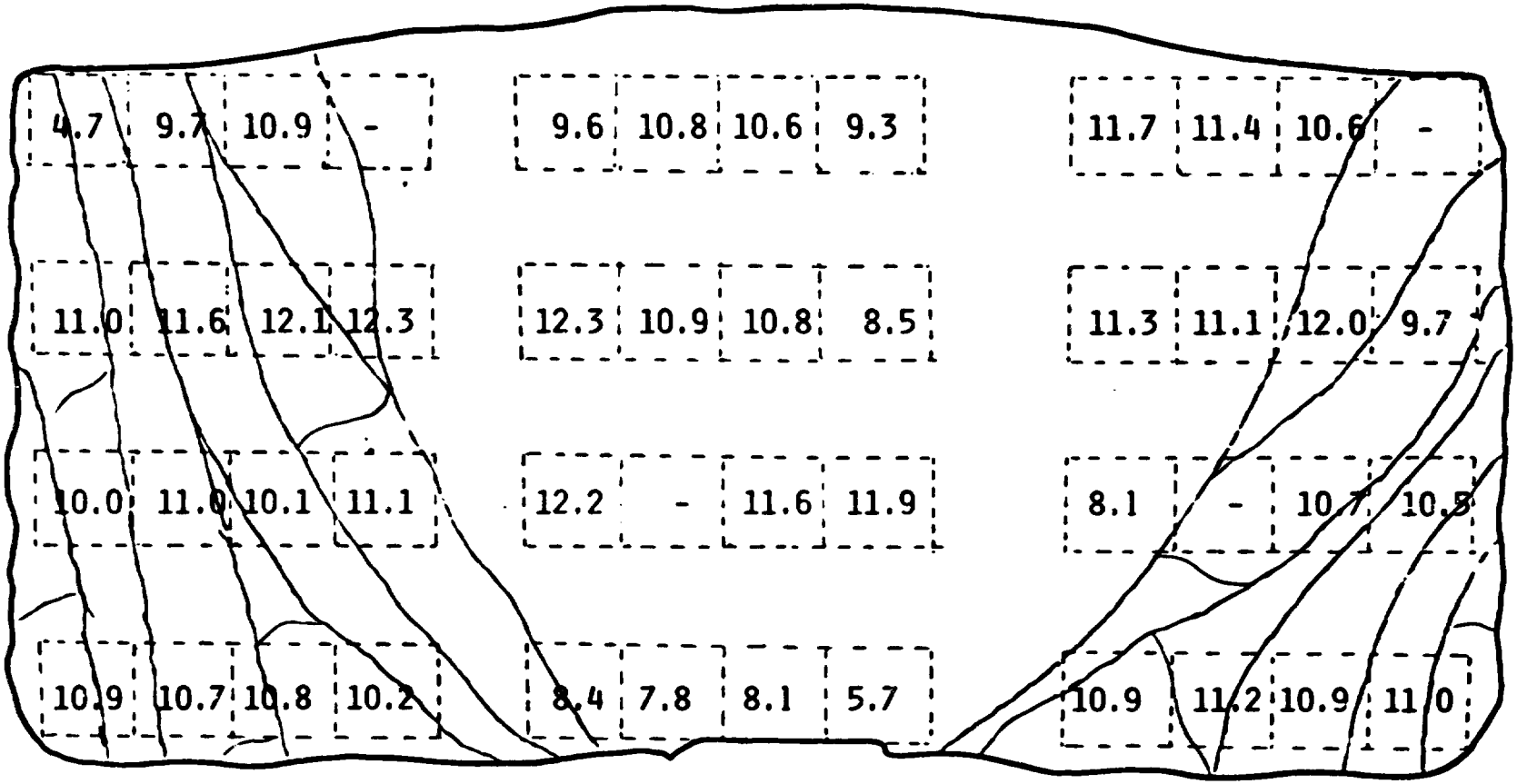

AVE.: 10.4%
CONTROL AVE: 12.2%

A MAPPING OF Voc (mV) FOR A QUARTER LAYER VERTICALLY CUT HEM (41-41C)

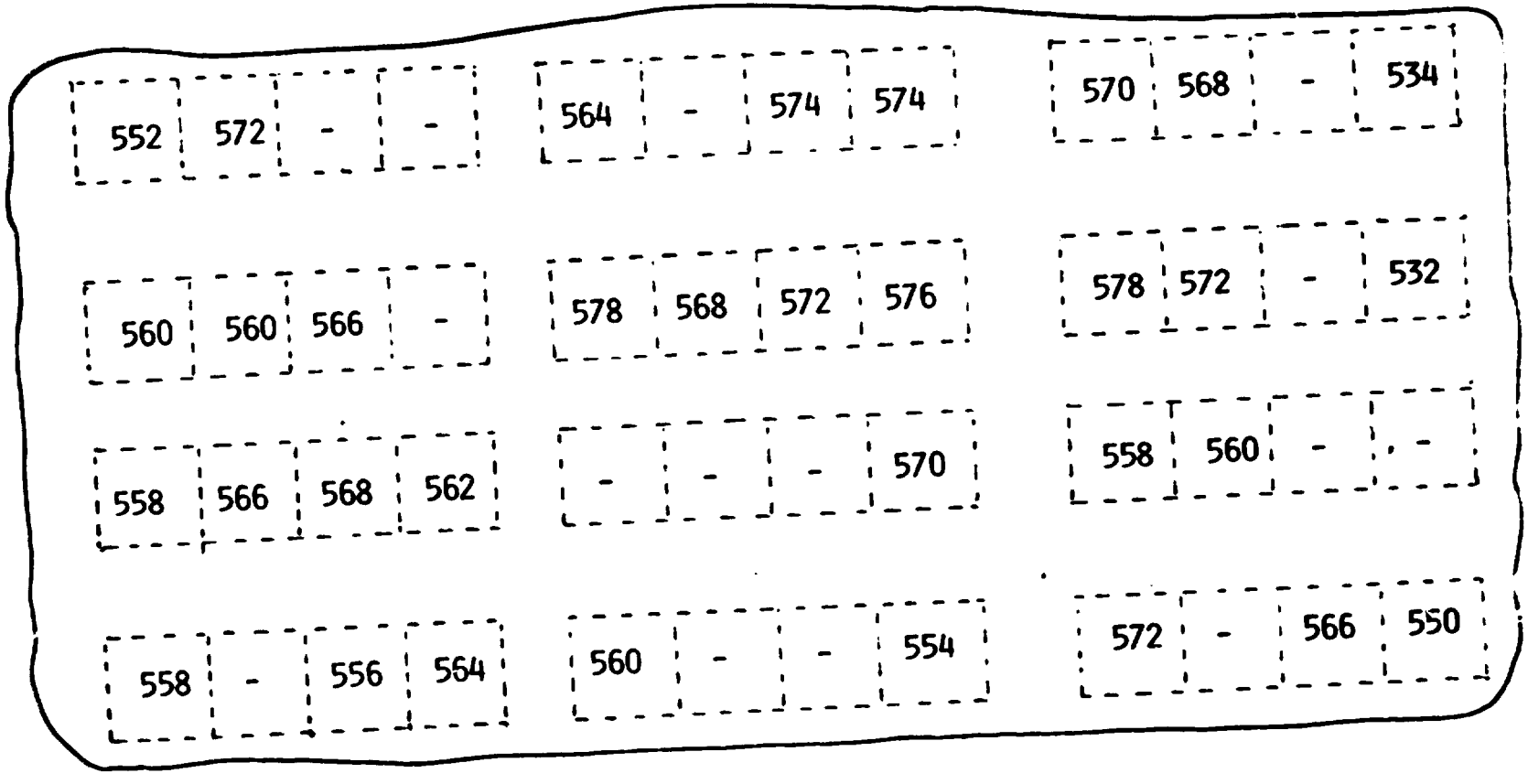

AVE. 563
CONTROL AVG. 572

A MAPPING OF Jsc (mA/cm^2) FOR A QUARTER LAYER OF VERTICALLY CUT HEM (41-41C)

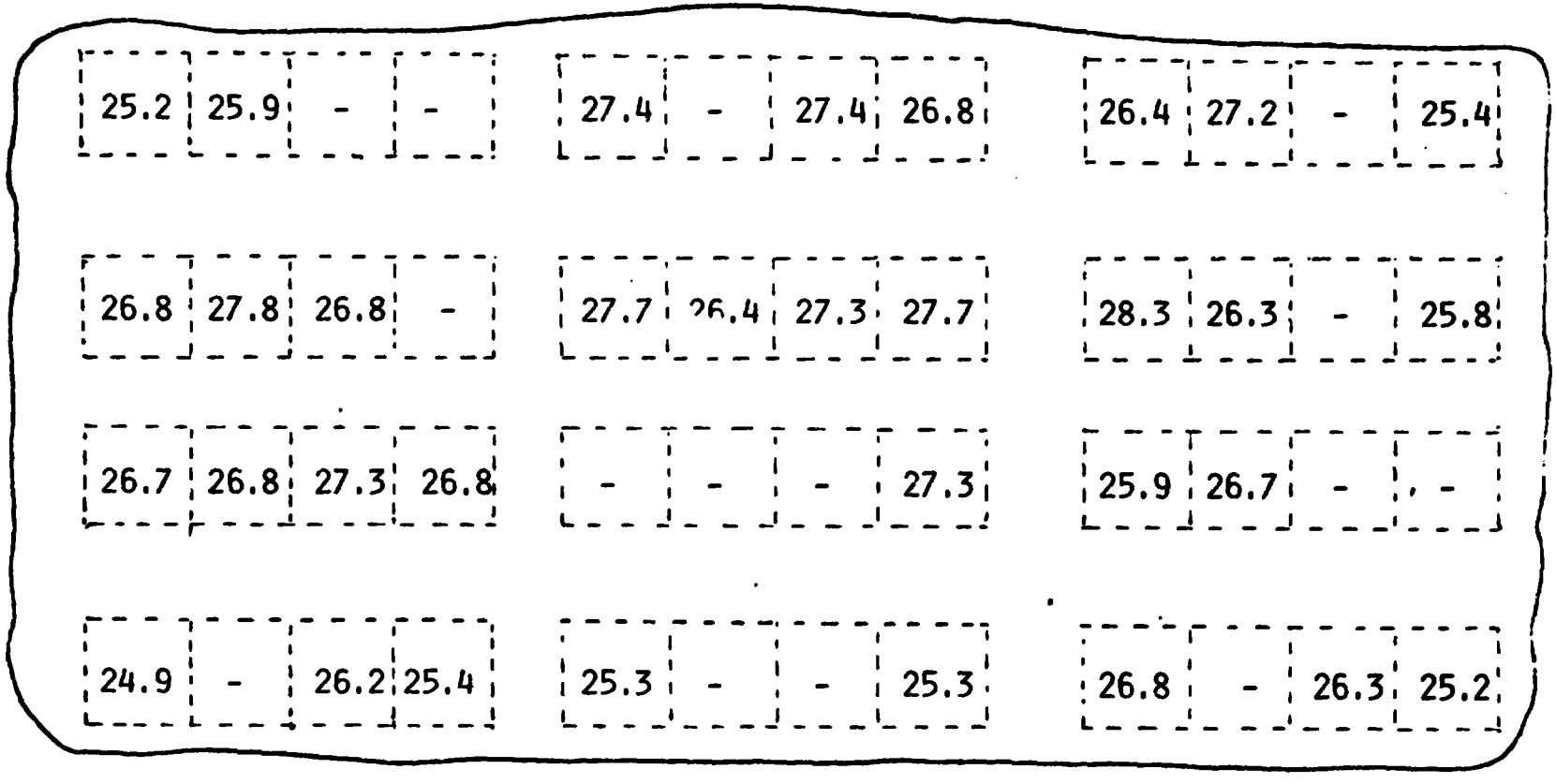

AVE: 26.4

CONTROL AVE: 28.6

A MAPPING OF CFF (%) FOR A QUARTER LAYER OF VERTICALLY CUT HEM(41-41C)

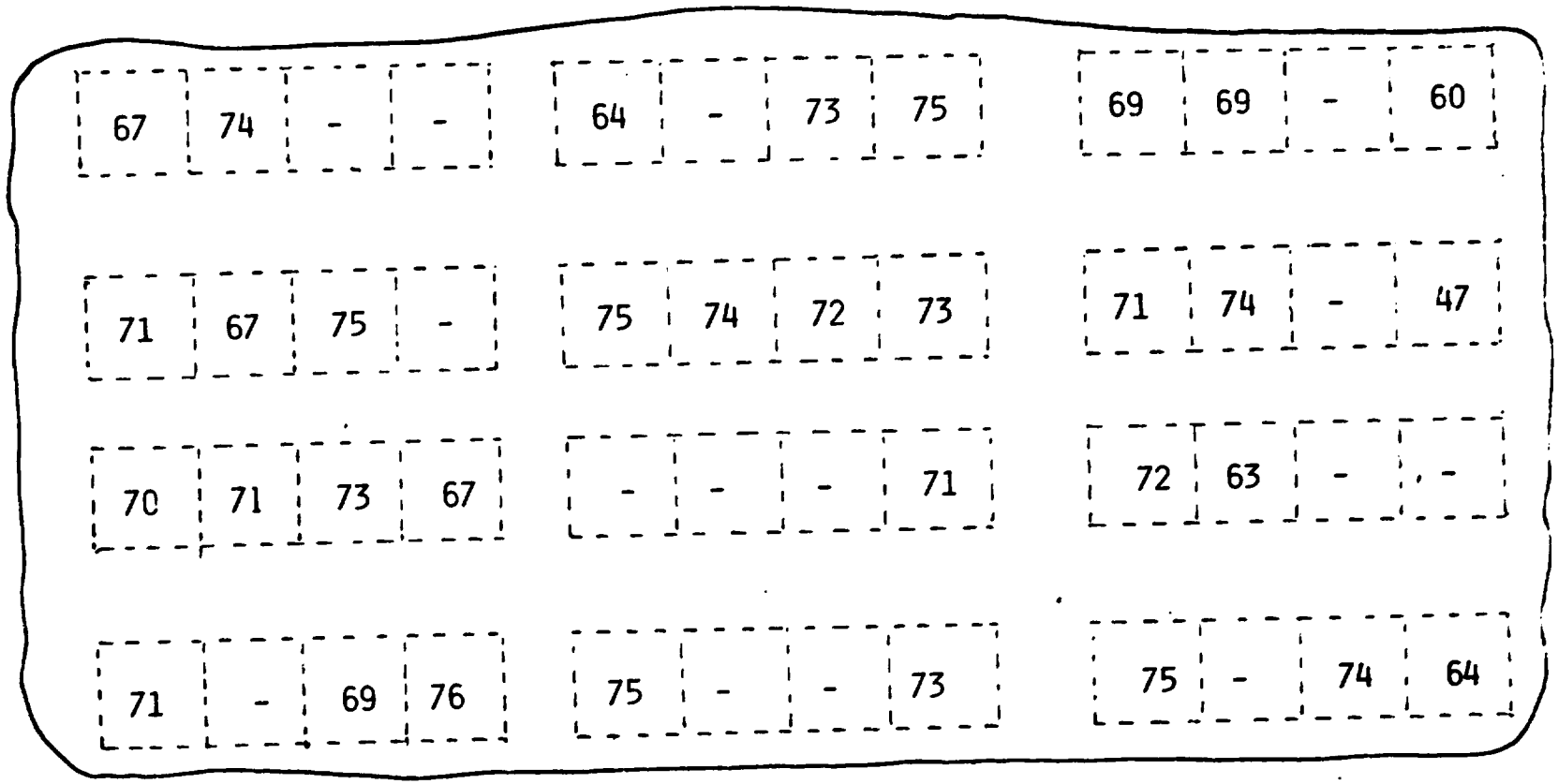

AVE. : 70.1

CONTROL AVE. 71

A MAPPING OF η (%) FOR A QUARTER LAYER OF VERTICALLY CUT HEM (41-41C)

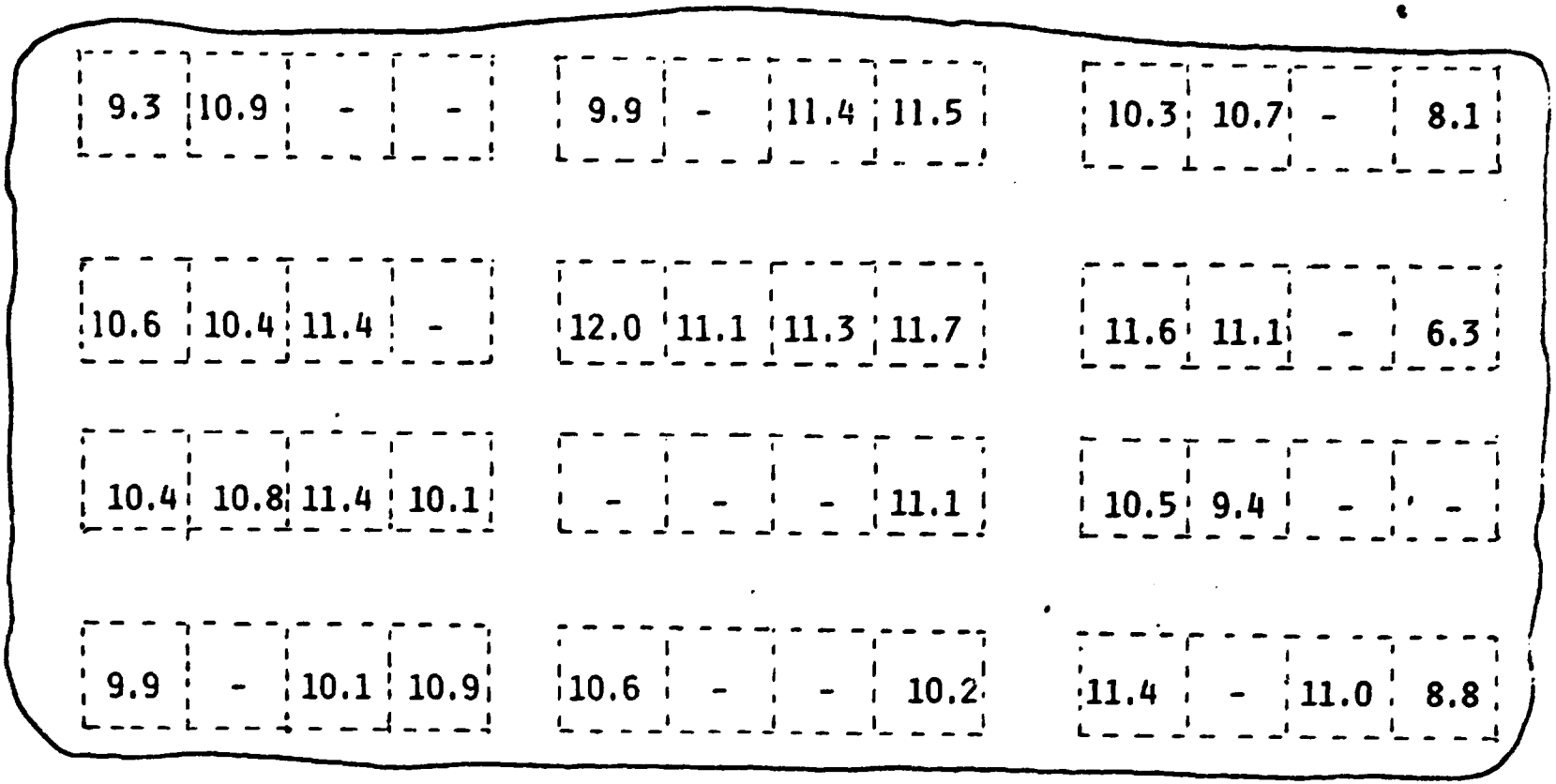

AVE: 10.5
CONTROL AVE: 11.6

A MAPPING OF Voc (mV) FOR A EDGE LAYER OF VERTICALLY CUT HEM (41-41C)

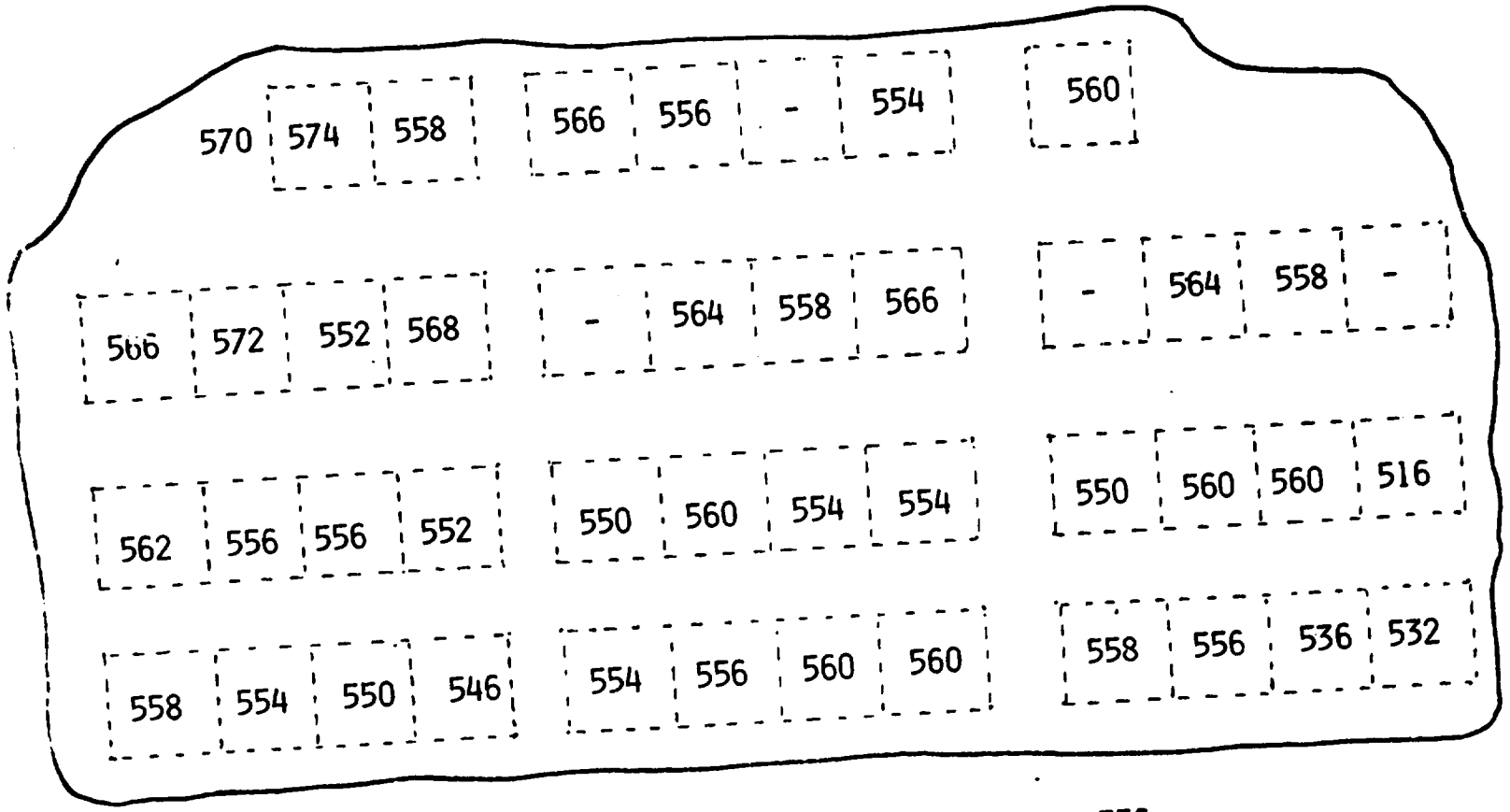

AVE. 556
CONTROL AVE. 572

A MAPPING OF Jsc (mA/cm^2) FOR A EDGE LAYER OF VERTICALLY CUT HEM
(41 - 41C)

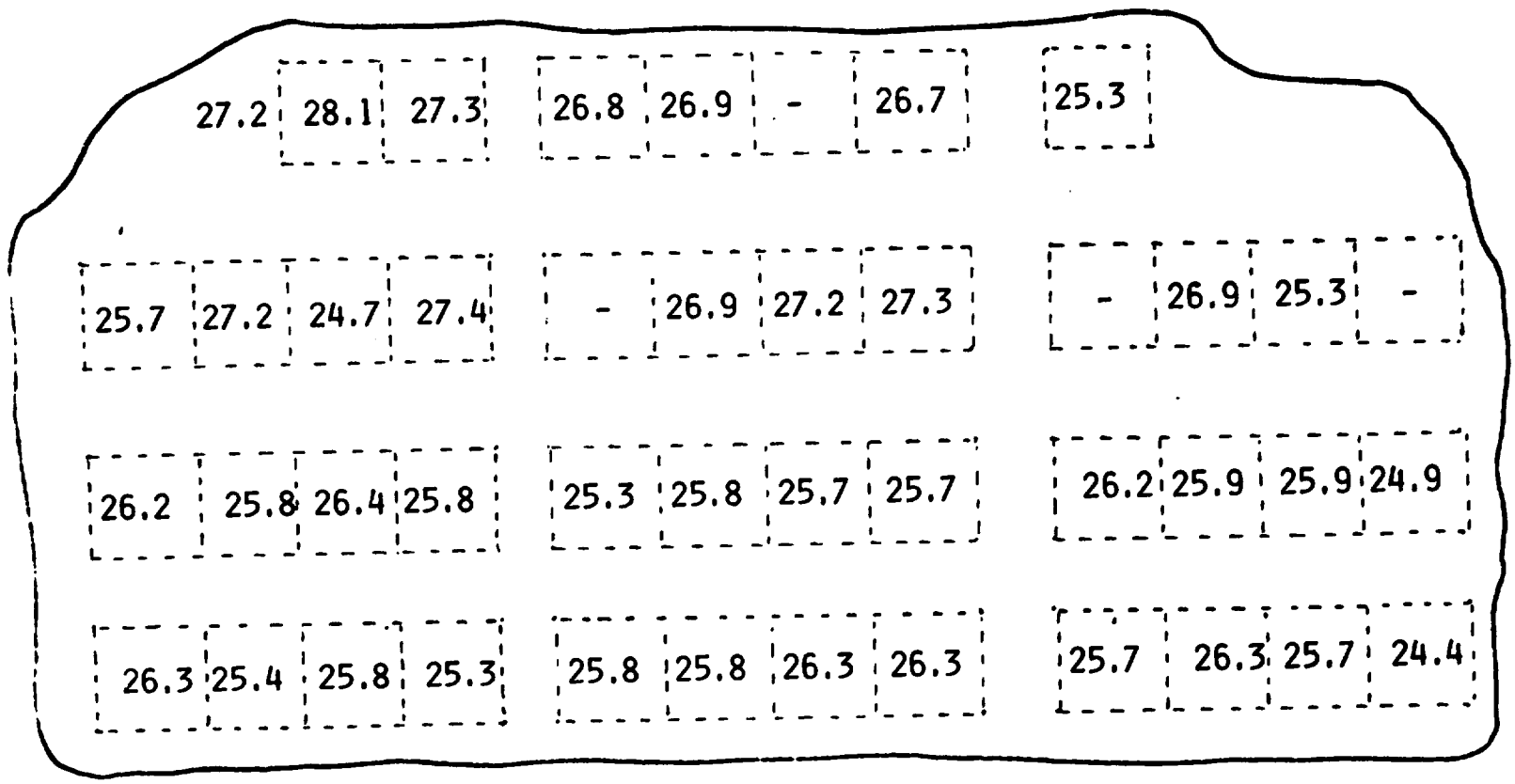

AVE.: 26.2
CONTROL AVE.: 28.6

A MAPPING OF CFF (%) FOR A EDGE LAYER OF VERTICALLY CUT HEM (41-41C)

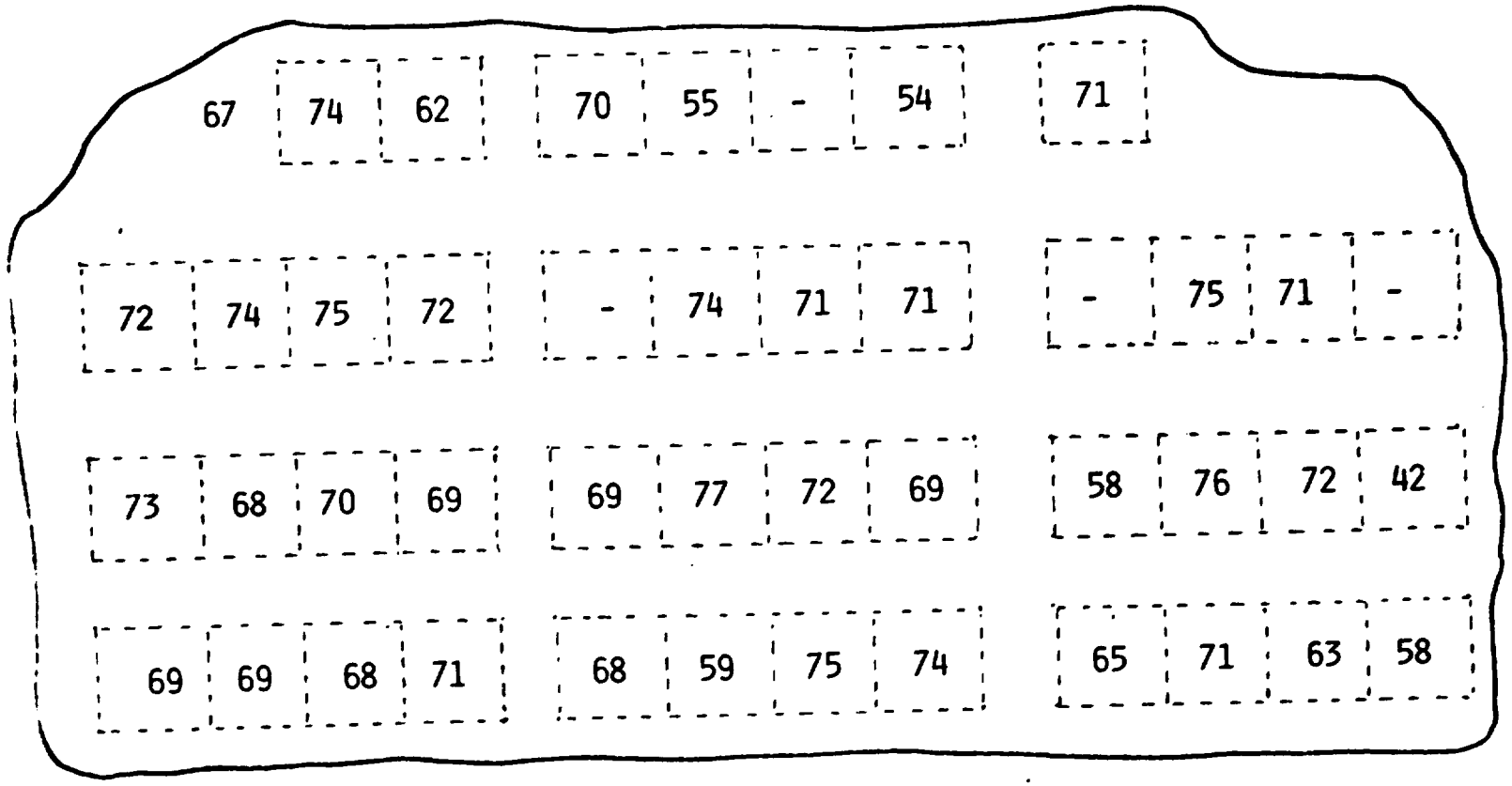

AVE. 68.3
CONTROL AVE. 71

A MAPPING OF η (%) FOR A EDGE LAYER OF VERTICALLY CUT HEM (41-41C)

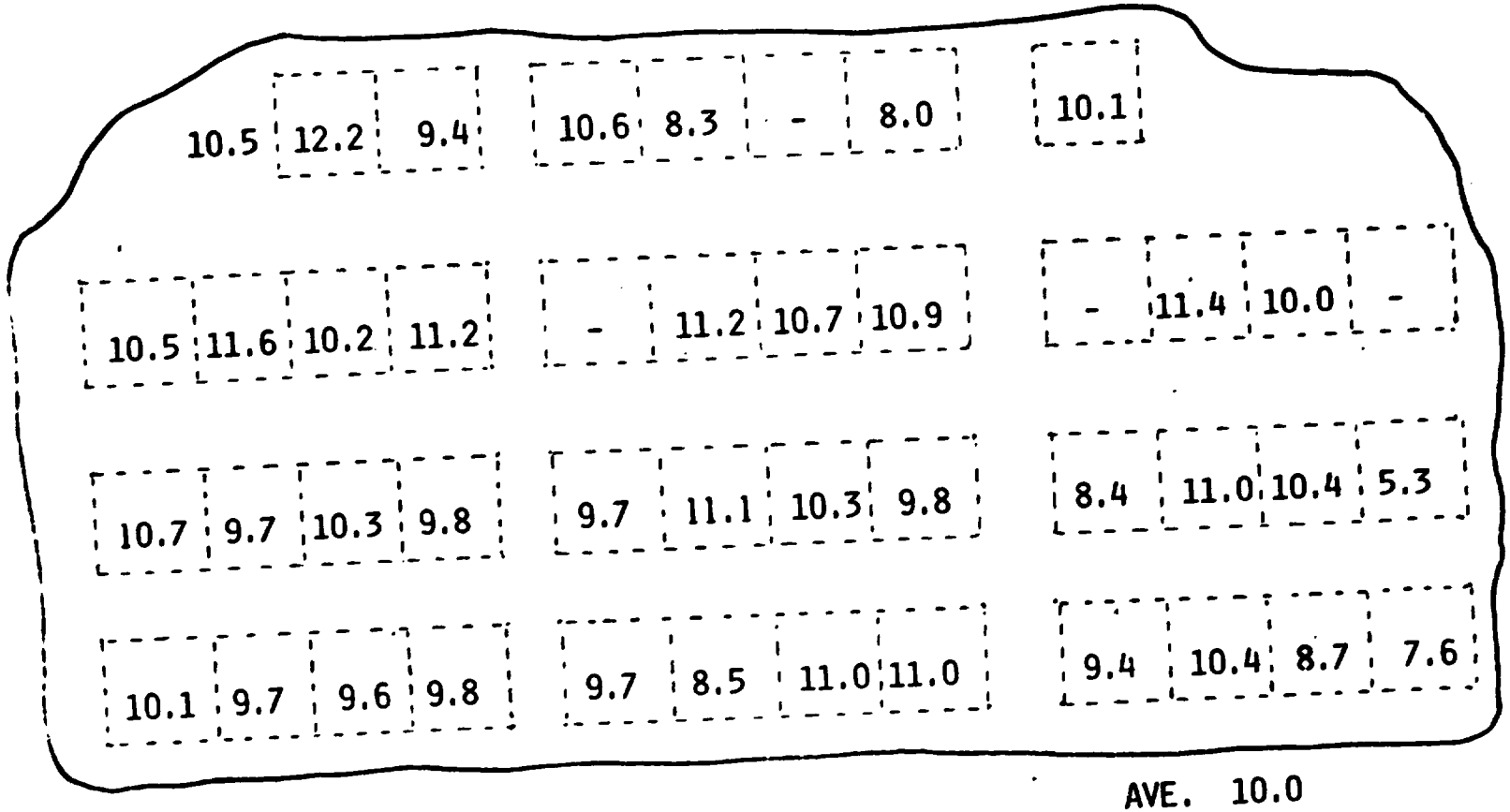

AVE. 10.0
CONTROL AVE. 11.6

APPENDIX IV

MAPPING OF SOLAR CELL PARAMETERS

FROM HORIZONTALLY CUT HEM (41-41C) LAYERS

A MAPPING OF Voc (mV) FOR THE TOP LAYER OF THE HORIZONTALLY CUT HEM (I.D. 41-41C)

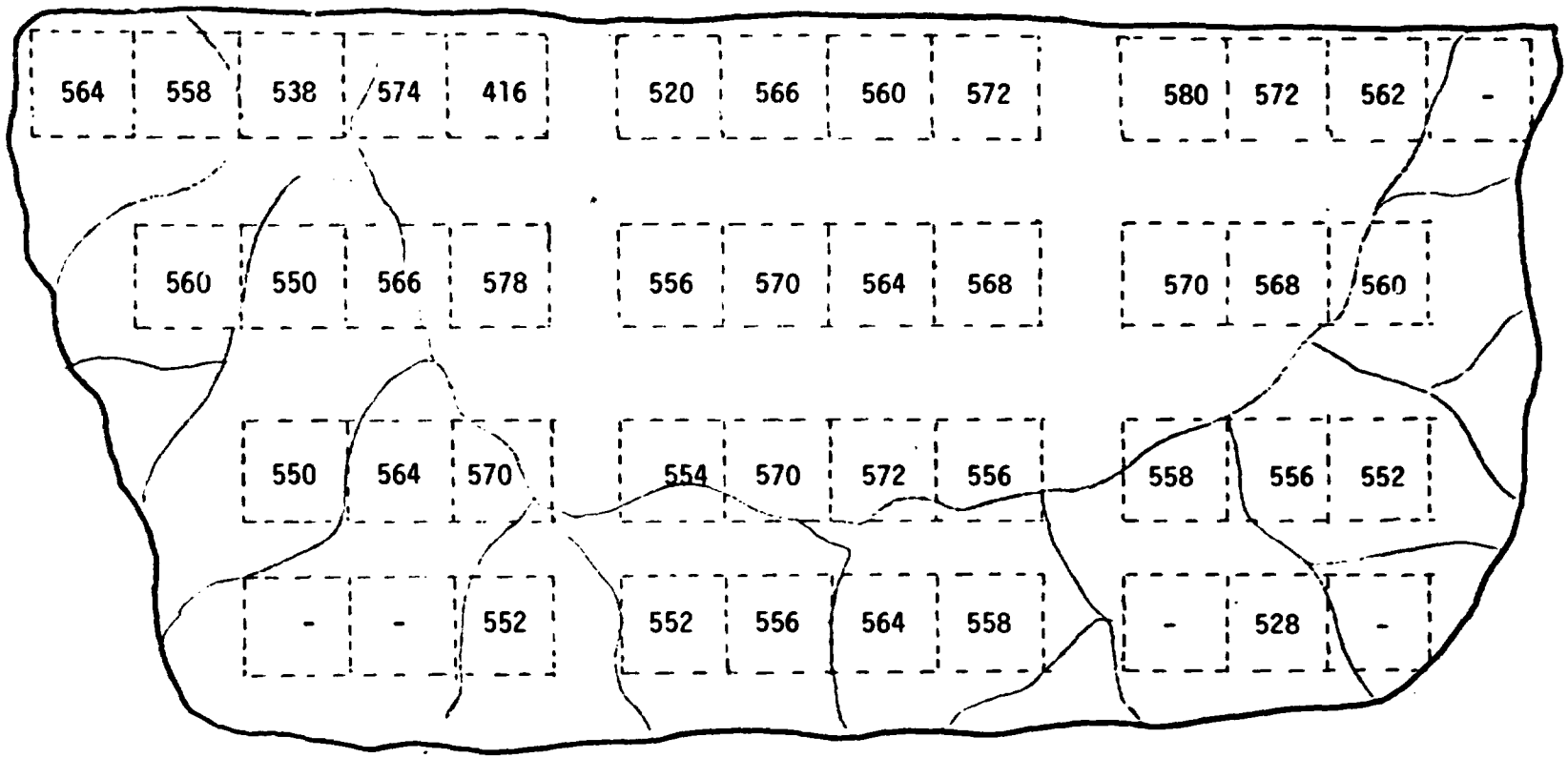

AVE. 557 mV

CONTROL AVE. 577 mV

A MAPPING OF Jsc (mA/cm^2) FOR THE TOP LAYER OF THE HORIZONTALLY CUT HEM (I.D.41-41C)

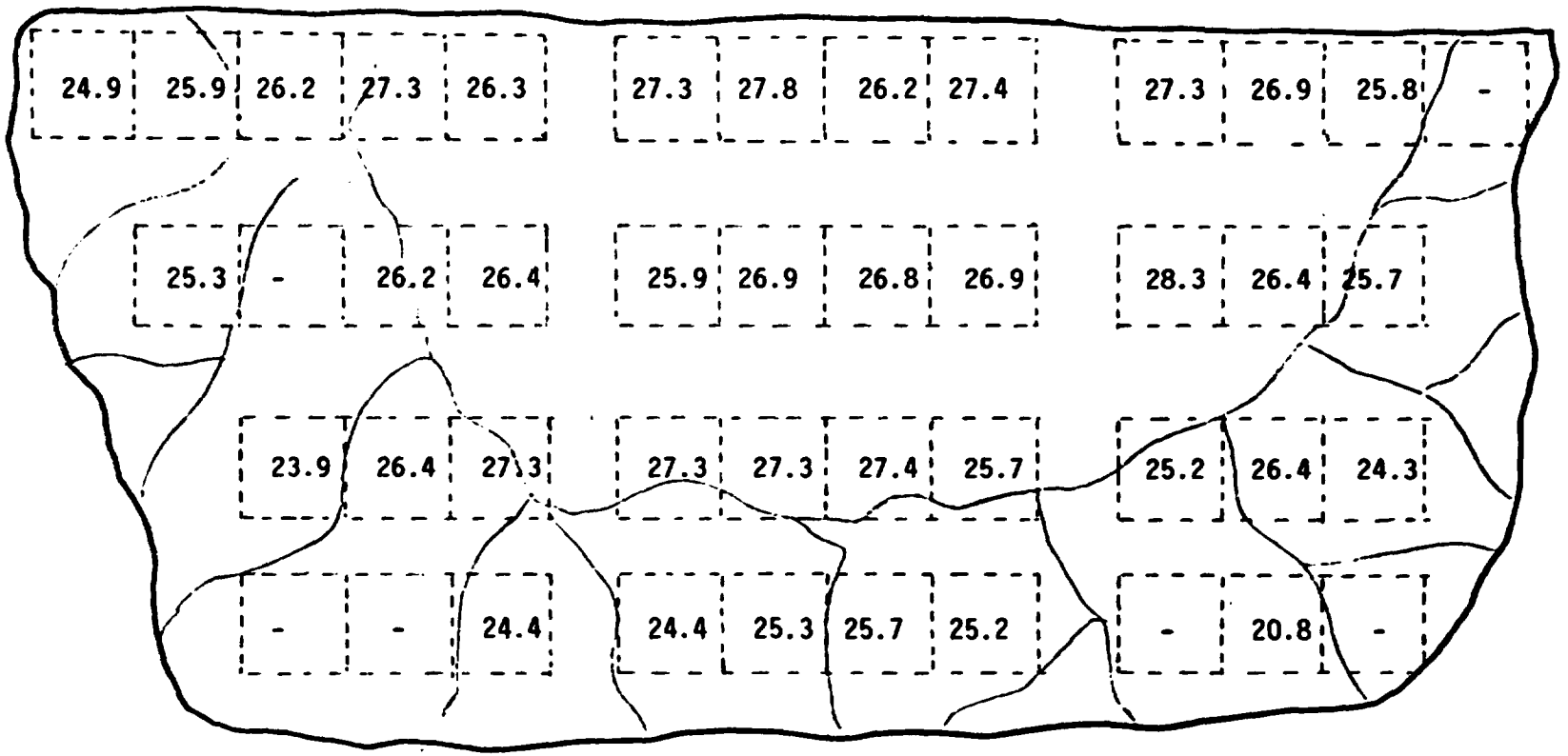

AVE. 26.1 mA/cm^2

CONTROL AVE. 28.2 mA/cm^2

A MAPPING OF CFF (%) FOR THE TOP LAYER OF THE HORIZONTALLY CUT HEM
(HEM I.D. 41-41C)

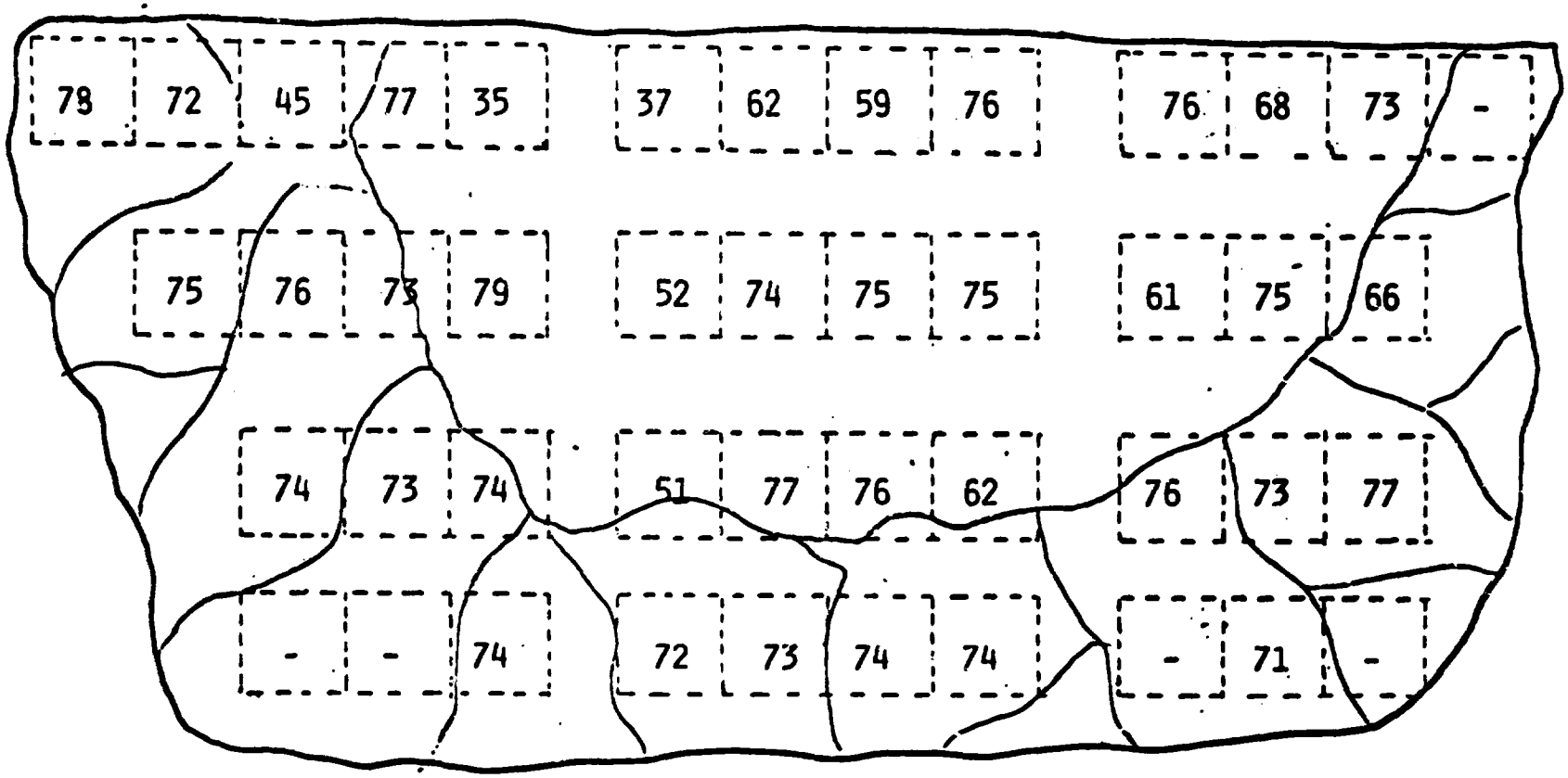

Ave 68%
Control Ave 76%

A MAPPING OF η (%AM1) FOR THE TOP LAYER OF THE HORIZONTALLY CUT HEM (I.D.41-41C)

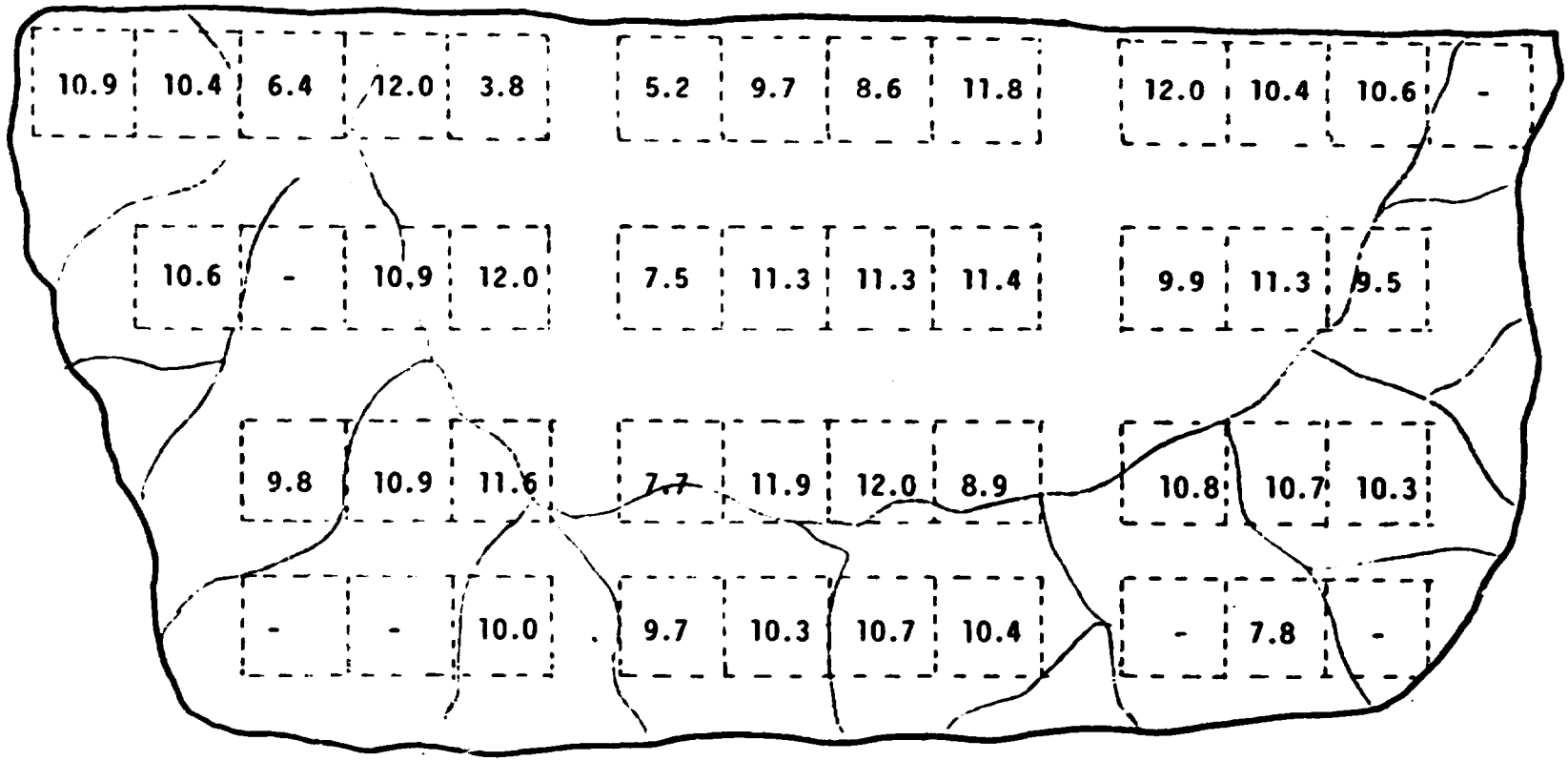

AVE. 10.0%

CONTROL AVE. 12.3

A MAPPING OF Voc (mV) FOR THE MIDDLE LAYER OF THE HORIZONTALLY CUT HEM (I.D.41-41C)

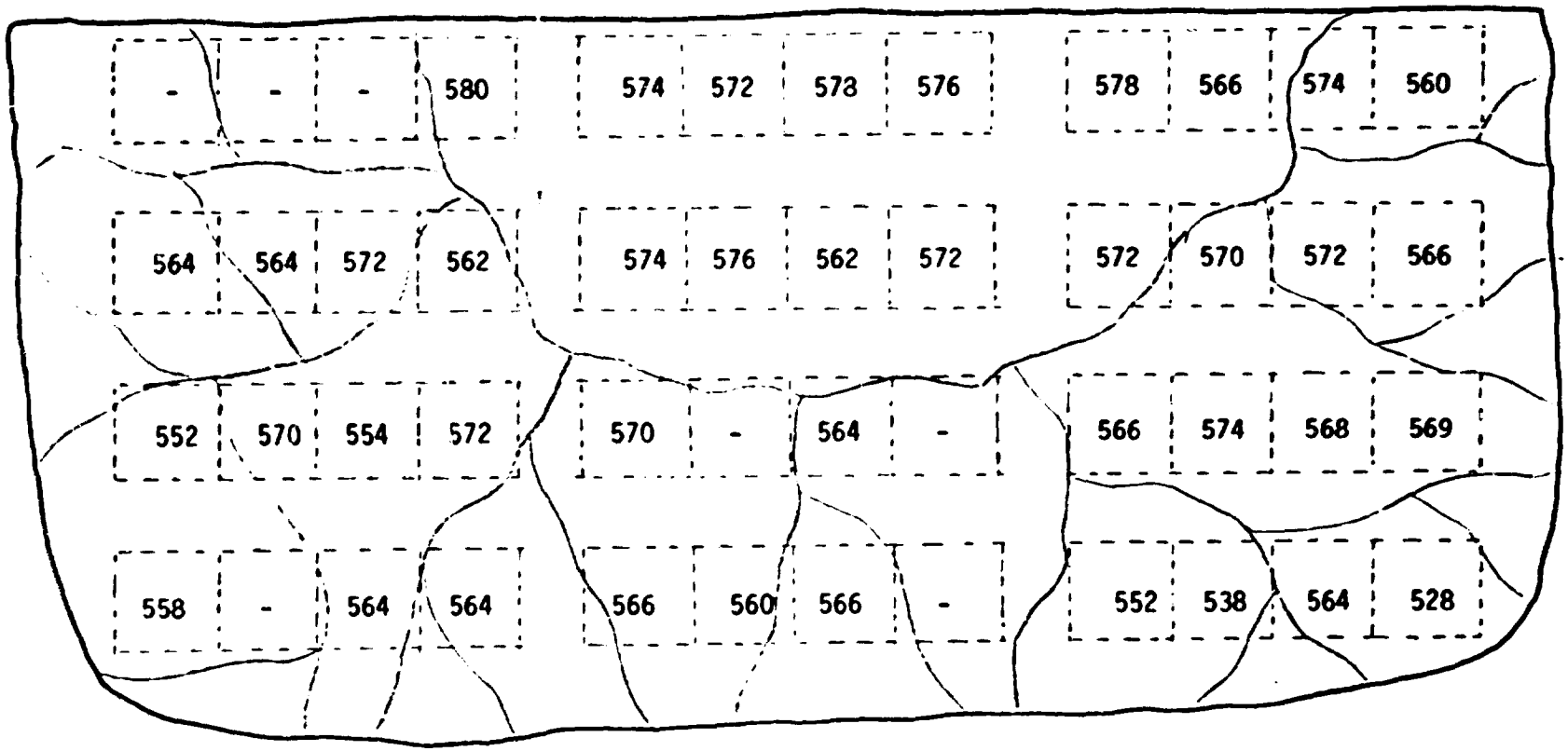

AVE. 556 mV

CONTROL AVE. 577 mV

A MAPPING OF Jsc (mA/cm^2) FOR THE MIDDLE LAYER OF THE HORIZONTALLY CUT HEM(I.D.41-41C)

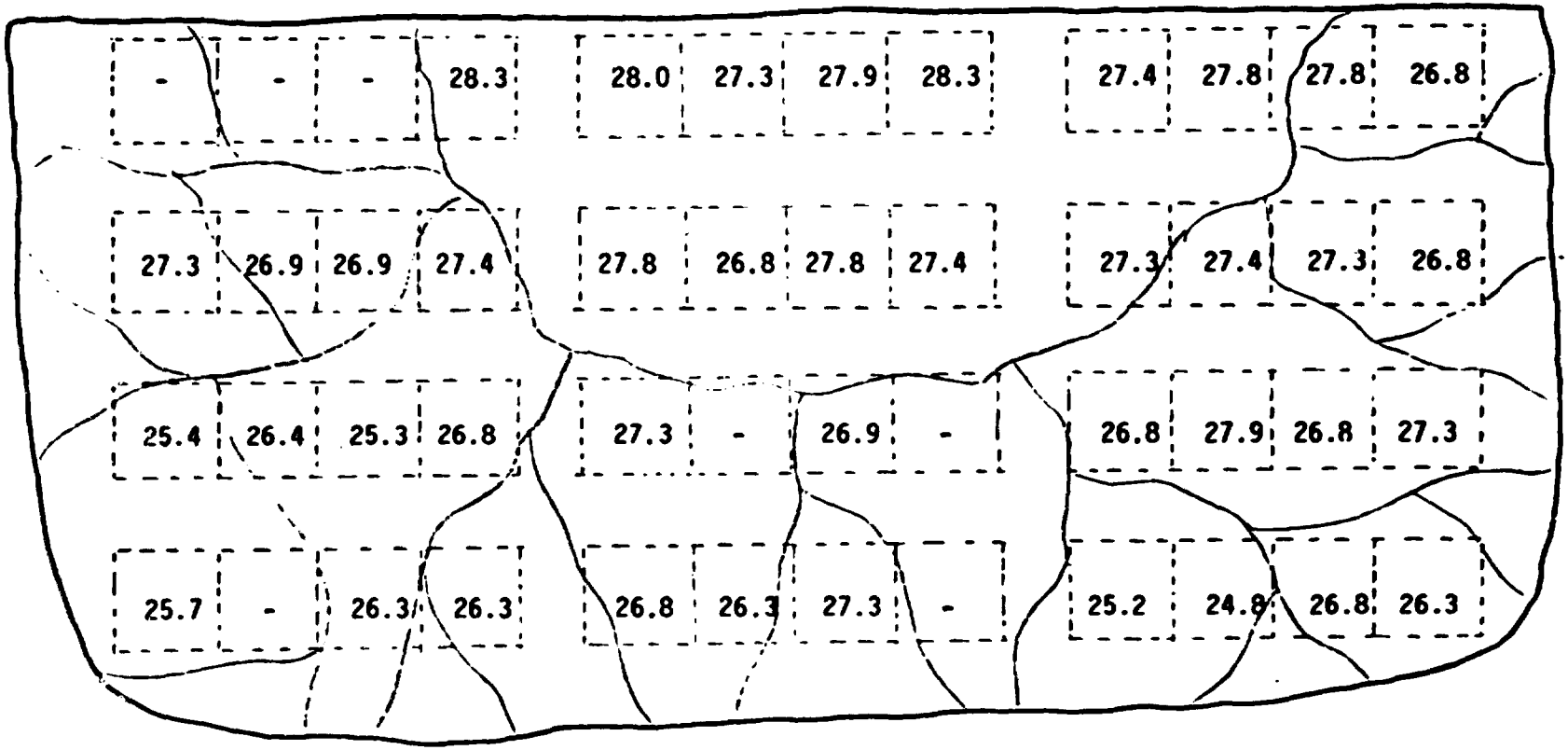

AVE. 27

CONTROL AVE. 28.2

A MAPPING OF CFF (%) FOR THE MIDDLE LAYER OF THE HORIZONTALLY CUT HEM (I.D.41-41C)

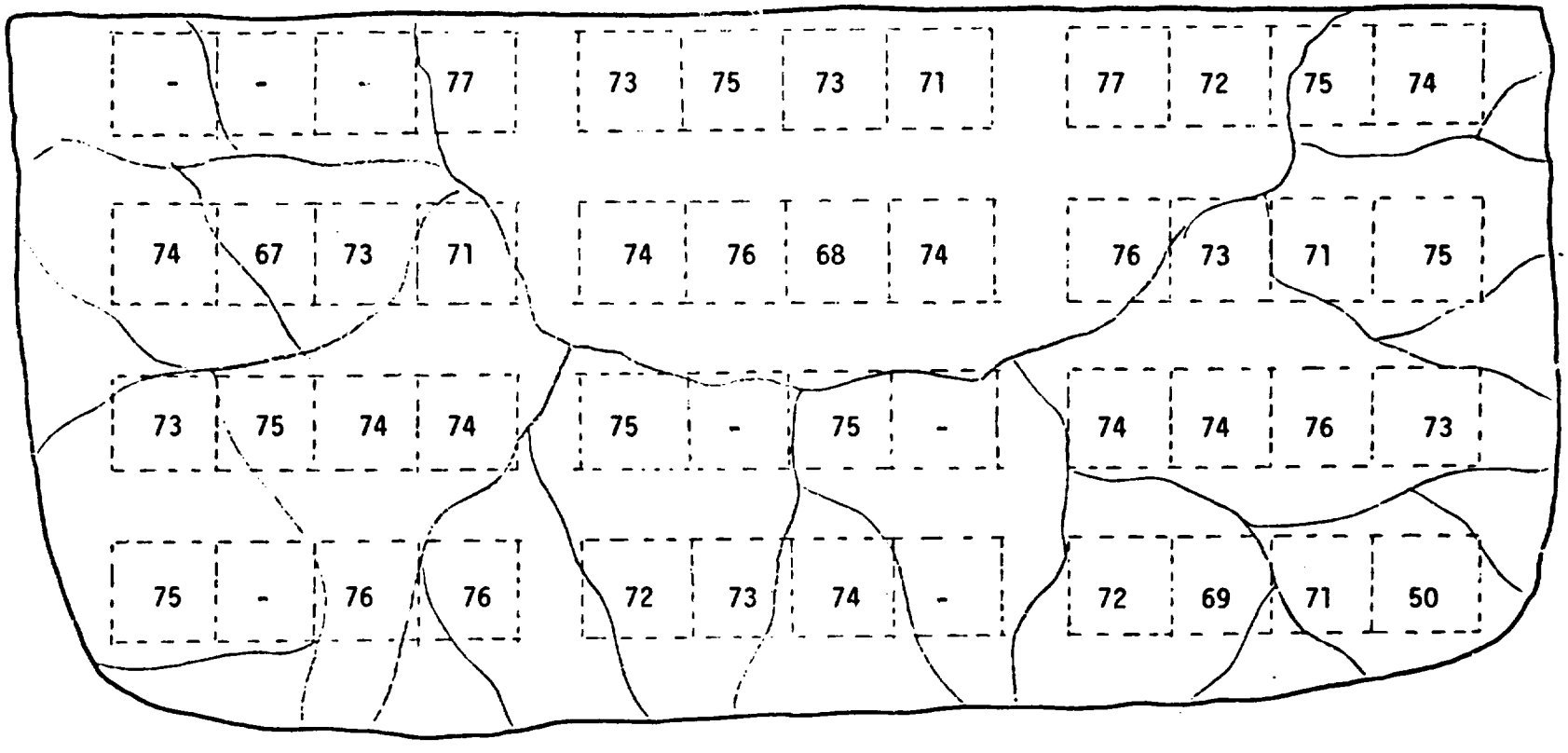

AVE. 73%

CONTROL AVE. 76%

A MAPPING OF η (% AM1) FOR THE MIDDLE LAYER OF THE HORIZONTALLY CUT HEM (I.D.41-41C)

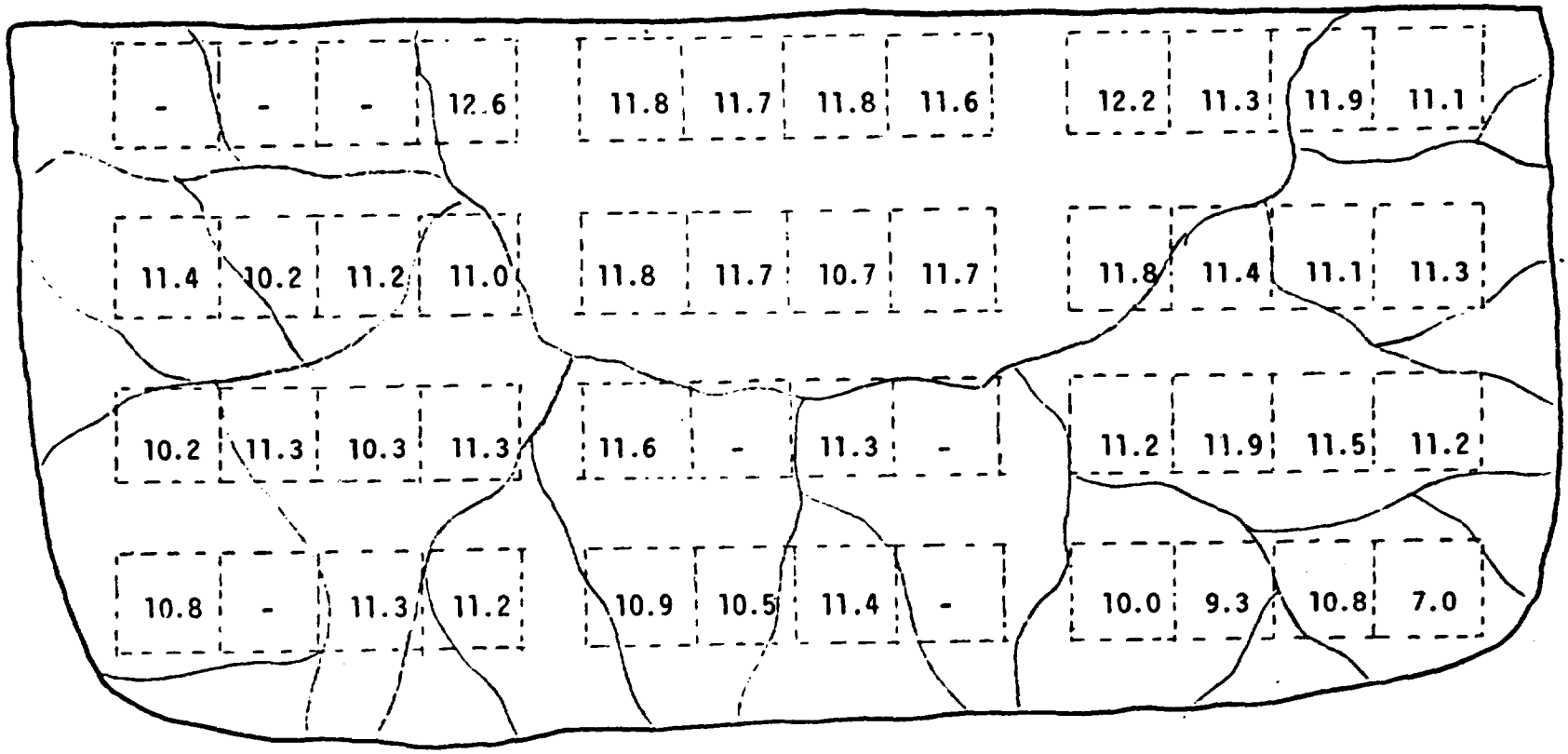

AVE. 11.1%

CONTROL AVE. 12.3%

A MAPPING OF Voc (mV) FOR THE BOTTOM LAYER OF THE HORIZONTALLY CUT HEM (I.D.41-41C)

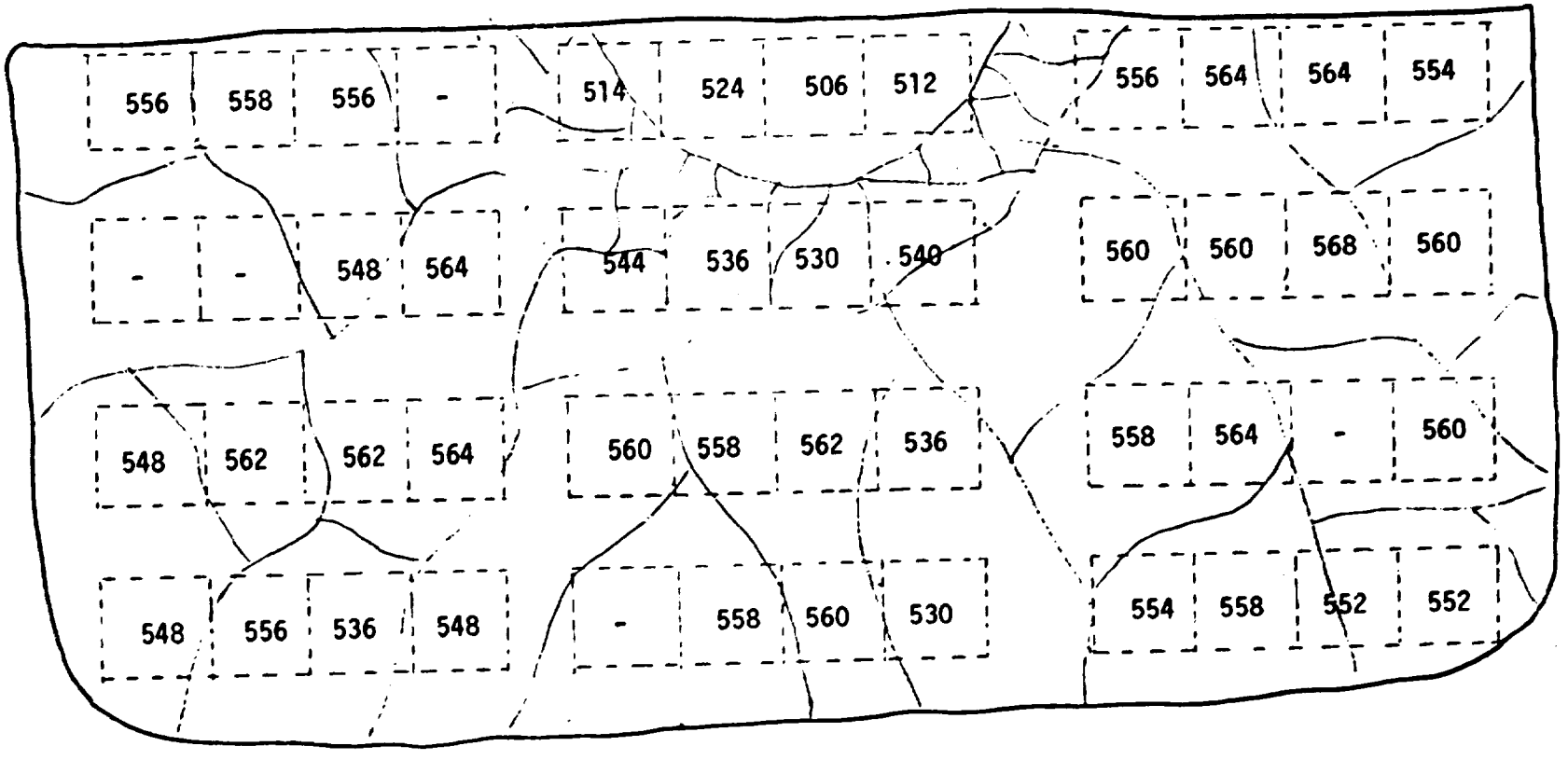

AVE. 550 mV

CONTROL AVE. 577 mV

A MAPPING OF Jsc (mA/cm^2) FOR THE BOTTOM LAYER OF THE HORIZONTALLY CUT HEM (HEM I.D.41-41C)

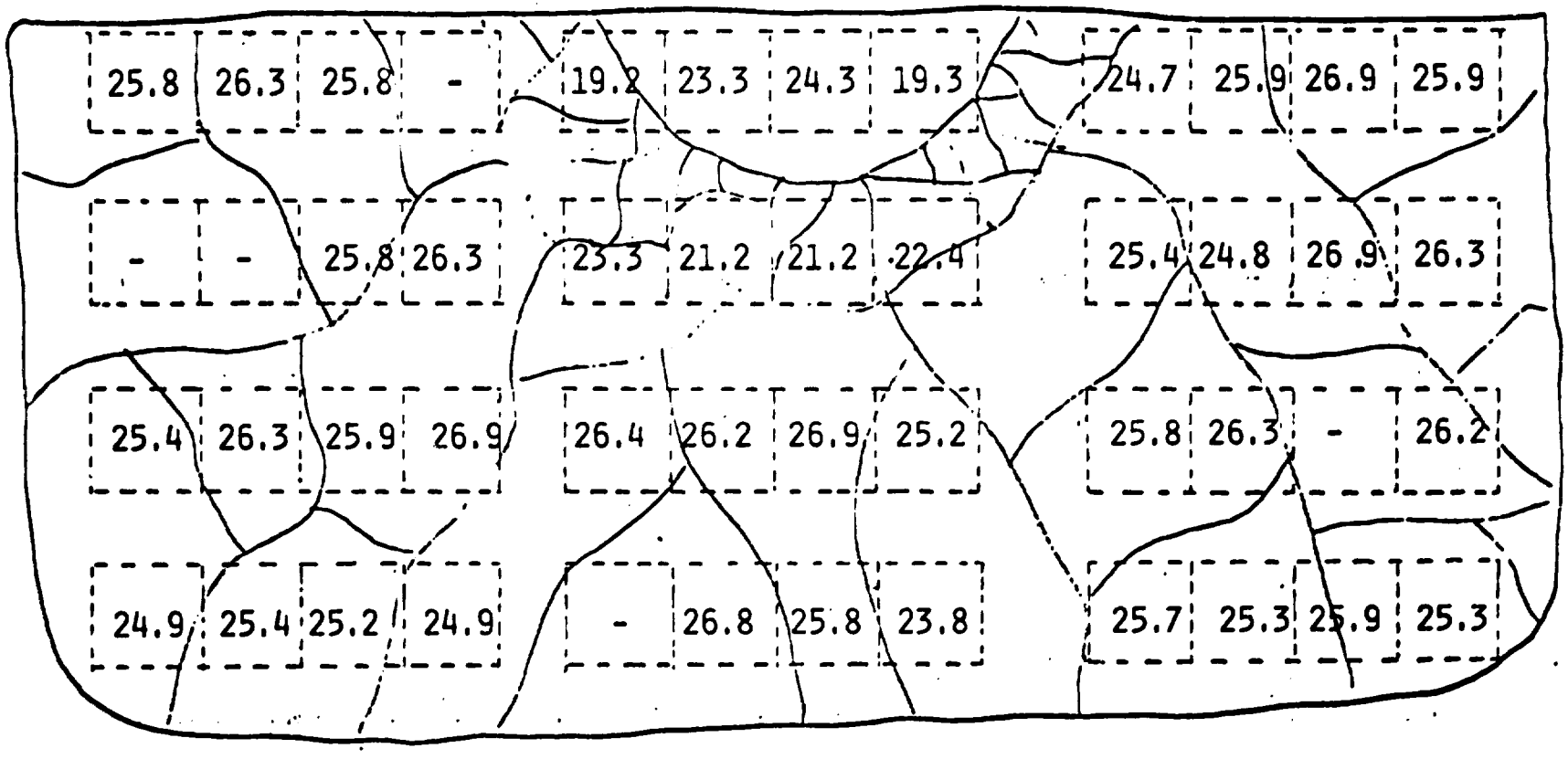

Ave 25.1
Control Ave 28.2

A MAPPING OF CFF (%) FOR THE BOTTOM LAYER OF THE HORIZONTALLY CUT HEM (I.D.41-41C)

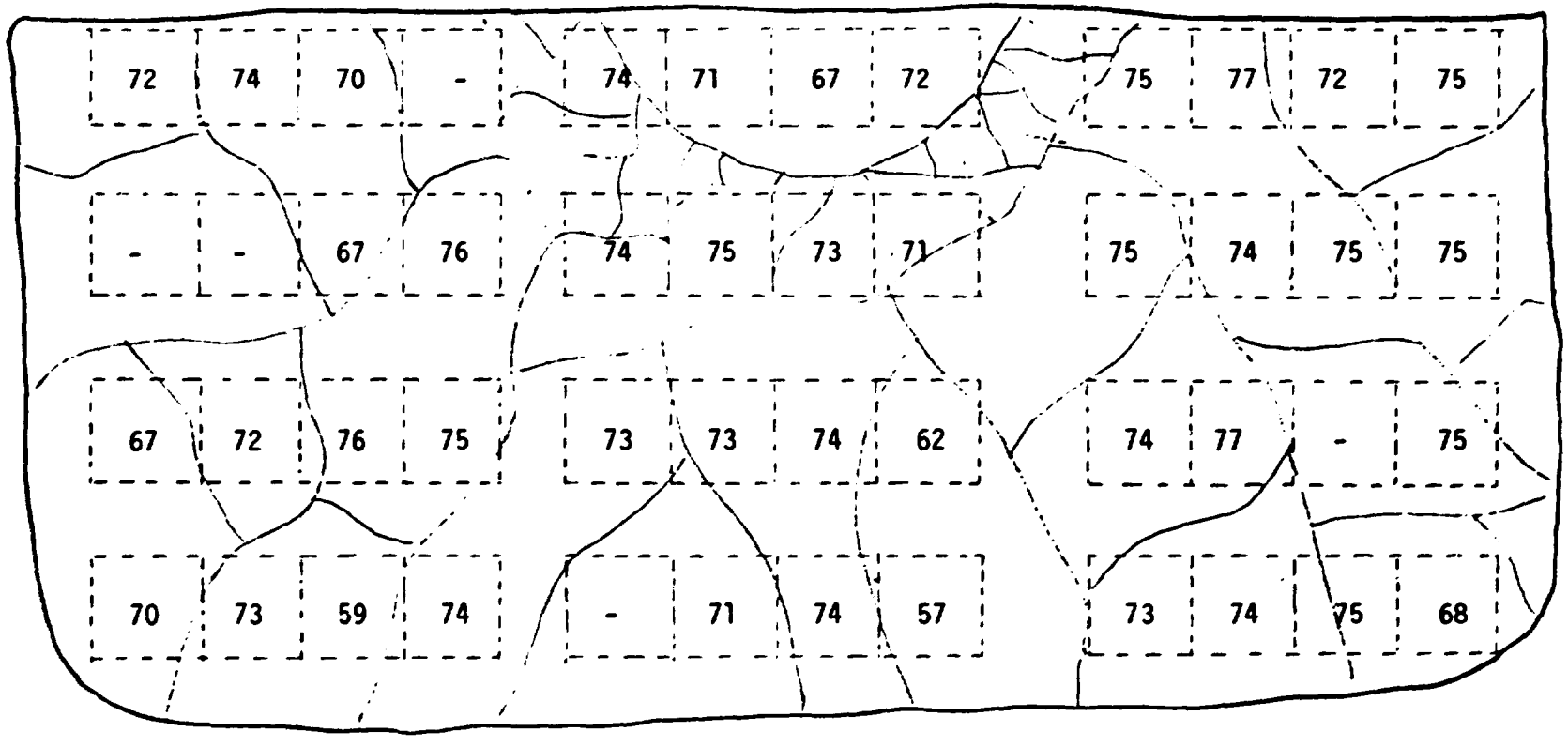

AVE. 73%

CONTROL AVE. 76%

A MAPPING OF η (%AMI) FOR THE BOTTOM LAYER OF THE HORIZONTALLY CUT HEM (I.D.41-41C)

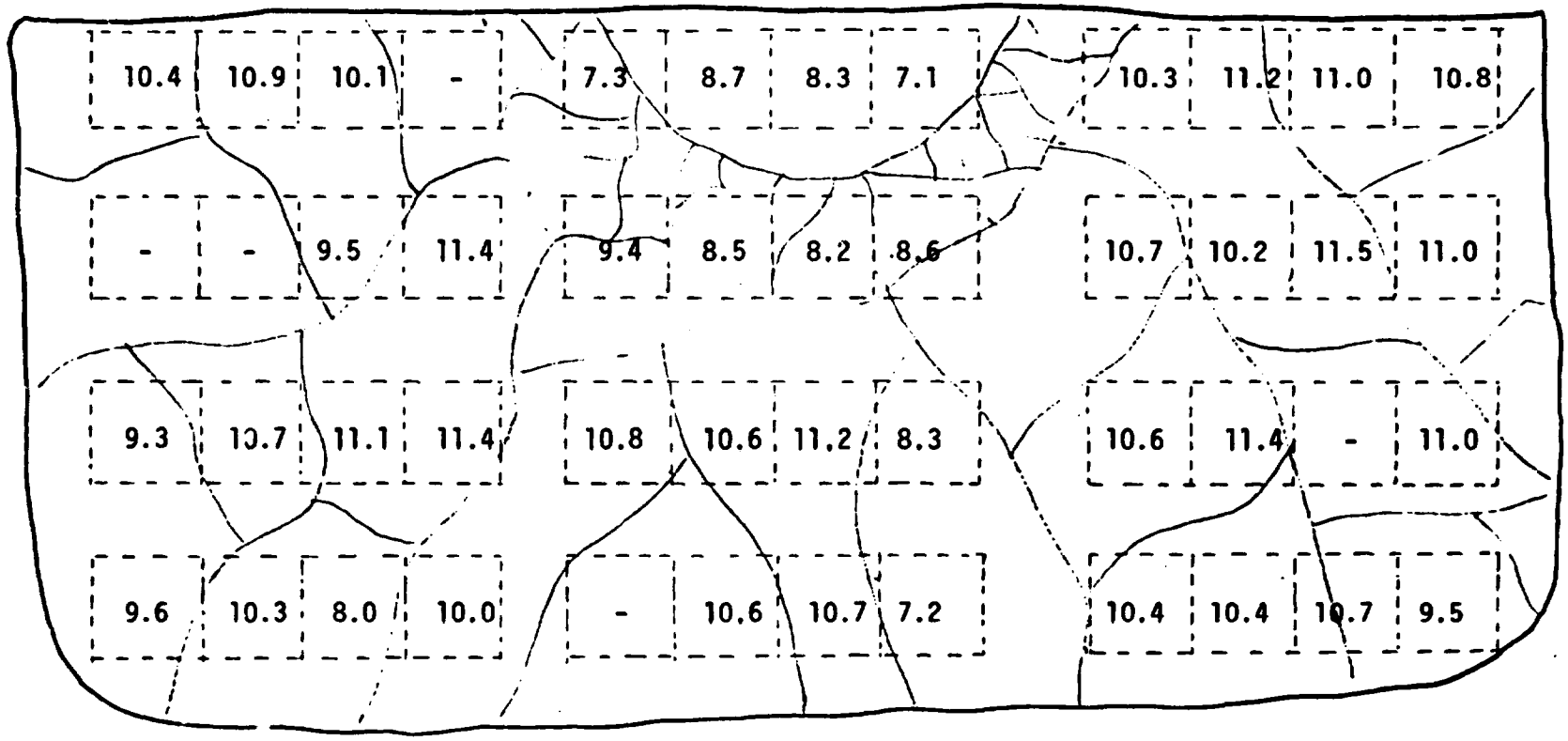

AVE. 10%

CONTROL AVE. 12.3%

APPENDIX V

MAPPING OF SOLAR CELL PARAMETERS FROM VERTICALLY CUT HEM (41-48) LAYERS

A MAPPING OF Voc (mV) FOR A CENTER LAYER OF VERTICALLY CUT HEM (41-48)

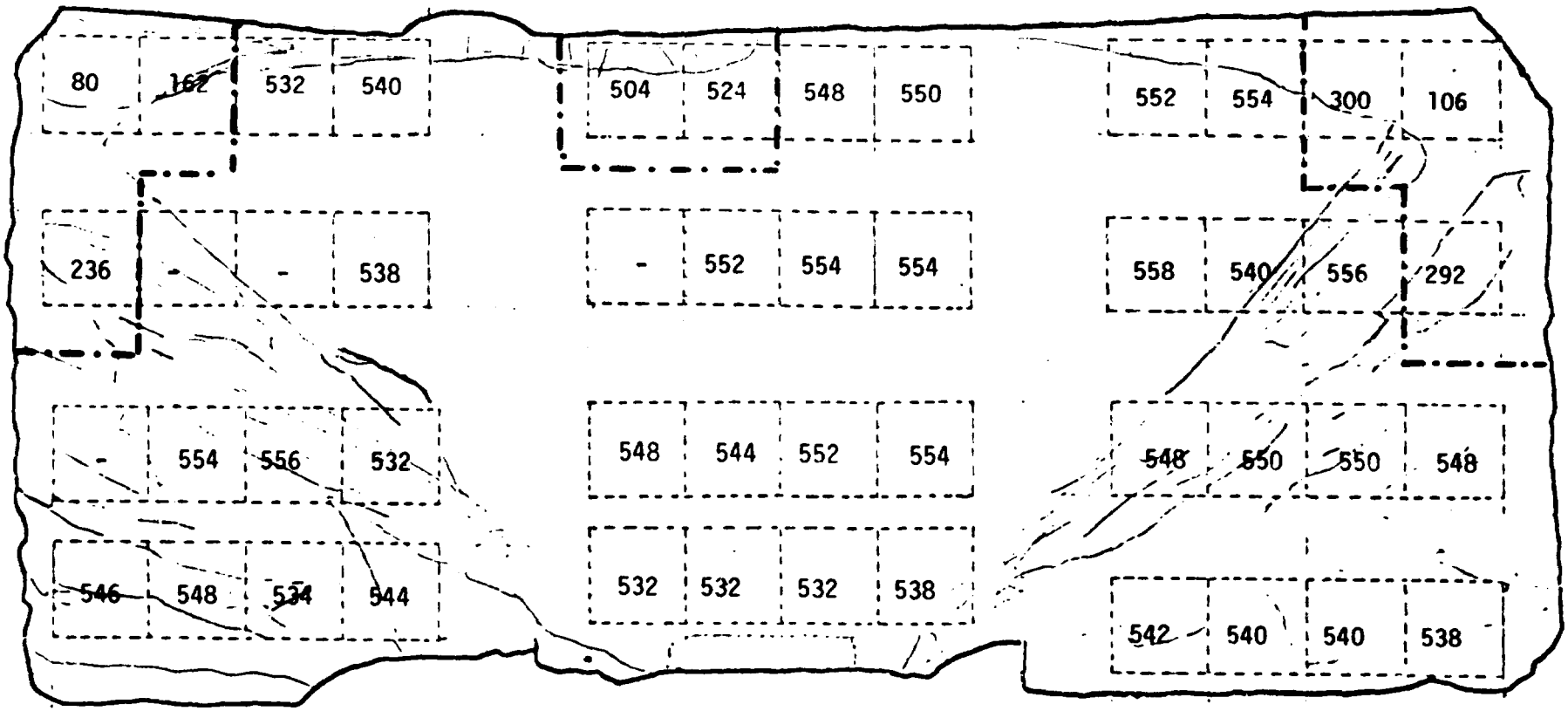

AVE. OF USABLE AREA: 545 (Regions separated by -·- lines are excluded due to shunting)

AVE. OF CONTROL: 578

A MAPPING OF Jsc (mA/cm^2) FOR A CENTER LAYER OF VERTICALLY CUT HEM (41-48)

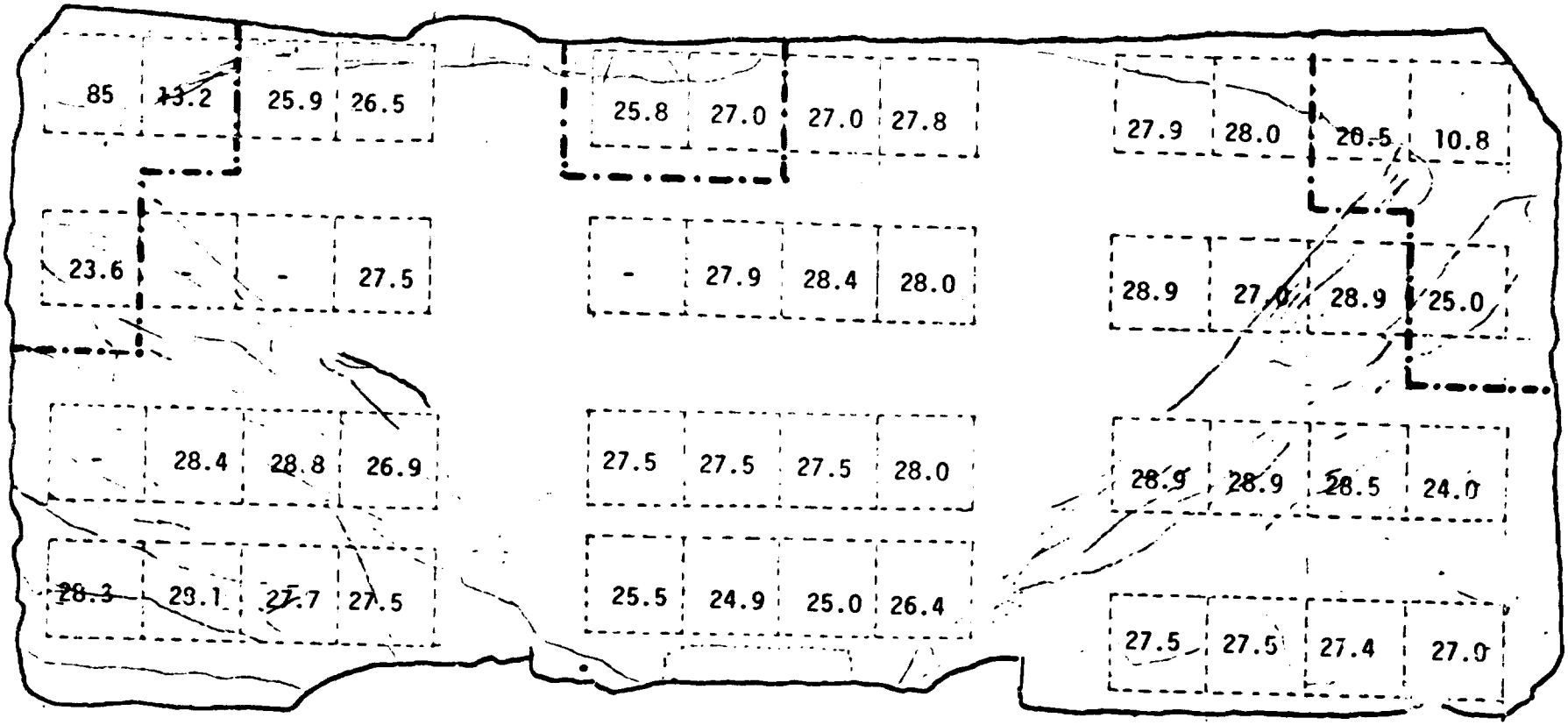

Ave. of Usable Area : 27.4 (Regions separated by -·- line are excluded due to shunting.)

Ave. of Control: 29.0

A MAPPING OF CFF (%) FOR A CENTER LAYER OF THE VERTICALLY CUT HEM (41-48)

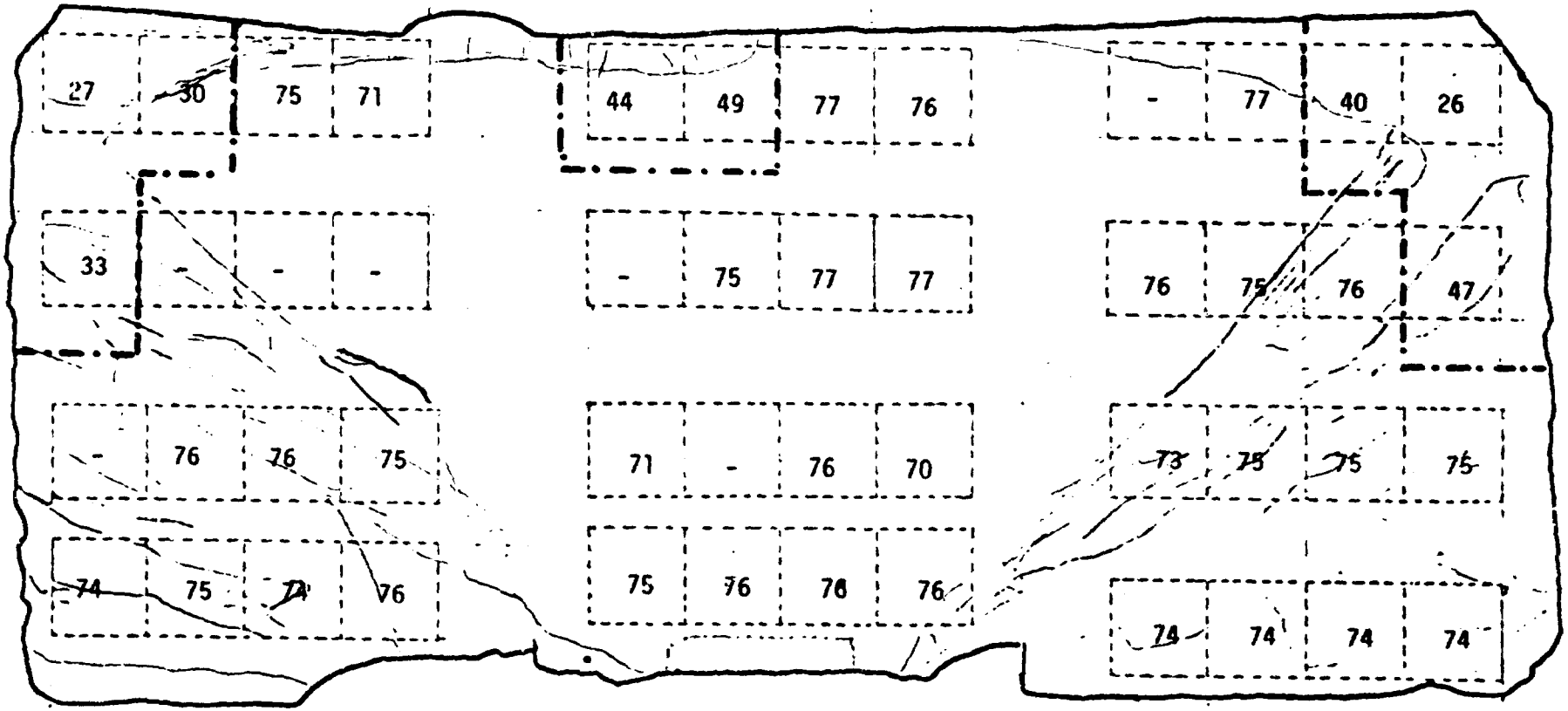

AVE. OF USABLE AREA: 75 (Regions separated by -·- lines are excluded due to shunting.)

AVE. OF CONTROL: 75

A MAPPING OF η (%) FOR A CENTER LAYER OF THE VERTICALLY CUT HEM (41-48)

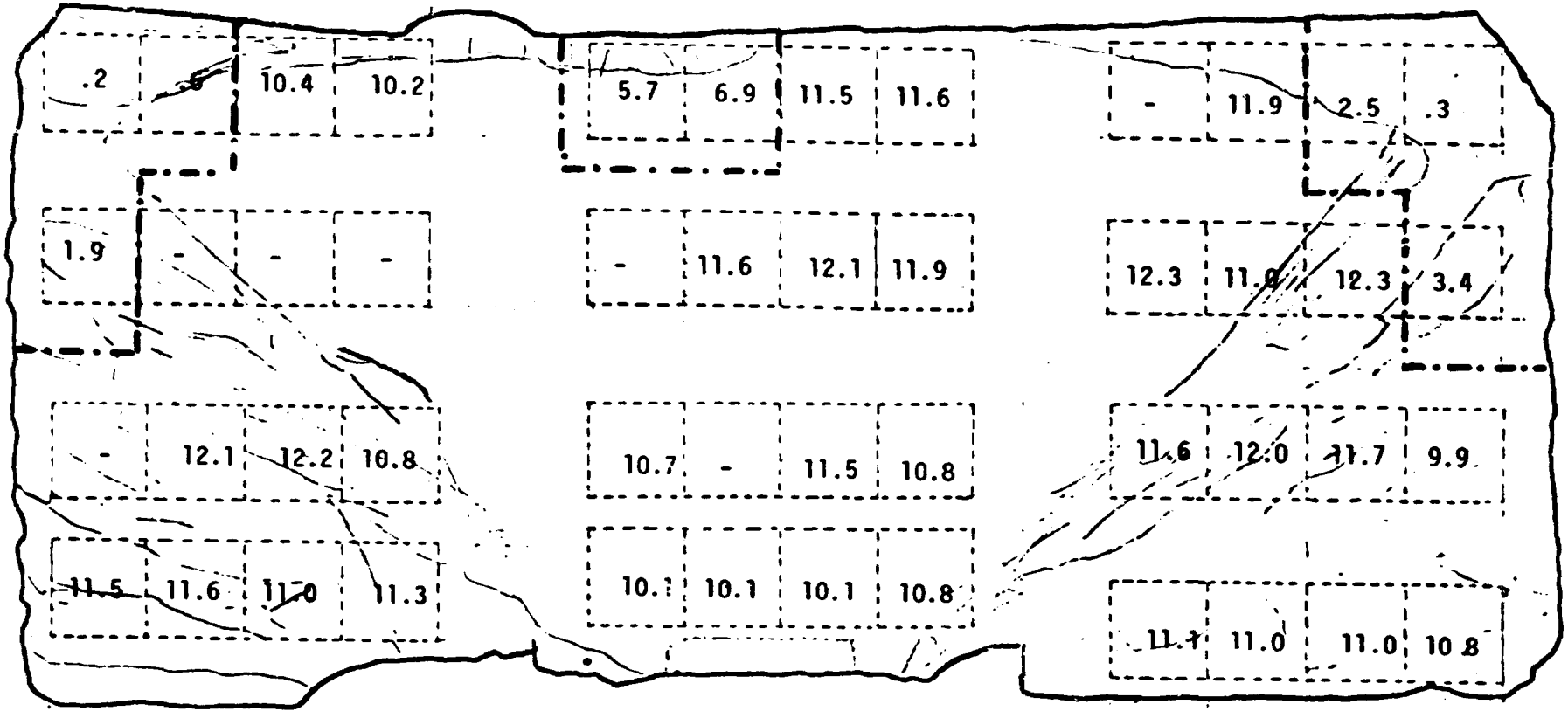

AVE. OF USABLE AREA: 11.2 (Regions separated by -.- lines are excluded due to shunting.)

AVE. OF CONTROL: 12.5

A MAPPING OF Voc (mV) FOR A QUARTER LAYER OF VERTICALLY CUT HEM (41-48)

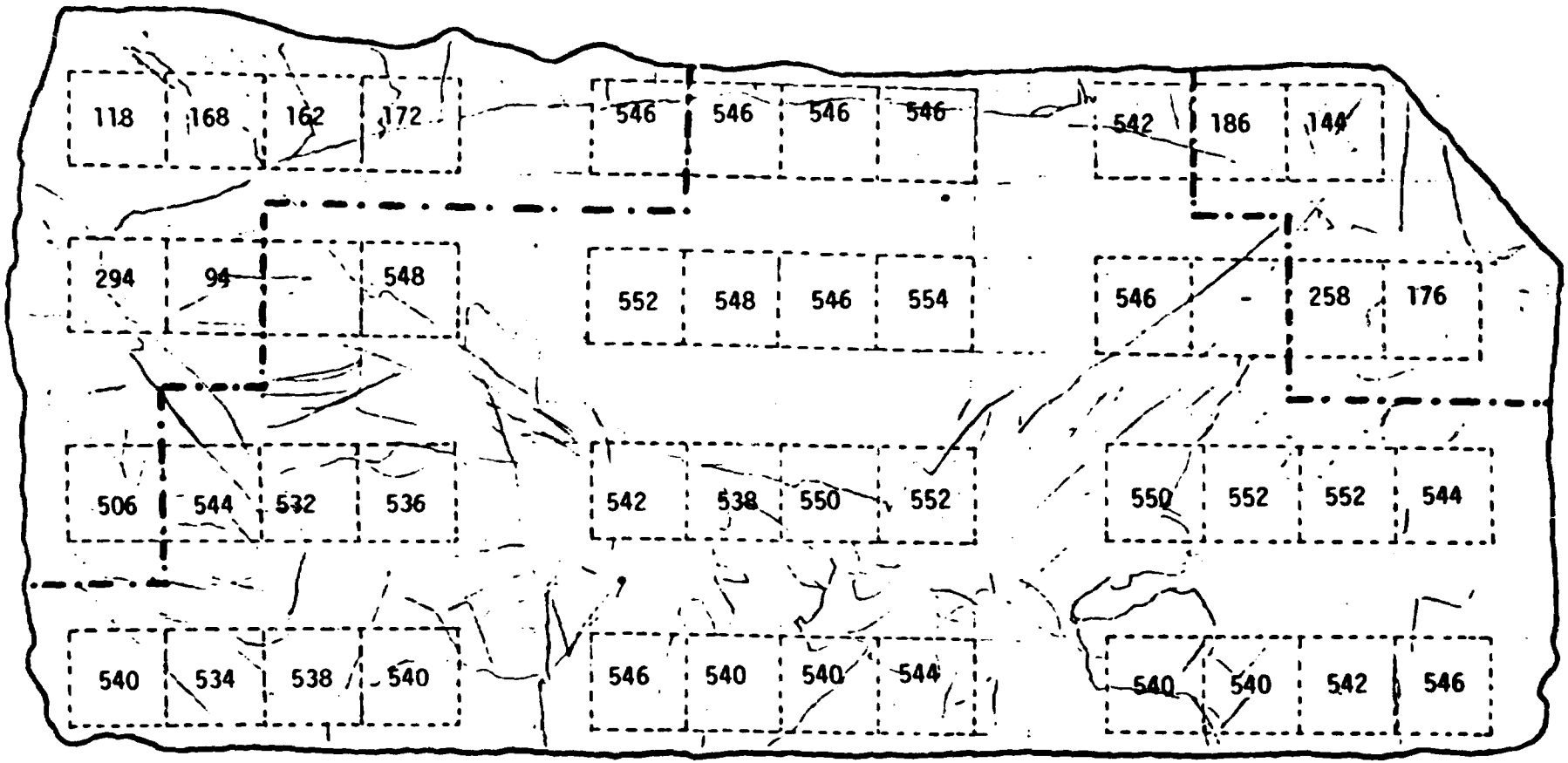

AVE. OF USABLE AREA: 528 (Regions separated by—·— lines are excluded due to shunting)

AVE. OF CONTROL: 578

A MAPPING OF Jsc (mA/cm^2) FOR A QUARTER LAYER OF VERTICALLY CUT HEM (41-48)

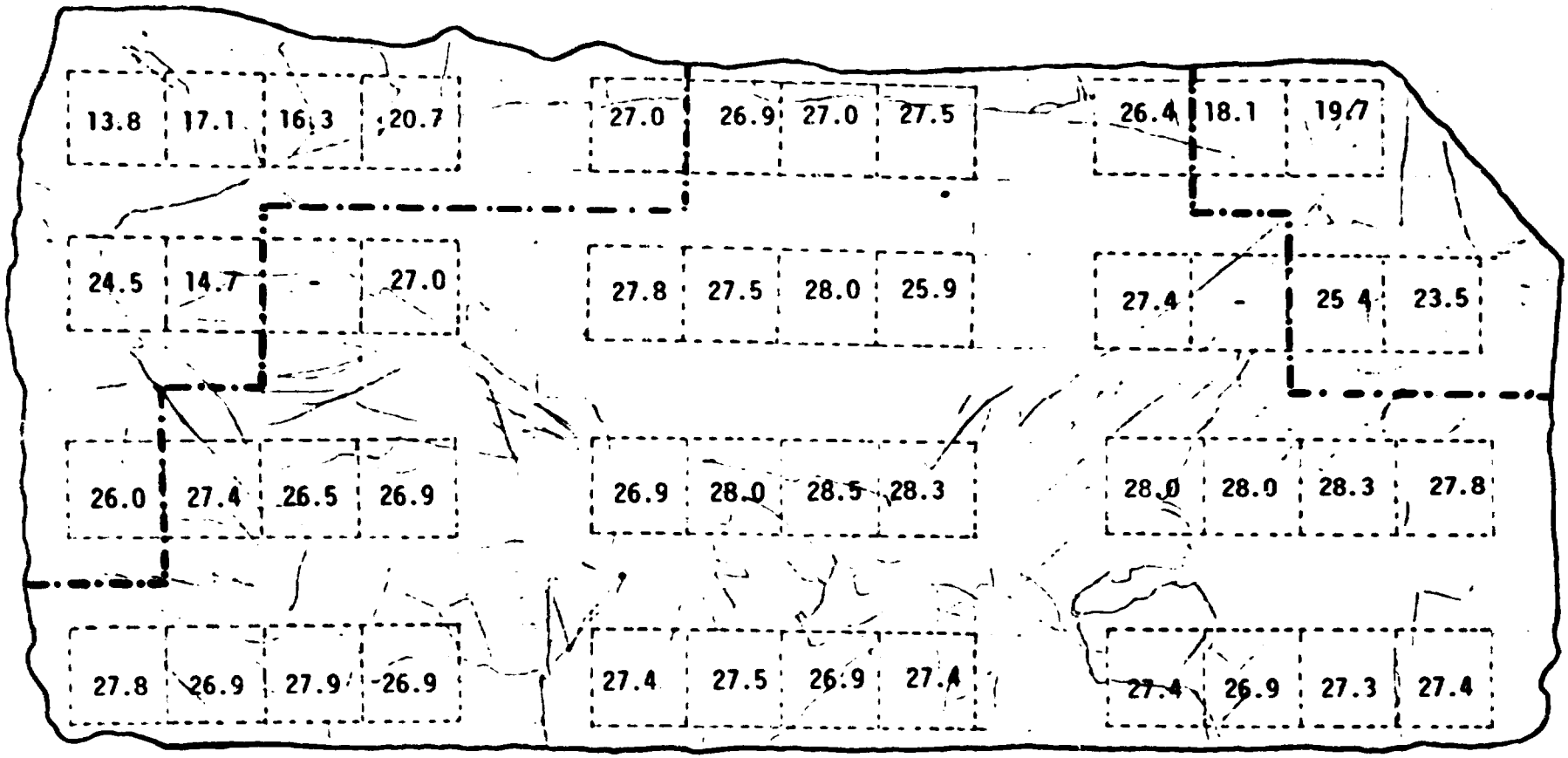

Ave. of Usable Area 27.4 (Regions separated by —·— line are excluded due to shunting)

Ave. of Control: 29.0

A MAPPING OF CFF (%) FOR A QUARTER LAYER OF THE VERTICALLY CUT HEM (41-48)

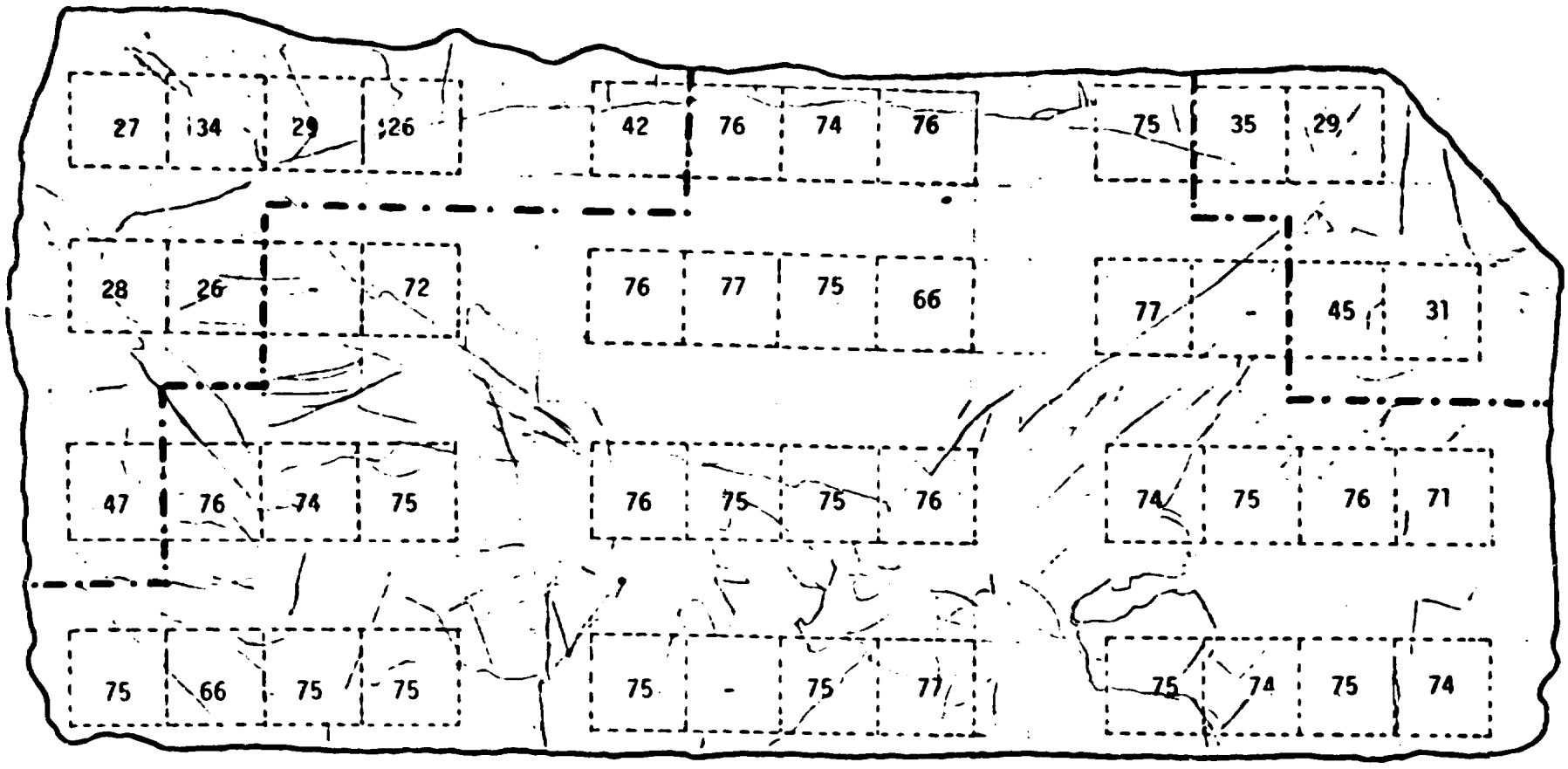

AVE. OF USABLE AREA: 75 (Regions separated by —·— lines are excluded due to shunting.)

AVE. OF CONTROL: 75

A MAPPING OF η (%) FOR A QUARTER LAYER OF THE VERTICALLY CUT HEM (41-48)

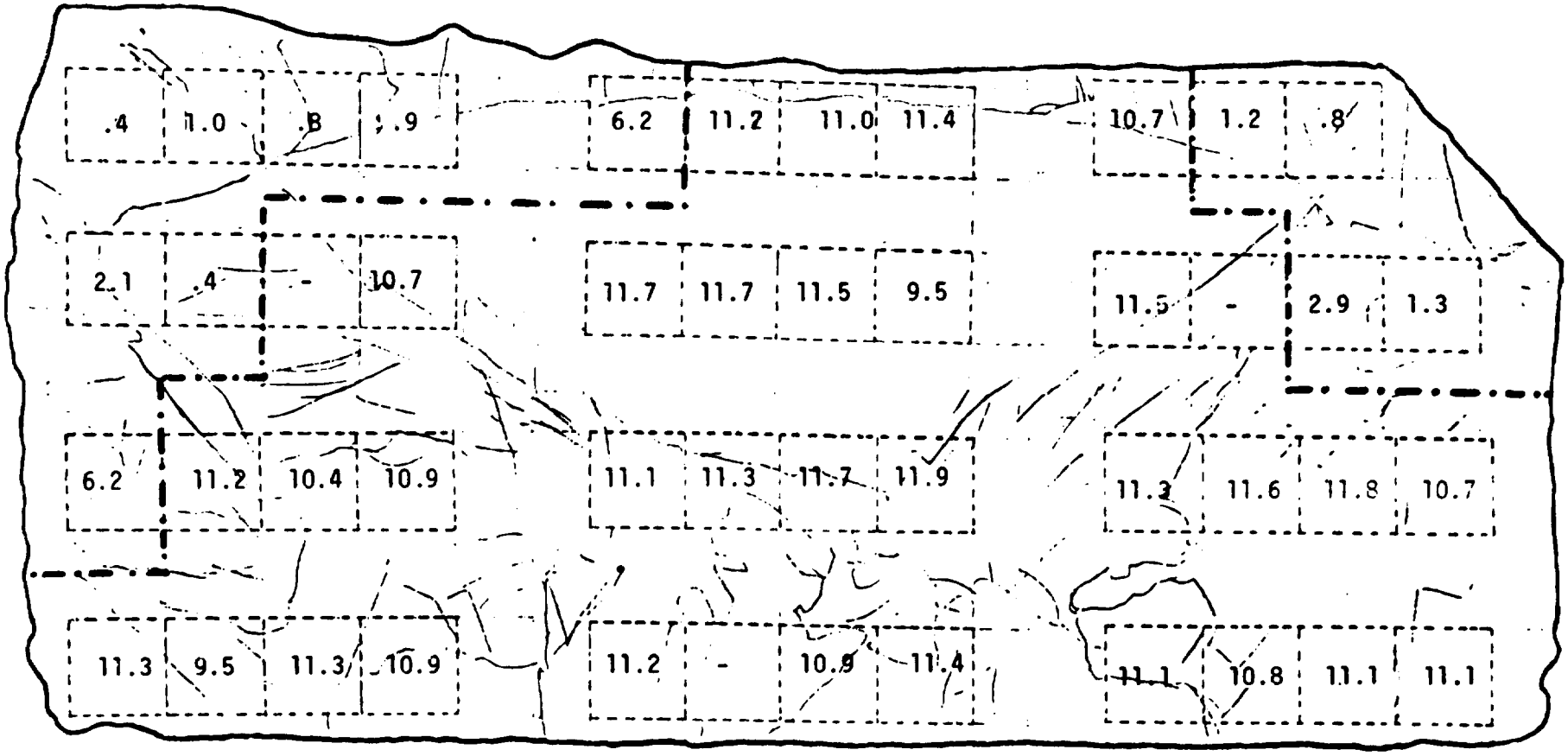

AVE. OF USABLE AREA: 11.1 (Regions separated by —·— lines are excluded due to shunting.)

AVE. OF CONTROL: 12.5

A MAPPING OF Voc (mV) FOR A EDGE LAYER OF VERTICALLY CUT HEM (41-48)

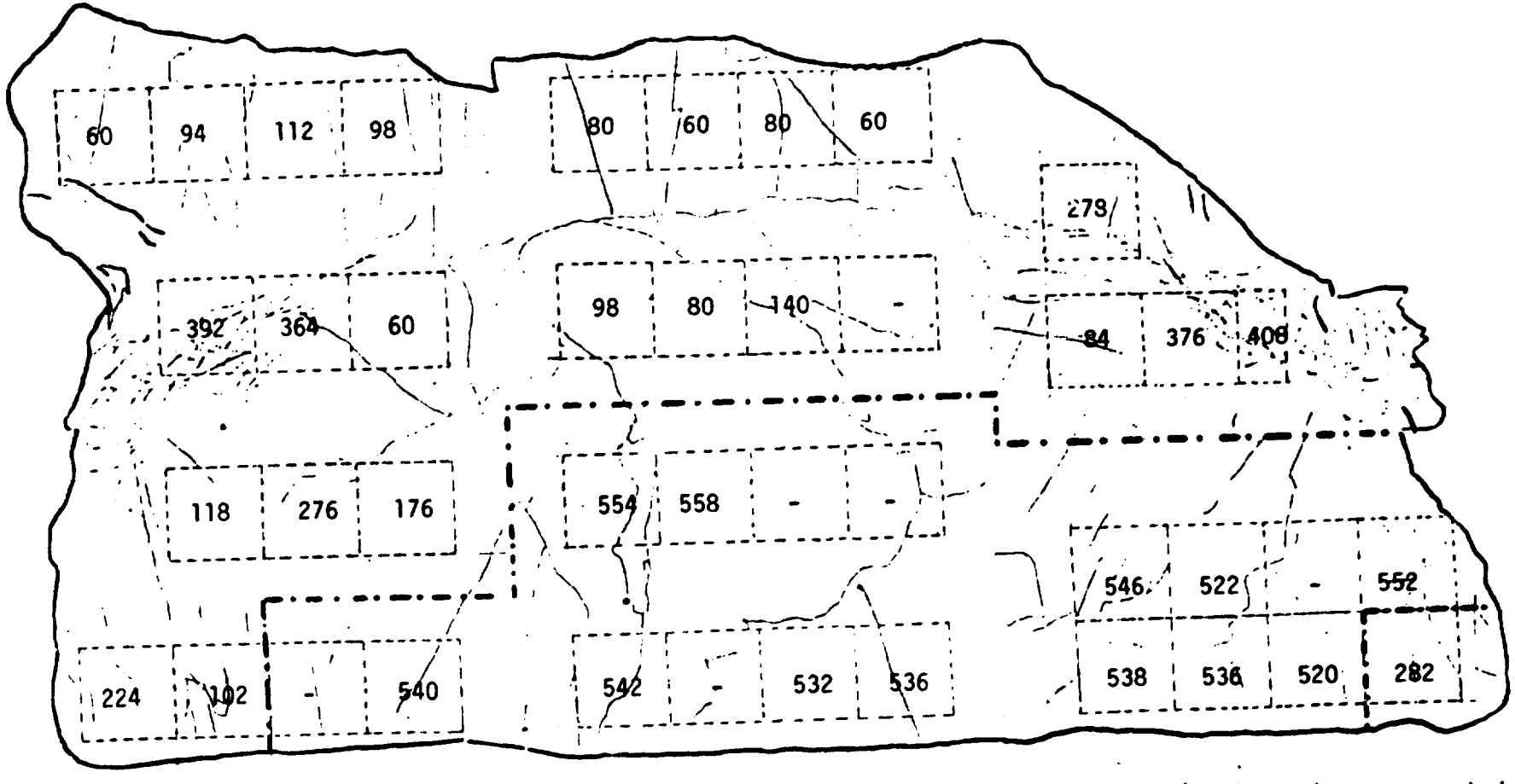

AVE. OF USABLE AREA: 540 (Regions above separated by —·— lines are excluded due to shunting. In this case, the whole upper region is excluded.)

AVE. CONTROL: 578

A MAPPING OF Jsc (mA/cm^2) FOR A EDGE LAYER OF VERTICALLY CUT HEM (41-48)

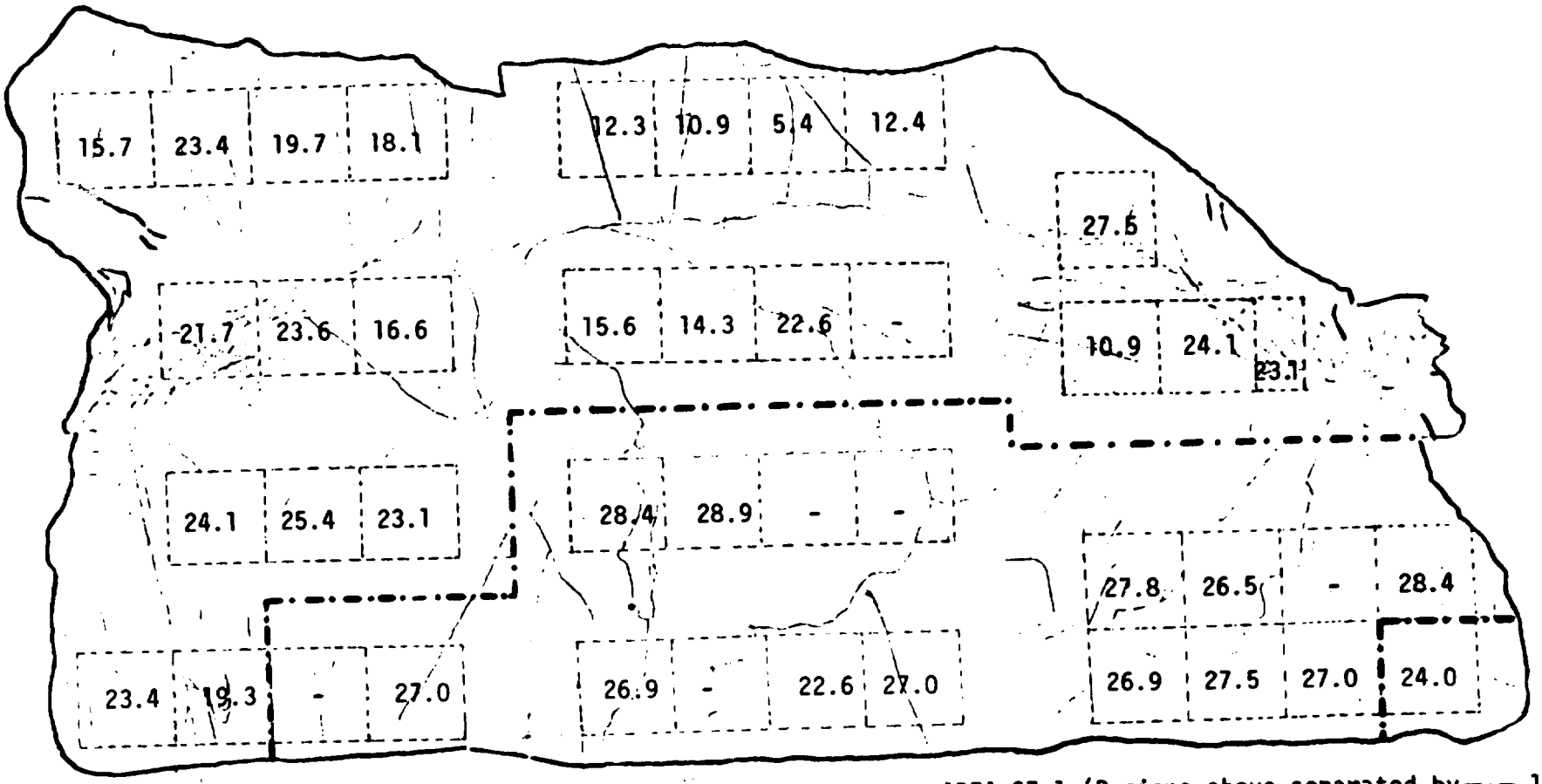

AVE. OF USABLE AREA 27.1 (Regions above separated by —·— lines Are excluded due to shunting. In this case, the whole upper region is excluded)

AVE. OF CONTROL 29.0

A MAPPING OF CFF (%) FOR A EDGE LAYER OF THE VERTICALLY CUT HEM (41-48)

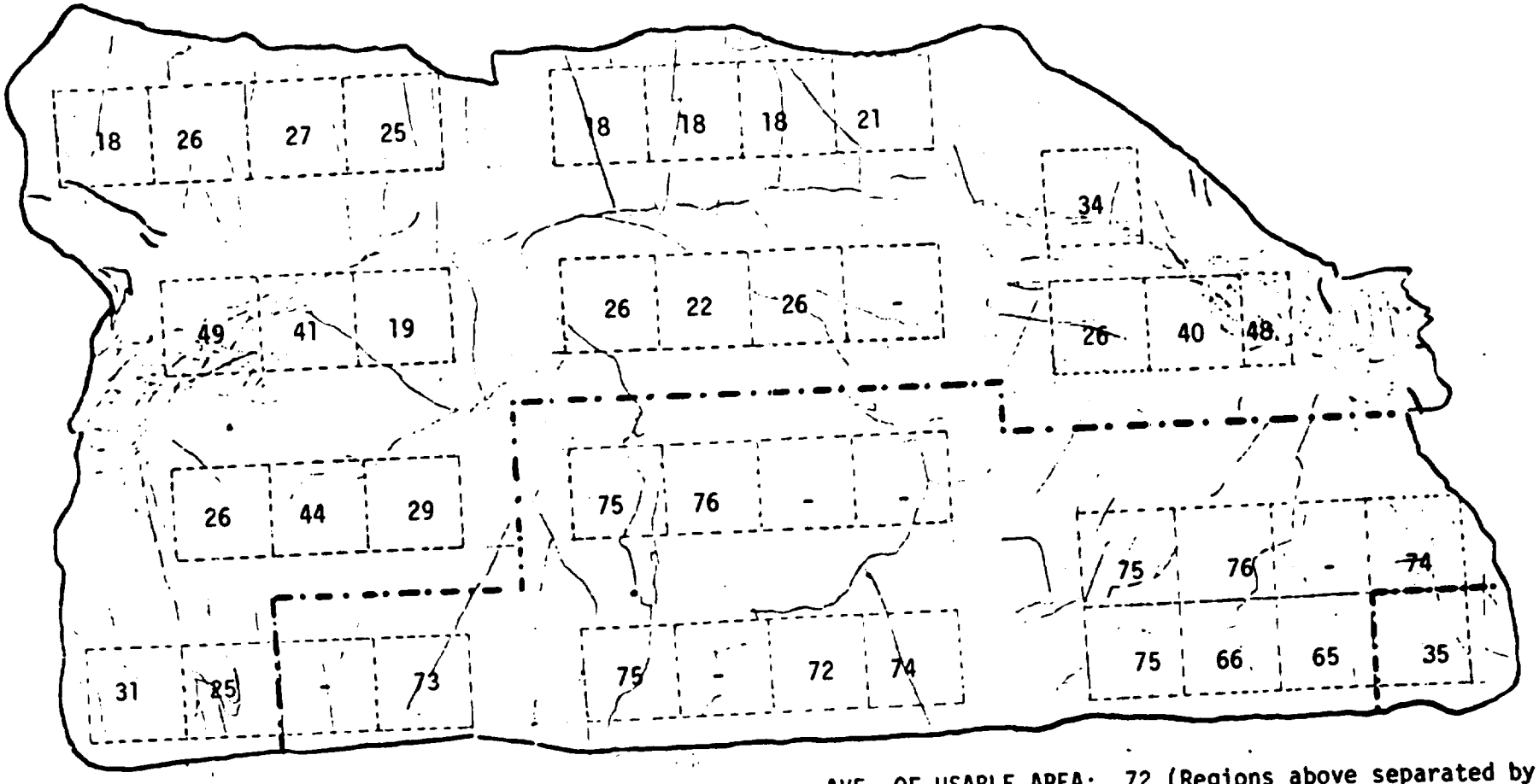

AVE. OF USABLE AREA: 72 (Regions above separated by -·- lines are excluded due to shunting. In this case the whole upper region is excluded.)

AVE, OF CONTROL: 75

A MAPPING OF η (%) FOR A EDGE LAYER OF THE VERTICALLY CUT HEM (41-48)

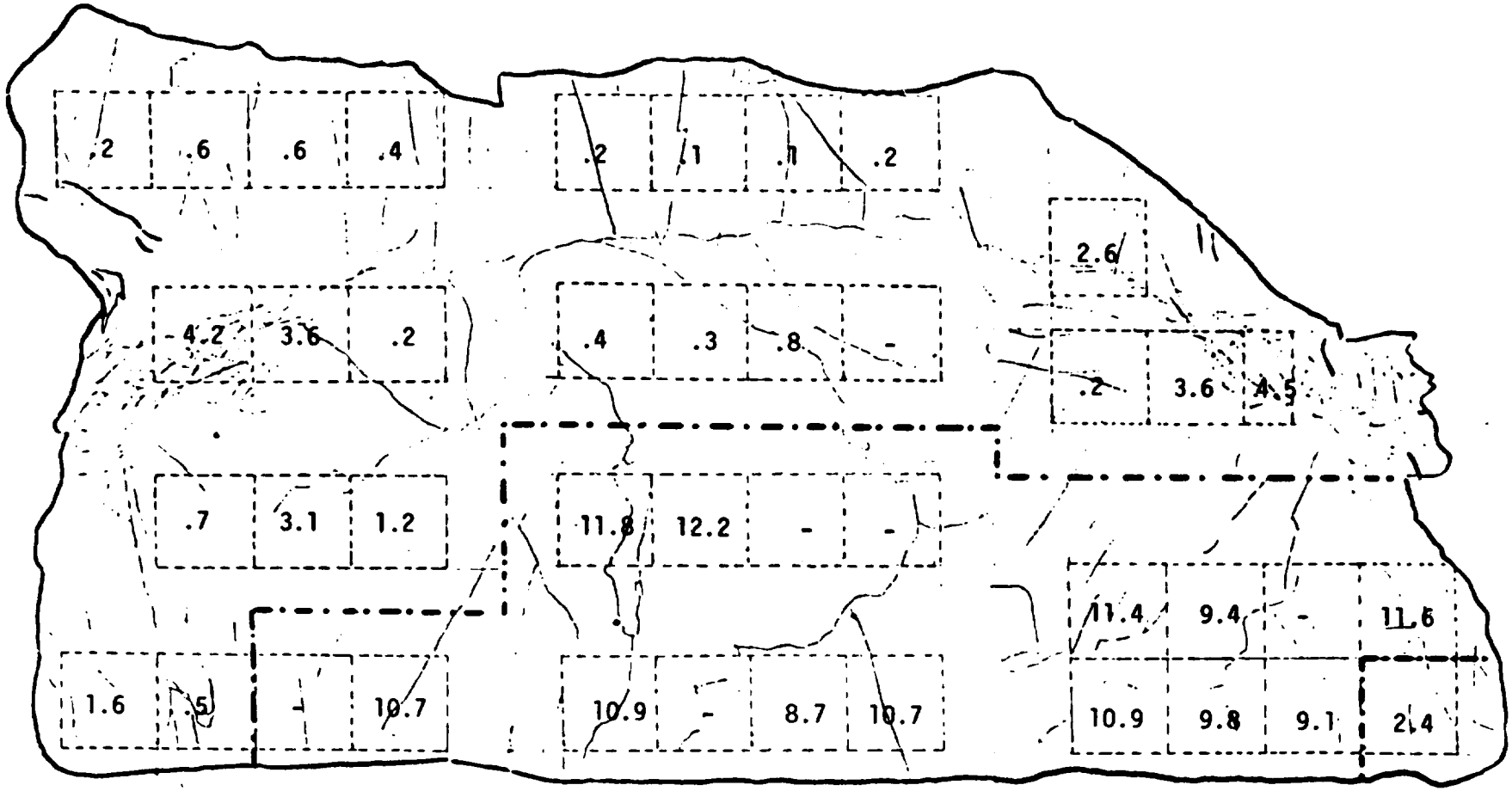

AVE. OF USABLE AREA: 10.5 (Regions above separated by —·— lines are excluded due to shunting. In this case, the whole upper region is excluded.)

AVE. OF CONTROL: 12.5

APPENDIX VI

ELECTRICAL DATA SHEETS FOR DENDRITIC WEB SOLAR CELLS

TABLE 2

SOLAR CELL ELECTRICAL DATA

CELL DESCRIPTION: Dendritic Web (characterized by MRI) Solar Cells
Baseline Solar Cell with SiO AR coating

TEST CONDITION: AM 1

TEMPERATURE: 28°C Feb. /81

NO.	V_{OC} mV	J_{SC} mA/cm^2	P_{Max} mW	CFF %	n %	AREA cm^2
C	534	26.5		77	10.9	4.04
E	534	26.2		78	10.9	4.03
F	534	26.3		77	10.8	4.03
K1	532	26.3		76	10.6	2.02
K2	534	26.2		76	10.6	2.01
(*) L2	530	24.7		79	10.3	1.83
	CZ (7~14 Ωcm) control cell					
1	536	28.5		77	11.8	4.03
2	536	28.9		76	11.7	"
3	534	28.0		77	11.5	"
4	536	28.8		76	11.7	"

Note: (*) Low J_{SC} is due to low active area caused by (1) Front grid line smearing, and (2) smaller cell size.